

2006

Linking land to ocean: Flux and fate of water and sediment from the Yangtze River to the East China Sea

Kehui Xu

College of William and Mary - Virginia Institute of Marine Science

Follow this and additional works at: <https://scholarworks.wm.edu/etd>



Part of the [Geology Commons](#), [Hydrology Commons](#), and the [Oceanography Commons](#)

Recommended Citation

Xu, Kehui, "Linking land to ocean: Flux and fate of water and sediment from the Yangtze River to the East China Sea" (2006). *Dissertations, Theses, and Masters Projects*. Paper 1539616915.

<https://dx.doi.org/doi:10.25773/v5-82xh-xm55>

This Dissertation is brought to you for free and open access by the Theses, Dissertations, & Master Projects at W&M ScholarWorks. It has been accepted for inclusion in Dissertations, Theses, and Masters Projects by an authorized administrator of W&M ScholarWorks. For more information, please contact scholarworks@wm.edu.

LINKING LAND TO OCEAN: FLUX AND FATE OF WATER AND SEDIMENT
FROM THE YANGTZE RIVER TO THE EAST CHINA SEA

A Dissertation
Presented to
The Faculty of the School of Marine Science
The College of William and Mary in Virginia

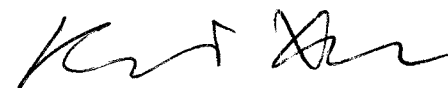
In Partial Fulfillment
Of the Requirements for the Degree of
Doctor of Philosophy

by

Kehui Xu
2006

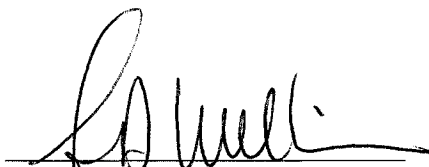
APPROVAL SHEET

This dissertation is submitted in partial fulfillment of
the requirements for the degree of
Doctor of Philosophy



Kehui Xu

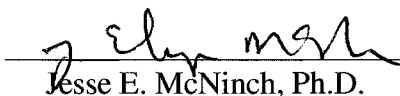
Approved, June 2006



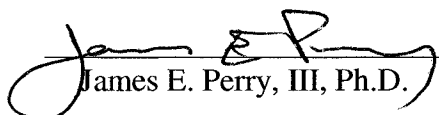
John D. Milliman, Ph.D.
Committee Chairman/Advisor



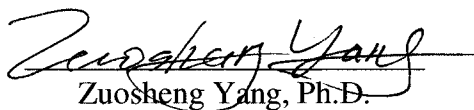
Steven A. Kuehl, Ph.D.



Jesse E. McNinch, Ph.D.



James E. Perry, III, Ph.D.



Zuosheng Yang, Ph.D.
Ocean University of China
Qingdao, China

TABLE OF CONTENTS

	Page
ACKNOWLEDGMENTS.....	v
LIST OF TABLES.....	vi
LIST OF FIGURES.....	vii
ABSTRACT	x
CARTOON.....	xi
CHAPTER 1: Introduction.....	2
Background.....	2
The Yangtze River.....	3
The East China Sea.....	4
The Dissertation.....	5
References.....	6
CHAPTER 2: Water-Budget Trends in Major Chinese Watersheds, 1951-2000.....	11
Abstract.....	12
Introduction.....	12
Methods.....	15
Elements of the Water Budget.....	16
Discussion.....	21
Conclusions.....	25
References.....	26
CHAPTER 3: Climatic and Anthropogenic Impacts on the Water and Sediment	
Discharge from the Yangtze River (Changjiang), 1950-2004.....	42
Abstract.....	43
Introduction.....	43
Physical Setting.....	46
Data and Methods.....	47
Spatial Variations of Water and Sediment.....	48
Temporal Variations of Water and Sediment.....	48
Discussion.....	52
Conclusions.....	59

References.....	60
CHAPTER 4: Yangtze Sediment Decline Partly from Three Gorges Dam.....	81
Introduction.....	82
Changes in Yangtze Sediment Transport.....	83
Future Changes to the Yangtze Watershed.....	84
References.....	86
CHAPTER 5: Yangtze- and Taiwan-Derived Sediments in the Inner Shelf of	
East China Sea.....	91
Abstract.....	92
Introduction.....	92
Sediments in the East China Sea.....	93
Material and Methods.....	97
Results.....	99
Discussion and Conclusions.....	102
References.....	107
CHAPTER 6: Structure and Formation of the Yangtze-derived Holocene Clinoform,	
Inner Shelf of the East China Sea.....	134
Abstract.....	135
Introduction and Background.....	136
Material and Methods.....	138
Results and Analyses.....	140
Discussion.....	143
Conclusions.....	149
References.....	150
VITA	174

ACKNOWLEDGMENTS

Over the four years I have spent at VIMS, so many people (from both U.S.A. and China) have helped me and made my interdisciplinary (land+ocean) study an enjoyable and colorful one.

First I must thank Dr. John D. Milliman, my advisor, for his great advice, guidance and support through my study and research. With insight, patience and encouragement, John has helped me greatly in both my study and life, and led me to several new and fascinating disciplines/fields on Marine Geology. Second, I am grateful to my committee members (Drs. Kuehl, McNinch, Perry and Yang) for their thoughtful comments and suggestions; especially, I thank Dr. Kuehl for his patience and kindness in revising my prospectus, and Dr. Z.S. Yang for collecting and providing the precious data of the Yangtze River. Moreover, I particularly appreciate Drs. J.P. Liu (North Carolina State University) and A.C. Li (Institute of Oceanology, Chinese Academy of Sciences - IOCAS) for their suggestions and helps. Without the great guidance from Dr. Liu, I can not gain the in-depth knowledge of sequence stratigraphy and sea level.

The crew of R/V Golden Star II, S. Wan, P. Huang and N. Jin (IOCAS), H. Xu (Institute of Atmospheric Physics, CAS), Z. Chen and J. Chen (East China Normal University), Z.X. Chu (Ocean University of China), S.J. Kao (Academia Sinica, Taiwan), Saulwood Lin (National Taiwan University), K.L. Farnsworth (U.S. Geological Survey) as well as H. Wadman (VIMS) are acknowledged for collecting and analyzing samples as well as processing data. Finally, I must thank my parents for their supports, as well as my wife and newborn son, Yanxia and James, for their patience, encouragement and love.

LIST OF TABLES

Table	Page
CHAPTER 2	
Table 1 Precipitation and runoff of five watersheds in China.....	29
CHAPTER 4	
Table 1 Comparison of the Yangtze River with the Choshui River.....	115
Table 2 Clay percentages of smectite, illite, kaolinite and chlorite.....	116
Table 3 Mineral ratios in fine-sand fraction (63-90 μm).....	117

LIST OF FIGURES

Figure	Page
CHAPTER 1	
Fig. 1 Dynamics of water withdrawal & consumption by natural-economic regions.....	9
Fig. 2 Calculated fluvial discharge of suspended solids to the global ocean.....	10
CHAPTER 2	
Fig. 1 Isohyet and major watersheds in China.....	30
Fig. 2 Temperature (a) and precipitation (b) changes from 1951 to 2000.....	31
Fig. 3 Precipitation, runoff, and water consumption of the Pearl River.....	32
Fig. 4 Precipitation, runoff, and water consumption of the Yangtze River.....	33
Fig. 5 Precipitation, runoff, and water consumption of the Yellow River.....	34
Fig. 6 Individual precipitation and runoff of the Liao River and Songhua River.....	35
Fig. 7 Precipitation, runoff, and water consumption of the Liao-Songhua rivers.....	36
Fig. 8 Relation between precipitation and runoff of Chinese rivers.....	37
Fig. 9 Total water withdrawal and consumption in China from 1949 to 2002.....	38
Fig. 10 (a) Comparison of change (%) in precipitation and runoff and (b) classification of major Chinese watersheds.....	39
Fig. 11 Water discharges in stations entering and exiting the sub-basin Upper2 in the Yellow.....	40
Fig. 12 Comparison of precipitation with the ratio of evapotranspiration and consumption to precipitation in Chinese watersheds.....	41
CHAPTER 3	
Fig. 1 Yangtze River drainage basin.....	68
Fig. 2 Water discharge and sediment load at Yichang (upstream) and Datong (lower stream) gauging stations.....	69
Fig. 3 Mean annual precipitation (mm/yr) in Yangtze drainage basin, 1951- 2000.....	70
Fig. 4 Runoff, sediment yield and concentration along the Yangtze River.....	71
Fig. 5 Yangtze River sediment budget.....	72
Fig. 6 Precipitation change (mm) in 1951-2000.....	73

Fig. 7 Spatial and temporal variation of precipitation and runoff in the Yangtze.....	74
Fig. 8 Precipitation, runoff and sediment loads between Pingshan and Cuntan gauging stations.....	75
Fig. 9 Temporal Sediment Trends of the Yangtze River.....	76
Fig. 10 Monthly water discharge and sediment loads at Yichang, Hankou and Datong...	77
Fig. 11 Monthly sediment trapped in the Three Gorges Dam (TGD) in 2003-04.....	78
Fig. 12 Temporal sediment budget in the Dongting Lake.....	79
Fig. 13 Measured and future sediment loads at Datong Station.....	80

CHAPTER 4

Fig. 1. (a) Yangtze River drainage basin. (b and c) Water discharge and sediment load at Yichang and Datong stations, respectively.....	88
Fig. 2. (a) Sediment load at seven stations along the mainstream of the Yangtze River (locations shown in Figure 1). (b and c) Mean annual sediment concentrations at Pingshan and Beibei, respectively.....	89
Fig. 3. Comparison of 2002 and 2004 thalweg profiles between Yichang and Shashi, connecting the lowest points of the river valley.....	90

CHAPTER 5

Fig. 1 Bathymetry and major currents in the East China Sea and Yellow Sea.....	118
Fig. 2 Dispersal of total suspended solids (TSS) in the surface and water-column of ECS.....	119
Fig. 3 Total suspended solids (TSS) concentration in profiles of L1, L2, L3 and L4.....	120
Fig. 4 Relative sediment loads entering the inner shelf of East China Sea.....	121
Fig. 5 Comparison of monthly loads of Yangtze sediment (transported southward) with that of Choshui.....	122
Fig. 6 Samples collected in the inner shelf of East China Sea and nearby rivers (left), and their grain size distributions (right).....	123
Fig. 7 Feldspar to quartz ratios of sand samples in three grain-size fractions (180-125, 125-90 and 90-63 μm).....	124
Fig. 8 Glycolated XRD curves of clay samples (<2 μm) from Yangtze, Qiantang,	

Ou, Min and Choshui (Taiwan) rivers as well as the East Chins Sea.....	125
Fig. 9 Clay percentages in the inner East China Sea and nearby rivers.....	126
Fig. 10 (a) Full Width at Half Maximum (FWHM) of illite with a unit of 0.01 degree of 2 θ	127
Fig. 11 Average Full Widths at Half Maximum (FWHM) of illite in Choshui River, Taiwan Strait (<26°N), East China Sea (ECS, 26-30.5°N) and Yangtze Delta (>30.5°N).....	128
Fig. 12 Classification of clays in the inner shelf of East China Sea.....	129
Fig. 13 XRD curves of fine sand (63-90 μ m) samples from Yangtze, Min and Choshui rivers as well as the Taiwan Strait.....	130
Fig. 14 Mineral ratios of fine-sand (63-90 μ m) samples from ECS and nearby rivers....	131
Fig. 15 Summer/winter currents and sediment transports in the inner shelf of East China Sea.....	132
Fig. 16 Preliminary clay assemblage in the East China Sea.....	133

CHAPTER 6

Fig. 1 Bathymetry and major currents in the East China Sea and Yellow Sea.....	158
Fig. 2 Surficial sediment distribution in the East China Sea.....	159
Fig. 3 Sediment accumulation rates based on ²¹⁰ Pb analysis in the East China Sea.....	160
Fig. 4 Seismic profiles and cores in the East China Sea.....	161
Figs. 5-9 Four facies in the seismic profiles of inner East China Sea.....	163-167
Fig. 10 Fence diagram of seismic profiles in the East China Sea.....	168
Fig. 11 (a) Late High-stand System Tract, (b) Early High-stand System Tract, (c) Transgressive System Tract and (d) Sedimentary feature.....	169
Fig. 12 Isopach of Holocene mud wedge in the inner shelf of East China Sea.....	170
Fig. 13 Down-core clay mineral variations in the north (DE2), middle (DE15) and south (737) of the mud wedge.....	171
Fig. 14 Triangle plot of clay mineral assemblage from Yellow, Min, Taiwan, Yangtze and cores collected in ECS.....	172
Fig. 15 Sediment load (mt/yr, million tons per year) from the Yangtze River to the East China Sea in the past 11,000 years and future decades.....	173

ABSTRACT

Occupying a watershed of 1.8×10^6 km² and being home to >400 million people, the Yangtze River (Changjiang) is the largest river in southern Asia, annually discharging 900 km³ of water into the East China Sea (ECS). As a result, the flux and fate of the Yangtze's sediment, generally cited to be 480 million tons per year (mt/yr), have both scientific and societal relevance.

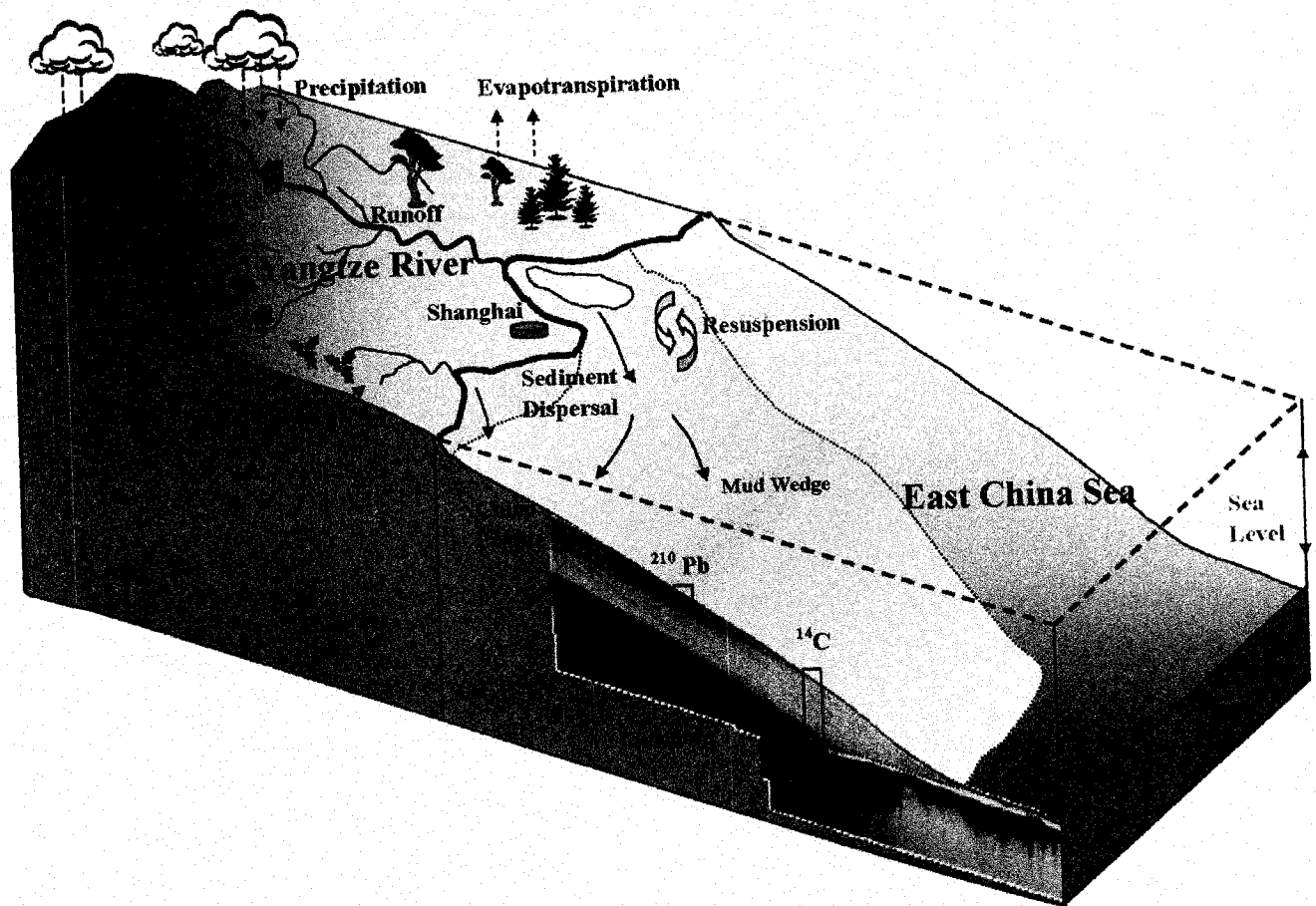
Although precipitation and runoff for the entire Yangtze watershed have changed little since 1950, the increase of runoff in Yangtze southern sub-basin has been much larger than that of precipitation, reflecting decreased temperatures and evapotranspiration. In contrast, the marked decreases in runoff in northern Yangtze have been due mainly to increased water consumption.

Since the 1980s, the Yangtze sediment load has declined dramatically, and 2004 loads at Yichang (just below the Three Gorges Dam - TGD) and Datong (lower stream) were only 12% and 33% of those in the 1950s and 60s, reflecting precipitation decline, landuse change, and most importantly, construction of >50,000 dams. Following the impoundment of the TGD, annual sediment load at Yichang dropped by 164 million tons (mt), but in the preceding 16 years it had decreased by ~300 mt/yr. Throughout the entire basin, the most significant sediment drops (>80%) occurred in two northern tributaries, one southern stream, and two passages between the mainstream and the shrinking Dongting Lake. Ongoing and proposed dams (collectively with greater storage capacity than the TGD) and north-south river diversions will probably decrease the Yangtze load to <100 mt/yr, thereby endangering the lower reaches of the river as well as the Yangtze delta.

Sediments on the inner shelf of the ECS reflect illite-dominated mud from the Yangtze River in the north as well as sandy silt and fine sand (low feldspar/quartz and low K-feldspar/plagioclase) from small mountainous rivers draining Taiwan to the south. Both sediments are significantly different from muds derived from the Yellow (smectite-rich) and Min (kaolinite-dominated) rivers. Grain-size distribution further confirms that ~25% of coarse sediments in northern Taiwan Strait (south of 26°N) are Taiwan-derived.

Along the inner shelf, an elongated (800 km) mud wedge, ~40 m thick at the 30-m isobath, overlies a transgressive sand layer; the mud wedge thins offshore to <2 m at the 80-m isobath. Four distinct acoustic facies can be delineated: late-Pleistocene, Transgressive System Tract (TST), and early and late High-Stand System Tracts (HST). The thin (<3 m) and acoustically transparent TST is only located between 40- and 90-m isobaths south of 30 °N. In contrast, early (2-11 ka BP) and late (0-2 ka BP, more opaque) sigmoidal HSTs are widely distributed in the inner shelf shallower than 70- and 50-m isobaths, respectively. Total volume of this Holocene mud wedge is 22×10^{11} m³, of which early and late HSTs account for 5.7 and 16.3×10^{11} m³, respectively. Assuming a density of 1.2 tons/m³, the average Yangtze sediment flux between 2 and 11 ka BP was 215 mt/yr, but increased to 330 mt/yr after 2 ka BP, primarily reflecting increased deforestation and agriculture. In the near future, however, extensive reforestation and dam construction may decrease the Yangtze load to less than half of its pre-anthropogenic level.

DISSERTATION CARTOON



**Linking Land to Ocean: Flux and Fate of Water and Sediment from the
Yangtze River to the East China Sea**

CHAPTER 1: Introduction

1.1. Background

Rivers form the major link between the lands and oceans, particularly in the transfer of water and sediment to the coastal ocean. Global rivers annually discharge $\sim 36,000 \text{ km}^3$ of water as well as $\sim 15\text{-}18 \times 10^9 \text{ t}$ of sediment to the oceans (Milliman and Syvitski, 1992). Water, perhaps the most widely distributed substance on our planet, plays an important role in the surrounding environment and human life (Shiklomanov, 1999). In addition to filling reservoirs and nourishing deltas, sediment is increasingly recognized as an important part of fluvial ecosystems, estuarine wetlands and biogeochemical cycles in the oceans.

Considering the growing demographic pressures and projected climate change (e.g. global warming), water availability and quality has become an increasing global concern (Gleick, 2000). In many managed watersheds, runoff has decreased dramatically due to decreased precipitation, increased water withdrawal or increased evapotranspiration. The lower reaches of several major rivers, such as the Nile, Colorado, Indus and Yellow, have essentially dried up in recent years, partially due to dramatically increased water consumption (e.g., Shiklomanov, 1999; Vorosmarty et al., 2003).

It can be argued that nowhere is water concern more acute than in southern Asia where large population pressure has increasingly affected freshwater usage and thereby availability. China and India alone (totalling ~ 2.5 billion people), for example, account for more than 40% of the global freshwater used for irrigation (Gleick, 2000). Their water withdrawals have increased by an order of magnitude over the past century and will continue to expend in the foreseeable future (Fig. 1). Coupled with these changes,

droughts and floods appear to have become more extreme and frequent in China. In the lower reaches of the Yellow, for example, dry-up days exceeded 220 in 1997, compared with severe floods in 1998 in the Yangtze causing tens of billion dollars damage and lost of life. Therefore, understanding hydrologic processes and quantifying the hydrologic parameters have become critical to the sustainable development of Chinese watersheds.

Much of the fluvial sediment is deposited in the coastal environment: in the deltas, estuaries and the continental shelf; only a small portion escapes to the deep sea (Meade, 1996). Mainly due to the tectonic control, approximately 2/3 of the fluvial load entering the global oceans comes from southern Asian rivers, such as the Indus, Ganges-Brahmaputra, Mekong, Yangtze and Yellow rivers (Fig. 2) (Milliman and Farnsworth, in prep.). Over the past 1-4 thousand years (the time depending on global locale), however, watershed degradation accelerated due to deforestation and agricultural cultivation, and more recently by road building and urbanization. In the past century, dam construction and related irrigation has caused local decreases in sediment delivery to the coastal zone (Syvitski et al., 2005), with corresponding delta erosion and shoreline retreat (e.g., Chu et al., 2006).

1.2. The Yangtze River

In terms of drainage basin area ($1.8 \times 10^6 \text{ km}^2$) and water discharge ($900 \text{ km}^3/\text{yr}$), China's Yangtze River (Changjiang) is the largest river in south Asia. Being home to >400 million inhabitants, the Yangtze annually delivers 480 million tons (mt) of sediment (measured at Datong Station in the lower stream) to the East China Sea. As a result, the studies of flux and fate of Yangtze water and sediment have both scientific and societal

relevance. Recent climatic change has caused rapid snow melting in the Yangtze headwaters, decline in regional precipitation, as well as more frequent floods over the past half-century. At the same time, anthropogenic impact has increased, water withdrawal expanding ~4 times since the 1950s, in response to an expanding population and increased irrigation. Since the 1980s, Yangtze sediment load has dramatically declined to 147 mt/yr at Datong Station in response to more than 50,000 dams (including the Three Gorges Dam, the world's largest) and reforestation throughout the watershed.

Given these changes in the drainage basin, the Yangtze has been and will continue to be impacted by both natural and anthropogenic changes. How have local and basin-wide Yangtze runoff and sediment responded to climatic (e.g., precipitation) as opposed to anthropogenic (e.g., dam construction and reforestation) forcings? How (and why) has the sediment budget changed regionally as well as throughout the entire Yangtze basin? What can we expect in the future and what will be the coastal responses to these changes?

1.3. The East China Sea

Debouching onto a wide and flat epicontinental shelf (>600 km wide and <100 m deep) in the East China Sea, the large annual flux of Yangtze sediments (480 mt/yr) has facilitated the preservation of high-resolution records of both stratigraphic sequences and sea-level change. The majority of Yangtze sediments dispersed southward along the inner shelf and formed an elongated mud wedge stretching south from Yangtze mouth 800 km to northern Taiwan Strait. Despite the obvious importance of inner shelf mud wedge in the East China Sea, there has been relatively little written on the fate of Yangtze sediment.

Of the 480 mt/yr sediment load measured at Datong Station (600 km upstream from the Yangtze mouth), channel aggradation and delta progradation trap about 70% of the sediment before reaching the East China Sea, leaving ~150 mt/yr exiting the estuary (Milliman et al., 1985). To complicate the situation, the Yangtze may not be the only sediment source for the inner-shelf mud wedge. Along the mainland side south of the Yangtze, the Qiantang, Ou and Min rivers totally discharge ~15 mt/yr directly into the mud wedge. More importantly, small mountainous rivers draining Taiwan (small red dot in the lower right panel of Fig. 2) collectively can discharge 175 to 380 mt/yr sediment into the ocean, often during typhoon-generated floods (Dadson et al., 2003; Kao et al., 2005). A super-typhoon in 1996, for example, resulted in nine Taiwanese rivers discharging 217 million tons of sediment (Milliman and Kao, 2005), more than the total Yangtze load in 2004.

Given these circumstances, how much of the Yangtze's sediment has accumulated in the mud wedge along the inner shelf during Holocene? How much of the sediment in the mud wedge was derived from the Yangtze as opposed to the rivers draining Taiwan? How have climatic and anthropogenic changes affected the sediment flux from the Yangtze?

1.4. The Dissertation

In this dissertation, I attempt to delineate the flux and fate of water and sediment from the Yangtze River to the East China Sea by incorporating and integrating both *land* and *ocean* parts into the study. In addition to this Introduction, the dissertation consists of five subsequent chapters.

For the land part of the study, water-budget trends for five major Chinese watersheds (Pearl, Yangtze, Yellow, Liao and Songhua) between 1950 and 2000 are analyzed by quantifying precipitation, runoff, water storage, water consumption, and evapotranspiration (Chapter 2, prepared for *Journal of Hydrometeorology*). In the following chapter (Chapter 3, prepared for *Journal of Hydrology*), I discuss the spatial as well as temporal variations of water and sediment from the entire Yangtze River over the past 50 years. In Chapter 4 (published in *EOS Transactions, AGU, 2006*), I explore the degree to which the recent decline in Yangtze sediment load was caused by construction of the Three Gorges Dam as opposed to the cumulative effect of upstream dams and reforestation.

The second part of the dissertation is concerned with the sediments in the East China Sea. In Chapter 5 (prepared for *Marine Geology*), mineralogical analyses (both clay and sand) are used to identify the sediment provenances (Yangtze vs. Taiwan) in the mud wedge along the inner shelf of the East China Sea. In the final chapter (Chapter 6, prepared for *Continental Shelf Research*), using chirp seismic profiles and geochronology (^{14}C and ^{210}Pb) as well as grain-size and mineralogical data, the structure and formation as well as the history of Holocene clinoform development of the mud wedge are discussed.

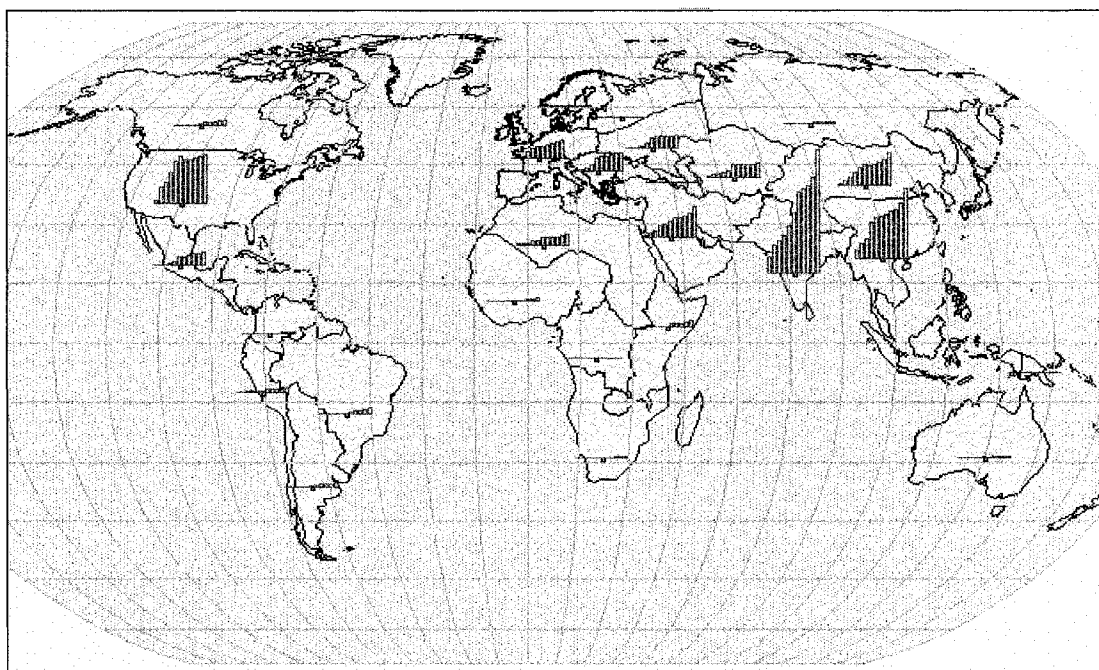
References

- Chu, Z.X., Sun, X.G., Zhai, S.K. and Xu, K.H., 2006. Changing pattern of accretion/erosion of the modern Yellow River (Huanghe) subaerial delta, China: Based on remote sensing images. *Marine Geology*, 227(1-2), 13-30.

- Dadson, S.J. et al., 2003. Links between erosion, runoff variability and seismicity in the Taiwan orogen. *Nature*, 426(6967): 648-651.
- Gleick, P., 2000. The World's Water 2000-2001. The Biennial Report on Freshwater Resources. Pacific Institute for Studies in Development, Environment, and Security, Oakland, California, USA.
- Meade, R.H. 1996. River-sediment inputs to major deltas. In: J. Milliman and B. Haq (Editors), *Sea-Level Rise and Coastal Subsidence*. Kluwer, London, pp. 63-85.
- Milliman, J.D., Shen, H.T., Yang, Z.S. and Meade, R.H., 1985. Transport and deposition of river sediment in the Changjiang estuary and adjacent continental shelf. *Continental Shelf Research*, 4(1-2): 37-45.
- Milliman, J.D. and Syvitski, J.P.M., 1992. Geomorphic/tectonic control of sediment discharge to the ocean: the importance of small mountainous rivers. *Journal of Geology*, 100(5): 525-544.
- Milliman, J.D. and Kao, S.-J., 2005. Hyperpycnal Discharge of Fluvial Sediment to the Ocean: Impact of Super-Typhoon Herb (1996) on Taiwanese River. *J. of Geology*, 113, 503-516.
- Milliman, J.D. and Farnsworth, K. L. in prep. *Flux and Fate of Fluvial Sediment to the Coastal Oceans*. Oxford University Press.
- Kao, S.J., Lee, T.Y. and Milliman, J.D., 2005. Calculating highly fluctuated suspended sediment fluxes from mountainous rivers in Taiwan. *Terres. Atmos. Ocean. Sci.*, 16(3): 441-432.
- Shiklomanov, I.A., 1999. *World Water Resources and Their Use*. State Hydrological Institute (SHI), Russia, St. Petersburg.

Syvitski, J.P.M., Vorosmarty, C.J., Kettner, A.J. and Green, P., 2005. Impact of Humans on the Flux of Terrestrial Sediment to the Global Coastal Ocean. *Science*, 308(5720): 376-380.

Vorosmarty, C.J. et al., 2003. Anthropogenic sediment retention: major global impact from registered river impoundments. *Global and Planetary Change*, 39(1-2): 169-190.



Dynamics of water withdrawal by natural-economic regions of the world (km cub.)

years: 1900, 1940, 1950, 1960, 1970, 1980, 1990, 1995, 2000, 2010, 2025

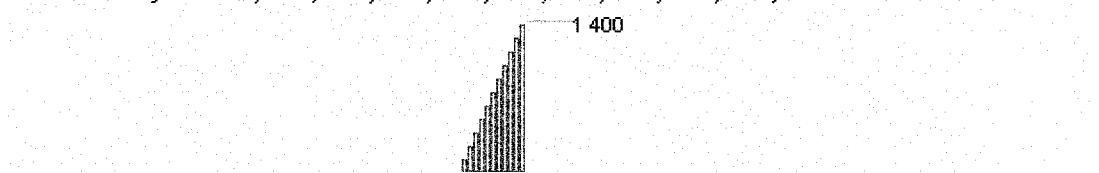


Fig. 1 Dynamics of water withdrawal & consumption by natural-economic regions of the world (from Shiklomanov, 1999). Note that total China's water withdrawal includes both southeast and northern China shown above.

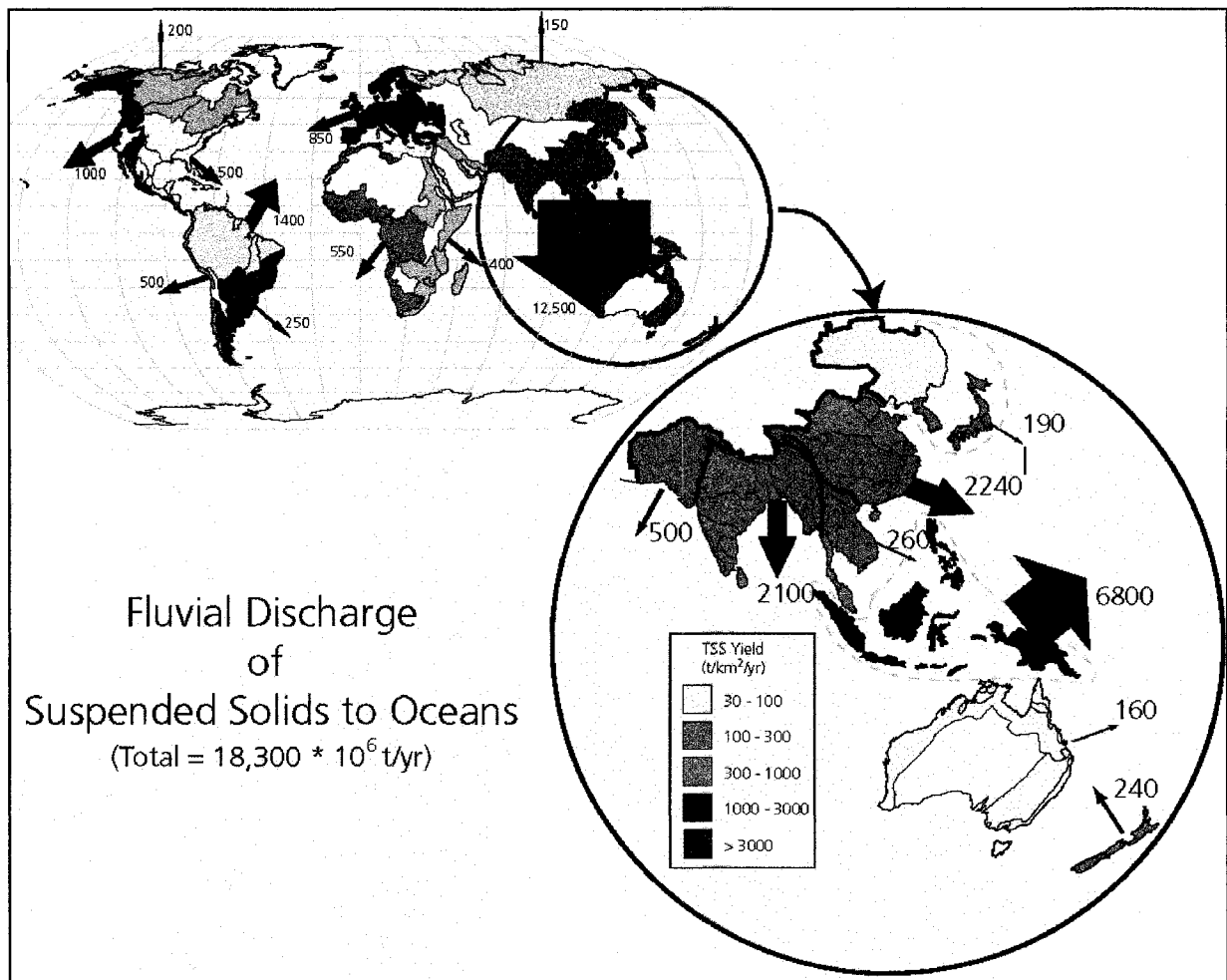


Fig. 2 Calculated fluvial discharge of suspended solids to the global ocean (upper left). Of the approximately 2/3 of the global load emanating from southern Asia, more than half comes from high-standing islands in the East Indies and the Philippines (from Milliman and Farnsworth, in preparation).

CHAPTER 2: Water-Budget Trends in Major Chinese Watersheds, 1951-2000*

Kehui Xu^{1,a}, John D. Milliman¹ and Hui Xu²

¹ School of Marine Science, College of William & Mary, Gloucester Point, VA 23062, USA;

² Institute of Atmospheric Physics, Chinese Academy of Sciences, Beijing 100029, People's Republic of China;

^a Corresponding author. Tel.: +1-804-684-7739; Fax: +1-804-684-7250; E-mail: kxu@vims.edu

* Prepared for *Journal of Hydrometeorology*

Abstract

Records from 160 meteorological stations throughout China show that since 1951 temperature has decreased slightly in the south but increased $>2^{\circ}\text{C}$ in the north. Over the same period, precipitation has increased slightly ($\sim 3\%$) in the south but decreased ($4\text{--}11\%$) in the north. Hydrologic data from five major watersheds show that Pearl River runoff increased by $\sim 9\%$, Yangtze runoff had little net change, whereas flows in the Yellow, Liao and Songhua rivers decreased by 80% , 52% and 13% , respectively. Changes in reservoir storage, groundwater uptake, and lake area in all five watersheds appear to have been small compared to precipitation and runoff. Depending on the extent to which withdrawn water is lost to the drainage basin (i.e. water consumption), the difference between precipitation and runoff since 1951 - which can be regarded as actual evapotranspiration - decreased 5% to 6% in the Pearl and Yangtze watersheds, whereas there has been no apparent change in the northern rivers. Runoff in the southern Yangtze has increased more than increased precipitation would suggest, perhaps reflecting decreased temperatures and evapotranspiration. In contrast, the marked decreases in runoff in northern China (including northern Yangtze, Liao, Songhua and most of the Yellow) reflect increased water consumption.

1. Introduction

The present and future availability and quality of freshwater has become an increasing global concern, particularly in light of growing demographic pressures and projected climate change (e.g., Gleick 1993, 2000; Shiklomanov and Rodda 2003). This concern is especially acute in southern Asia, where ever-expanding large populations

have increasingly affected freshwater usage. China and India alone account for more than 40% of the global freshwater used for irrigation (Gleick 2000). Even where annual precipitation and river runoff are high, the monsoonal nature of seasonal precipitation can result in severe droughts or floods, sometimes within the same year.

It can be argued that nowhere is water availability more uneven than in China. The 1000-mm isohyet, which separates the northern Yangtze River from the southern Yellow River (Figs. 1a and 1b), provides an effective dividing line between the wet south and the dry north. Rainfall throughout much of the southeast exceeds 1400 mm yr⁻¹, whereas it is less than 400 mm yr⁻¹ throughout the north. The influence of the summer monsoon increases from south to north, summer (June-August) rains accounting for 30-40% of the annual precipitation in south-central China but > 65% in the north (Simmons et al. 1999; Chen et al. 2005).

Recent decades have seen a number of marked changes in both climate and fluvial regimes throughout China. Since 1951 temperature has decreased slightly in the south (especially in the upper Yangtze) but increased dramatically (>2°C) in the north (Fig. 2a). Precipitation also has changed, some areas along the southern coasts experiencing up to 300 mm increase in annual rainfall, whereas areas in the central part of the country have seen similar levels of decline (Fig. 2b). In the past decade, summer floods seem to have become more frequent and severe in southern China, in contrast to increased droughts in northern China (Menon et al. 2002). In 1998, for example, floods on the Yangtze and Songhua rivers caused tens of billion dollars of damage and lost of life, whereas in 1997 the number of no-flow days on the lower Yellow River exceeded 220.

Superimposed on these climatic trends have been anthropogenic changes, particularly those involving watershed management. Temporal variations and trends in precipitation (Huang and Chen 2002; Wang 2002; Wang et al. 2004) and water discharge of Chinese rivers (Yang et al. 1998; Chen et al. 2001a; Chen et al. 2001b; Ren et al. 2002; Xu, 2002) have been extensively studied, but few studies have attempted to address the relationship between precipitation and river runoff, taking into account evapotranspiration, water storage, and water consumption.

Under natural conditions, river discharge (Q) can be expressed as precipitation (P) minus the sum of evapotranspiration (ET , the combination of physical evaporation and plant transpiration) and water storage (both surface water, SW , in reservoirs and lakes, and groundwater, GW). In managed watersheds, such as those in China, one also must take into account water consumption (WC), withdrawn water directly lost to the watershed (mainly through evapotranspiration) and generally accounting for ~50% of water withdrawal in southern Asia (Shiklomanov, 1999). The water budget can then be quantified as:

$$Q = P - (ET + \Delta SW + \Delta GW + WC) \quad (1)$$

In this paper, we report the 50-yr (1951-2000) trends in precipitation and runoff for five major Chinese watersheds - the Pearl (Zhujiang), Yangtze (Changjiang), Yellow (Huanghe), Liao and Songhua (a tributary of the Amur) rivers (Table 1, Fig. 1b). Spanning a wide range of latitudes (22°N - 50°N), these five watersheds occupy a cumulative area of 3.8 million km², and are home to more than 755 million people (Fuggle et al., 2000).

In addition to a basin-wide analysis of these five rivers, we also performed sub-basin calculations for four Yangtze sub-basins and three Yellow sub-basins for inter-basin comparison. Precipitation and runoff for the adjacent Liao and Songhua rivers were analyzed separately, but because their water storage and consumption generally are reported as a single quantity in most Chinese publications, we sometimes discuss these two rivers as a single entity. By taking into account estimated changes in surface and groundwater storage and water consumption, we attempt to calculate actual evapotranspiration and thereby quantify the water budget in these five major Chinese watersheds.

2. Methods

In this study we have used monthly *temperature* and *precipitation* datasets (1951-2000) released by China Meteorological Administration, collected from 160 meteorological stations throughout China (Fig. 1a, red dots). Of these stations, 46 were located within the Yangtze watershed, 20 in the Yellow, 11 in the Pearl, and 13 in the Liao and Songhua. For each station, the trends of precipitation and temperature from 1951 to 2000 were determined by linear regression in Matlab 7. Since these stations are not evenly distributed in space, the annual average precipitation for basins and sub-basins was calculated by Krigging interpolation and gridding in the Golden Surfer program after equal-area projections in ArcView 3.2.

Discharge data for each river came from the downstream-most gauging station as reported in the Bulletin of Chinese Rivers and Sediments (2000, 2001 and 2002), Changjiang Sediment Bulletin (2000 and 2001), and other publications (Shiklomanov

1999; Fuggle et al., 2000; Chen et al. 2001a). Pearl River discharge was defined by collective discharge of its three main tributaries (West, North and East rivers) (Fig. 1b, Table 1). Watershed runoff was calculated by dividing river discharge by drainage basin area upstream from the gauging station, generally 70-95% of the total watershed areas except for the Liao (55%). After determining the precipitation and runoff, the correlation coefficients between them were then calculated in Matlab 7.

Post-1997 water withdrawal and consumption data for five watersheds were taken directly from the Bulletin of Water Resources in China (1997-2002). Before 1997, however, only total national withdrawal and consumption in China were available (Ren et al. 2002; Heilig 1999), thus making it impossible to obtain data for individual watersheds. However, since withdrawal of each watershed seems to have accounted for a relatively stable percentage of total national withdrawal between 1997 and 2002, we assumed that pre-1997 withdrawal in each river remained a fairly constant percentage to the total China (Bulletin of Water Resources in China, 1997-2000). Pre-1997 watershed withdrawal for each watershed could thus be calculated. Each watershed's pre-1997 consumption data were therefore calculated by multiplying its calculated pre-1997 withdrawal with its average ratio of consumption/withdrawal in 1997-2002.

3. Elements of the Water Budget

a. Precipitation

Combining data from the 160 meteorological stations, precipitation showed a broad belt of decline trending from the northeast to the southwest (Fig. 2b). Major decreases occurred in the northern upper Yangtze watershed as well as the middle-lower

Yellow, a region with historic water shortages and high population densities. In southern China, patterns of precipitation change were more mixed, with a station in upper Yangtze River decreasing by more than 250 mm, compared to increases as much as 150 mm in the Pearl River basin (Figs. 1b and 2b).

From 1951 to 2000, basin-wide annual precipitation (Figs. 3-7) increased slightly (3%) within the Pearl watershed, and there was almost no change (-1%) in the Yangtze. In contrast, there was a significant decline in rainfall in the north (e.g., 11% in the Yellow River) (Table 1). Regardless of long-term trend, these Chinese rivers experienced several major flood years, notably 1954 and 1998 in the Yangtze, 1964 in the Yellow, and 1998 in the Songhua and Liao.

b. River Discharge and Runoff

Runoff appears to have been more variable than precipitation over the past 50 years (Figs. 3-7). Annual runoff on the Pearl and Yangtze has varied by a factor of 2-4, the long-term runoff trend increasing by 9% and 5%, respectively. In contrast, runoff in the Yellow, Liao and Songhua has decreased 80%, 52% and 13%, respectively, reflecting primarily the influence of anthropogenic activities, such as water withdrawal and dam construction (discussed below).

Precipitation predicted runoff well for the Pearl, Yangtze and Songhua rivers (R^2 of 0.72, 0.81 and 0.63, respectively) from 1951 to 2000 (Fig. 8). For the Yellow and Liao rivers, precipitation correlated with runoff relatively well ($R^2 = 0.63$ and 0.67 , respectively) until construction of major dams in the early 1960s, after which runoff decreased dramatically primarily due to water withdrawal, resulting in poor correlations

with precipitation. For the entire 50-yr period, correlation coefficients (R^2) of the Yellow and Liao rivers were only 0.40 and 0.56 (Fig. 8 and Table 1).

c. Change in Water Storage

1) Change in Subsurface Storage (Groundwater)

In the natural environment, groundwater and runoff are highly exchangeable. In 2000, for example, the groundwater in the Yangtze watershed was reported to be 252 km³, of which 241 km³ overlapped with runoff. Since the runoff is already included in Equation (1), the change in non-overlapped groundwater (11 km³) can be regarded as ΔGW . From 1997 to 2000, the non-overlapped groundwater in the Yangtze fluctuated between 7 and 14 km³ yr⁻¹ (Bulletin of Water Resources in China, 1997- 2000), compared with a mean annual water discharge of 957 km³ yr⁻¹ (Table 1). Non-overlapped groundwater in 2000 for the Pearl also was small, 3 km³ yr⁻¹. Thus, groundwater withdrawal can be considered to be a minor component of the southern China water budget.

Using similar calculations, non-overlapped groundwater in 2000 for the Yellow and Liao-Songhua rivers was 11 and 17 km³ yr⁻¹, respectively. Change in the Yellow groundwater probably was not negligible considering its low water discharge (35 km³ yr⁻¹) and severe water withdrawal. Human water withdrawal has actually lowered the water table in many parts of northern China so that there probably has been negative storage (Bulletin of Water Resources in China, 1997- 2000). While limited groundwater data hinder us from quantifying this variable, groundwater withdrawal should be considered a potentially important factor in the northern China water budget.

2) Change in Surface Storage (Lakes and Reservoirs)

We also need to calculate annual storage of water in both natural lakes and man-made reservoirs for each of the basins. Natural lake area in China in the early 1950s was about 46,000 km². Using this area and assuming an evaporation rate of 500 mm yr⁻¹ (close to the means of precipitation-runoff in Figs. 3-5 and 7), annual lake storage in the early 1950s would have had to be ~23 km³ yr⁻¹ to maintain lake levels. Between 1950 and 2000, however, Chinese lakes lost an estimated area of 13,000 km²; three largest freshwater lakes - Poyang (5,340 km²), Dongting (4,350 km²), and Tai lakes (2,424 km²) - all within the Yangtze watershed - alone losing about 3,200 km² of area (Changjiang Sediment Bulletin, 2000). Thus, by 2000, change in lake storage due to decreased lake area probably amounted to ~16 km³ yr⁻¹. Assuming more than half of this occurred in Yangtze lakes, total lake-storage change probably amounted to no more than ~1% of the annual Yangtze freshwater budget.

Between 1950 and 1999 approximately 86,000 reservoirs were built on Chinese rivers (Fuggle et al., 2000). From 1997 to 2002, the total capacity of big- and middle-size reservoirs in total China varied between 165 and 197 km³. In 2000, reservoir capacity was 30, 74, 23 and 19 km³ in the Pearl, Yangtze, Yellow and Liao-Songhua rivers, respectively (Bulletin of Water Resources in China, 1997-2000). Assuming that water had been stored gradually over 50 years, annual stored water would be 0.6, 1.5, 0.5 and 0.4 km³ yr⁻¹, respectively. In addition to stored water, one must calculate reservoir filling to offset evaporation loss. Although we can find no estimate of total surface area of Chinese reservoirs, we can estimate this by assuming a mean dam height of 30 m, which we then divide into total reservoir volume. For the Pearl, Yangtze, Yellow and Liao-Songhua watersheds, calculated reservoir area would be 1, 2.5, 0.8 and 0.6 × 10³

km² (capacity/height), respectively. Using the evaporation rates of 780, 520, 400 and 420 mm yr⁻¹ (estimated by precipitation-runoff, Figs. 3-5 and 7), annual evaporated water would be about 0.78, 1.3, 0.32 and 0.25 km³ yr⁻¹ (area × evaporation rate), respectively, for the four watershed; again, very small numbers compared to annual discharge of these rivers.

Despite these uncertainties, compared with the water discharge of 35 to 957 km³ yr⁻¹ in major watersheds (Table 1), changes in groundwater and surface storage appear to have played relatively minor roles in the water budgets of the major Chinese watersheds.

d. Water Withdrawal and Consumption

Since 1950, both water withdrawal and consumption in China have increased ~5-fold and consumption has remained ~55% of withdrawal (Fig.9). In 2000, water consumption was 40, 83, 22, and 33 km³ yr⁻¹ for the Pearl, Yangtze, Yellow and Liao-Songhua, respectively, which translates to basin-averaged consumption 87, 46, 28 and 42 mm yr⁻¹ (Figs. 3c-5c and 7c). For the Yellow River (data from the Water Conservancy Committee of Yellow River) two big increases in consumption resulted from the impounding in the Sanmenxia Dam in 1959 and 1960 (Fig. 5c).

e. Evapotranspiration

Given the minor roles of groundwater and surface-water storage, particularly in southern China, Equation (1) can be simplified to:

$$Q = P - (ET + WC)$$

(2)

from which actual evapotranspiration, the only undocumented parameter in Equation (2), can be calculated:

$$ET = P - (Q + WC)$$

(3)

We are not sure how much of the water consumption is actually lost via evapotranspiration. If WC is mostly from ET loss (which we suspect it is), then it is already contained within the ET term and can be ignored in Equation (3). On the other hand, if some of the WC term derives from processes other than ET (which we find difficult to envision as being significant), the calculated ET would be somewhat greater. Assuming for the moment the former, basin-wide actual evapotranspiration since 1951 shows a decrease of 5% in the Pearl River and 6% in the Yangtze. In contrast, there has been little or no change in the northern watersheds (Figs. 3d-5d and 7d).

4. Discussion

a) Classification of basins and sub-basins

In order to quantify more detailed variations, two largest drainage basins, the Yangtze and Yellow, were divided into four (Upper-1, Upper-2, North and South) and three (Upper-1, Upper-2, and Middle) sub-basins, respectively (Fig. 10b). Sub-basin discharge was calculated by subtracting entering discharge from exiting discharge, and sub-basin runoff therefore was determined by dividing its discharge by area. This calculation, however, should be used with caution. For instance, in the lower part of the Yellow upstream (sub-basin Upper2; Figs. 10 and 11), annual precipitation is only ~200 mm yr⁻¹ (Figs. 1a and 1b) and a large amount of water is withdrawn for farming irrigation. Although before 1980s its exiting discharge (Y2) was generally higher than that entering (Y1), since then increased water withdrawal has decreased discharge through the

sub-basin Upper-2 (Fig. 11), leading to some *negative* sub-basin discharges. Although negative discharge seems to be counter-intuitive, the concept is valid for this paper since it indicates that water consumption stems not only from the sub-basin itself but also water entering from upstream.

Because changes in river runoff can reflect both climatic and anthropogenic forcings, we compared the 50-yr change in runoff with that in precipitation over the same period, classifying these five basins and seven sub-basins into three categories (Fig. 10). In the Pearl and Yangtze, as well as Yangtze sub-basins Upper-1 and Upper-2 and Yellow sub-basin Upper-1, discharge trend closely reflects that of precipitation. Following Milliman et al. (in prep.), we have termed these watersheds as “normal” (Green, Fig. 10). In the lower stream of the Yangtze, Datong Station is the seaward-most station 600 km from the Yangtze mouth, and we assumed the ungauged section downstream of Datong to be “normal” (Fig. 10). In contrast, increase in discharge of Yangtze sub-basin South (+18%) has been considerably greater than the change in precipitation would have predicted (+3%), suggesting that the “excess” (Blue) discharge must come from some other source, i.e decreased evapotranspiration rather than increased precipitation. Yangtze sub-basin North, most parts of the Yellow, Liao and Songhua, in contrast, were termed “deficient” (Red) rivers, as their discharges decreased far more than precipitation would suggest, mainly due, we submit, to increased water consumption.

Suffering an ongoing - and increasing - severe water crisis, the Yellow River is somewhat complex to classify. In sub-basin Upper-2 of the Yellow, post-1980s exiting discharge at times was lower than that entering, leading to a decrease of sub-basin runoff

(exiting-entering) larger than 100% (Fig. 11). Downstream, the Yellow River channel has been elevated to as high as 10 m above ground due to severe channel aggradation of 1 billion tons of sediment eroded annually from the Loess Plateau. Considering its severe water consumption and dry-up days in recent years, lower Yellow should be “deficit”.

b) Actual Evapotranspiration

Evapotranspiration is probably the most perplexing term in the entire water budget. Although climatic models can calculate the potential evapotranspiration (based on temperature, wind, cloudiness etc.) and pan evaporation can be measured in gauging stations, actual evapotranspiration is particularly challenging to quantify. By determining most terms in water budget, we regard actual evapotranspiration as the difference between precipitation and runoff. As such it has decreased in both Pearl (37mm) and Yangtze (32mm) rivers over the past 50 years, which agrees with both reported measured pan evaporation (Liu et al., 2004) and calculated potential evapotranspiration (Thomas, 2000) in China. Some of this decreased evapotranspiration may be related to the $\sim 0.5^\circ$ decrease in temperature (Fig. 2a), but also may be related to decreased solar radiation in response to increased aerosol concentrations (Roderick and Farquhar 2002; Liu et al. 2004).

Despite these variations, annual actual evapotranspiration in all “normal” rivers generally accounts for 50-60% of annual precipitation from 1951 to 2000 (Fig. 12). For the “deficit” rivers, however, actual evapotranspiration is more than 70% of precipitation, particularly in sub-basins Upper2 of Yellow, Songhua and Liao, where >90% of precipitation is lost by evapotranspiration (Fig. 12). In the “excess” southern Yangtze,

evapotranspiration slightly has fallen below the “normal” dashed line, reflecting decreased evapotranspiration trend in the past 50-yr (Fig. 12).

c) Dam Construction and Water Consumption

Since 1950s, anthropogenic activities have increased dramatically in the major Chinese watersheds, particularly through dam construction and water consumption. Total dams in China have increased from only a few in 1950s to about 86,000 in 2000 (Fuggle et al., 2000). In northern China, 3,150 dams on the Yellow River decreased its runoff significantly, particularly with the impounding of the Sanmenxia Dam in 1960 (Fig. 5). The dams on the Liao also decreased the runoff greatly after 1965, but since 1985 runoff had increase somewhat, presumably due to the filling-up of reservoirs (Fig. 7). In contrast, ~50,000 dams on the Yangtze and 13,700 dams on the Pearl appeared to have had little impact on river runoff (Figs. 3 and 4).

Both water withdrawal and consumption in China have increased to about 5-fold in the past 50 years (Fig. 9) because of doubling of population as well as increased irrigation and industrial activity. While decreased precipitation can partly explain the decreased runoff in northern China, increased water consumption appears to have been far more important. In the Yellow River, for example, pre-dam runoff in 1951-55 averaged 67 mm yr^{-1} . Based on Fig. 10a, the 11% decrease in 1951-2000 precipitation would have resulted in ~17% of drop in runoff, leading to a runoff of 56 mm yr^{-1} in 2000. In fact, average runoff in 1996-2000 was only 12 mm yr^{-1} , suggesting that 44 mm yr^{-1} (or 80% of the decreased runoff) was related to water consumption and other anthropogenic activities. Although water consumption within the Yangtze watershed actually has been greater than in the Yellow River ($83 \text{ vs. } 22 \text{ km}^3 \text{ yr}^{-1}$), Yangtze consumption represents

<10% of its annual discharge ($957 \text{ km}^3 \text{ yr}^{-1}$) whereas consumption along the Yellow River has been >60% of its annual discharge ($35 \text{ km}^3 \text{ yr}^{-1}$). This helps explain why the water crisis has been much more severe in northern than southern China.

5. Conclusions

Between 1951 and 2000, dramatic decreases (80% and 52%) of runoff were noted for the Yellow and Liao rivers, respectively, due to decreased precipitation and more importantly increased water consumption. Calculated actual evapotranspiration decreased by 4-6 % in the Pearl (37 mm) and Yangtze (32 mm) watersheds, whereas there was no apparent change in the northern rivers. Sub-basin water budgets indicated that “excess” flow in southern Yangtze was caused by decreased temperatures and evapotranspiration whereas the northern Yangtze, Yellow, Liao and Songhua were considered “deficit” rivers primarily due to increased water consumption. With nearly 85,000 dams presently on Chinese rivers and more under construction or being planned, increased water consumption – the combination of increased population pressures and economic activity - together changing evapotranspiration, may well exacerbate the water crisis in these major Chinese watersheds, particularly in northern China where precipitation has been declining over the past half century.

Acknowledgements

Thanks Z. Yang for the water consumption data of the Yellow River. This paper is supported by the US National Science Foundation (NSF) and Office of Naval Research

(ONR). This paper is Contribution No.xxxx of the Virginia Institute of Marine Science, the College of William and Mary.

References

- Bulletin of Chinese Rivers and Sediments, 2000, 2001, 2002, Changjiang (Yangtze) Water Resources Commission, Ministry of Water Resources of the People's Republic of China (in Chinese).
- Bulletin of Water Resources in China, 1997-2002, Ministry of Water Resources of the People's Republic of China, website: <http://sdinfo.chinawater.net.cn/index.asp> (in Chinese).
- Changjiang Sediment Bulletin, 2000, 2001, Changjiang (Yangtze) Water Resources Commission, Ministry of Water Resources of the People's Republic of China, website: <http://www.cjw.com.cn/> (in Chinese).
- Chen, M., D. Pollard, and E. J. Barron, 2005: Hydrologic processes in China and their association with summer precipitation anomalies. *Journal of Hydrology*, **301**, 14-28.
- Chen, Z., J. Li, H. Shen, and Z. Wang, 2001a: Yangtze River of China: historical analysis of discharge variability and sediment flux. *Geomorphology*, **41**, 77-91.
- Chen, X., Y. Zong, E. Zhang, J. Xu, and S. Li, 2001b: Human impacts on the Changjiang (Yangtze) River basin, China, with special reference to the impacts on the dry season water discharges into the sea. *Geomorphology*, **41**, 111-123.
- Fuggle, R., W. Smith, H. C. Inc., and A. C. Inc., 2000: *Large Dams in Water and Energy Resource Development in The People's Republic of China (PRC)*. Country review

paper prepared as an input to the World Commission on Dams, Cape Town, www.dams.org.

Gleick, P. H., 1993: *Water in Crisis: A Guide to the World's Fresh Water Resources*.

Oxford University Press, 504pp.

——, 2000: *The World's Water 2000-2001: The Biennial Report on Freshwater Resources*. Island Press, Washington, D.C.

Heilig, G. K., 1999: *China Food. Can China Feed Itself?* International Institute for Applied Systems Analysis (IIASA), Laxenburg.

Huang, R. and W. Chen, 2002: Recent Progresses in the Research on the Interaction between Asian Monsoon and ENSO Cycle. *Climatic and Environmental Research*, **7**, 146-159.

Liu, B., M. Xu, M. Henderson, and W. Gong, 2004: A spatial analysis of pan evaporation trends in China, 1955-2000. *Journal of Geophysical Research*, Vol. 109 D15102.

Milliman, J.D., C. Smith, P.D. Jones, K.L. Farnsworth and K.H. Xu, in prep. Climatic and anthropogenic factors in changing river discharge to the global ocean.

Menon, S., J. Hansen, L. Nazarenko, and Y. Luo, 2002: Climate Effects of Black Carbon Aerosols in China and India. *Science*, **297**, 2250-2253.

Ren, L., M. Wang, C. Li, and W. Zhang, 2002: Impacts of human activity on river runoff in the northern area of China. *Journal of Hydrology*, **261**, 204-217.

Roderick, M. L. and G. D. Farquhar, 2002: The Cause of Decreased Pan Evaporation over the Past 50 Years. *Science*, **298**, 1410-1411.

Shiklomanov, I. A., 1999: *World Water Resources and Their Use*. State Hydrological Institute (SHI), Russia, St. Petersburg.

- Shiklomanov, I. A. and J. C. Rodda, 2003: *World Water Resources at the Beginning of the Twenty-First Century (International Hydrology Series)*. Cambridge University Press, 435pp.
- Simmonds, I., D. Bi and P. Hope, 1999: Atmospheric water vapor flux and its association with rainfall over China in summer. *Journal of Climate*, **12**, 1353-1367.
- Thomas, A., 2000: Spatial and temporal characteristics of potential evapotranspiration trends in China. *International Journal of Climatology*, **20**, 381-396.
- Wang, H., 2002: Instability of the East Asian Summer Monsoon-ENSO Relations. *Advances In Atmospheric Sciences*, **19**, 1-11.
- Wang, S., J. Zhu, and J. Cai, 2004: Interdecadal Variability of Temperature and Precipitation in China since 1880. *Advances In Atmospheric Sciences*, **21**, 307-313.
- Xu, J., 2002: Implication of relationships among suspended sediment size, water discharge and suspended sediment concentration: the Yellow River basin, China. *CATENA*, **49**, 289-307.
- Yang, Z. S., J. D. Milliman, J. Galler, J P, and X. G. Sun, 1998: Yellow River's water and sediment discharge decreasing steadily. *Eos, Transactions, American Geophysical Union*, **79**, 589-592.

Table 1 Precipitation and runoff of five watersheds in China

River	Total area (10 ⁴ km ²)	Station	Area above stations in 10 ⁴ km ² (percentage to total area)	Average annual Precipitation (mm/yr)	Change of precipitation (%)	Average annual runoff (mm/yr)	Change of runoff (%)	Average annual water discharge (km ³ /yr)	R ² of correlation between precipitation and runoff
Songhua	55.7	Haerbin	39.0 (70%)	521	-4	113	-13	63	0.63
Liao	22.0	Tieling	12.1 (55%)	505	-8	28	-52	6	0.56
Yellow	79.5	Lijin	75.2 (95%)	442	-11	45	-80	35	0.40
Yangtze	180.0	Datong	170.5 (95%)	1045	-1	532	+5	957	0.81
Pearl	45.4	Gaoyao, Shijiao, Boluo	41.5 (91%)	1469	+3	691	+9	313	0.72

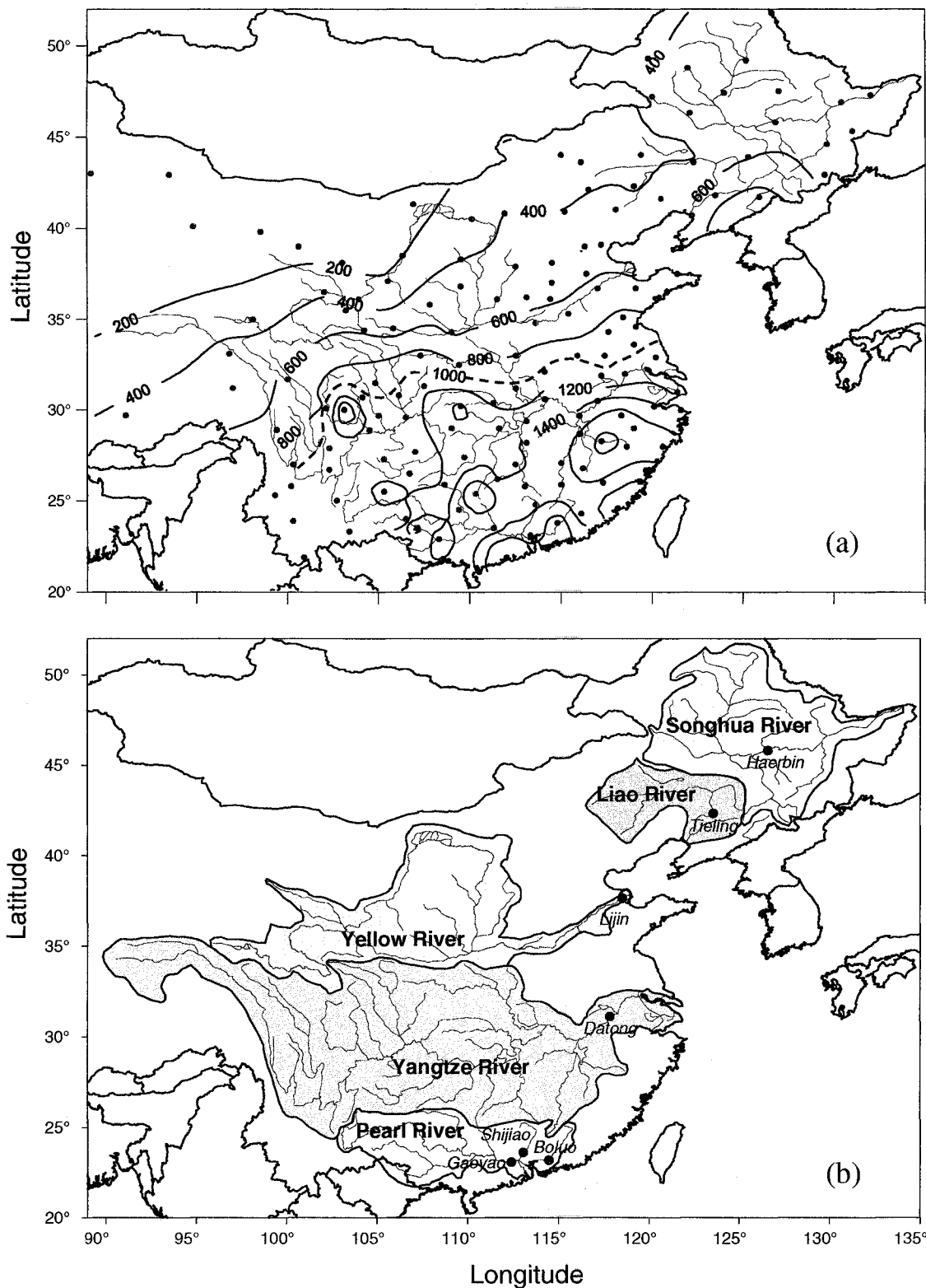


Fig. 1 Isohyet and major watersheds in China. (a) Isohyet. Meteorological stations are red dots and 1000-mm isohyet (blue dash line) can be regarded as the division line between dry northern and wet southern China. (b) Five major watersheds. Downstream-most hydrological stations are black dots.

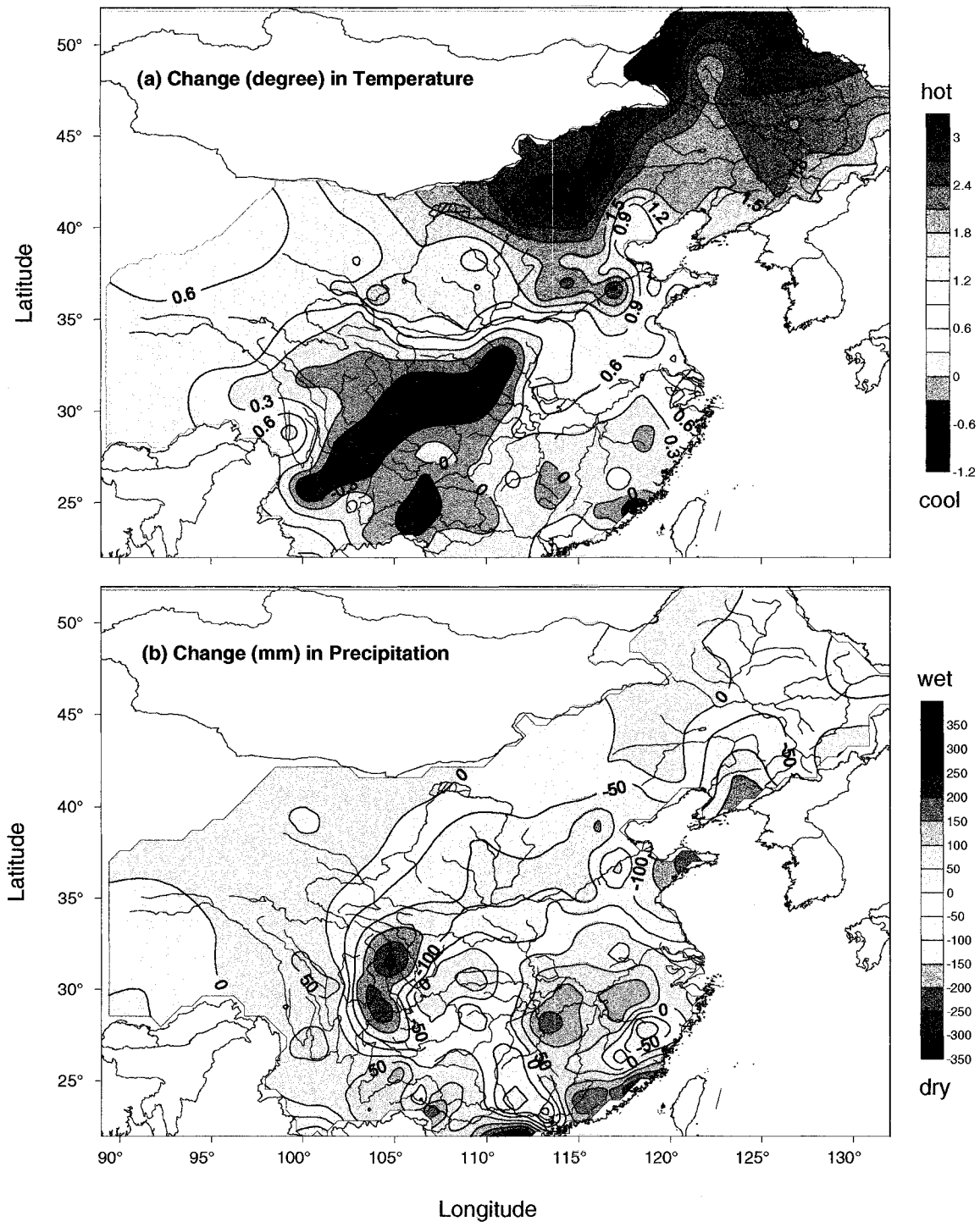


Fig. 2 Temperature (a) and precipitation (b) changes from 1951 to 2000. Temperature and precipitation datasets were released by China Meteorological Administration, collected from 160 meteorological stations throughout China. See Fig. 1a for locations of stations.

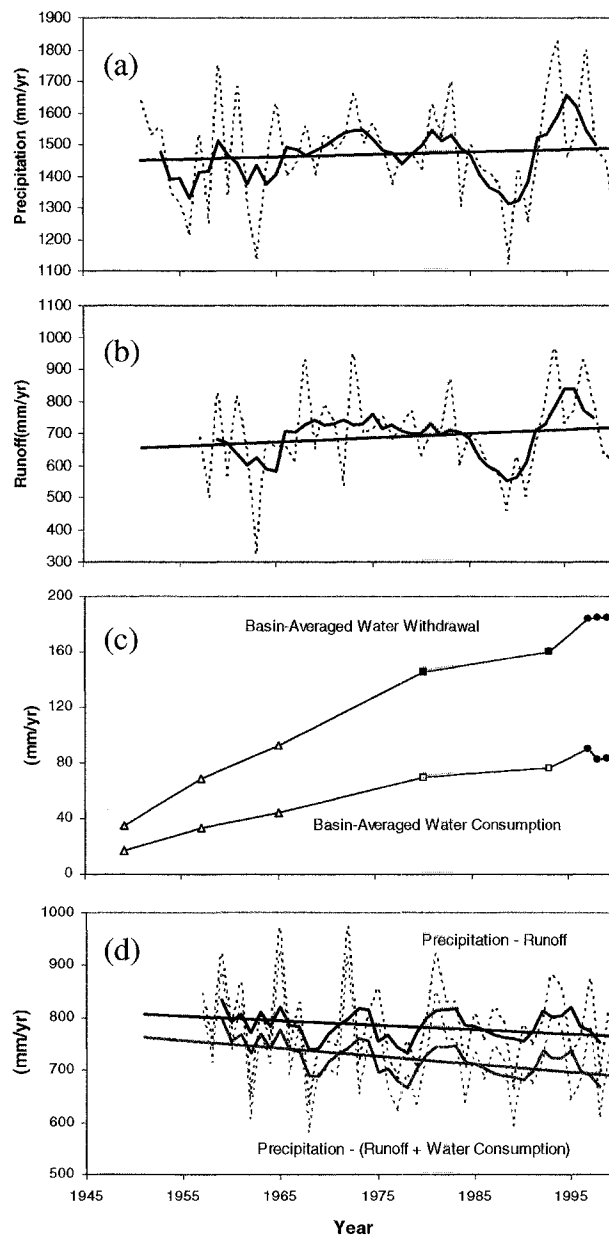


Fig. 3 Precipitation, runoff, and water consumption of the Pearl River. In (a), (b) and (d), dashed lines are annual data whereas bold lines are running 5-yr means. In (c), solid circles are from Bulletin of Water Resources in China (1997- 2000); solid squares are from Heilig (1999). Open triangles and squares are calculated using the percentages of watershed to total China withdrawal, and the percentages of consumption to withdrawal, see detailed explanation in *Section 2*.

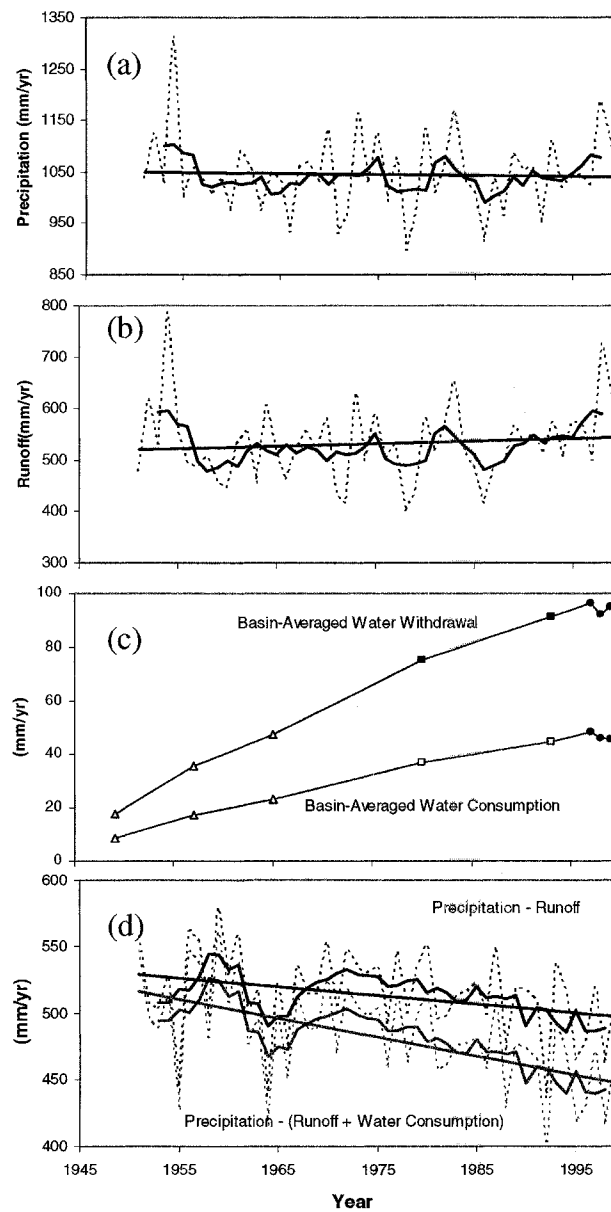


Fig. 4 Precipitation, runoff, and water consumption of the Yangtze River. See explanation in Fig. 3

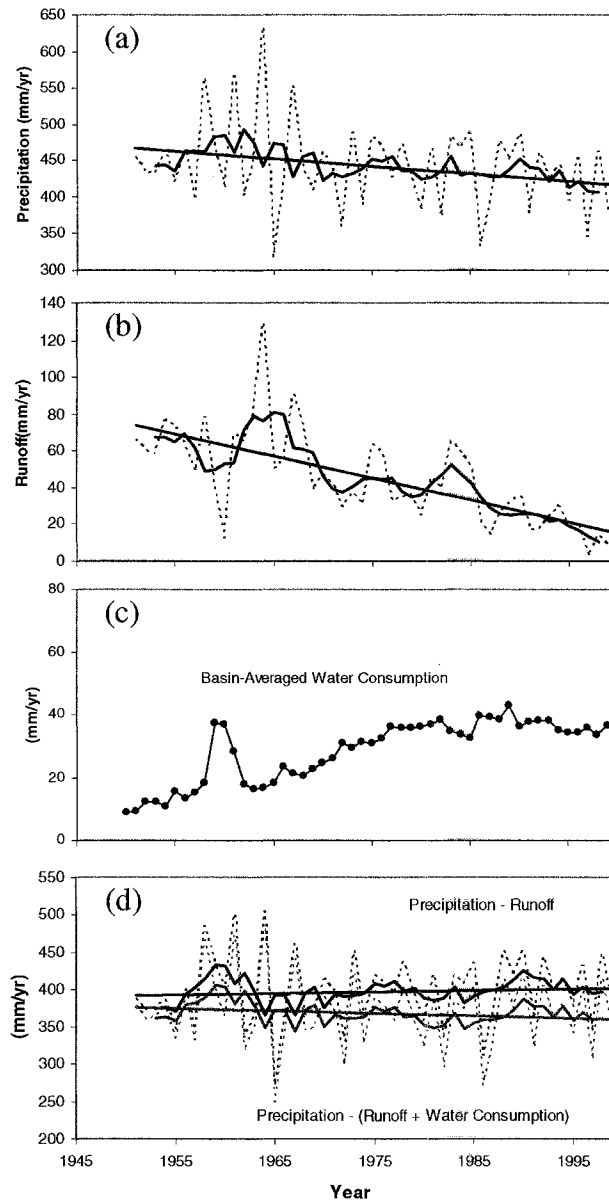


Fig. 5 Precipitation, runoff, and water consumption of the Yellow River. See explanation in Fig. 3

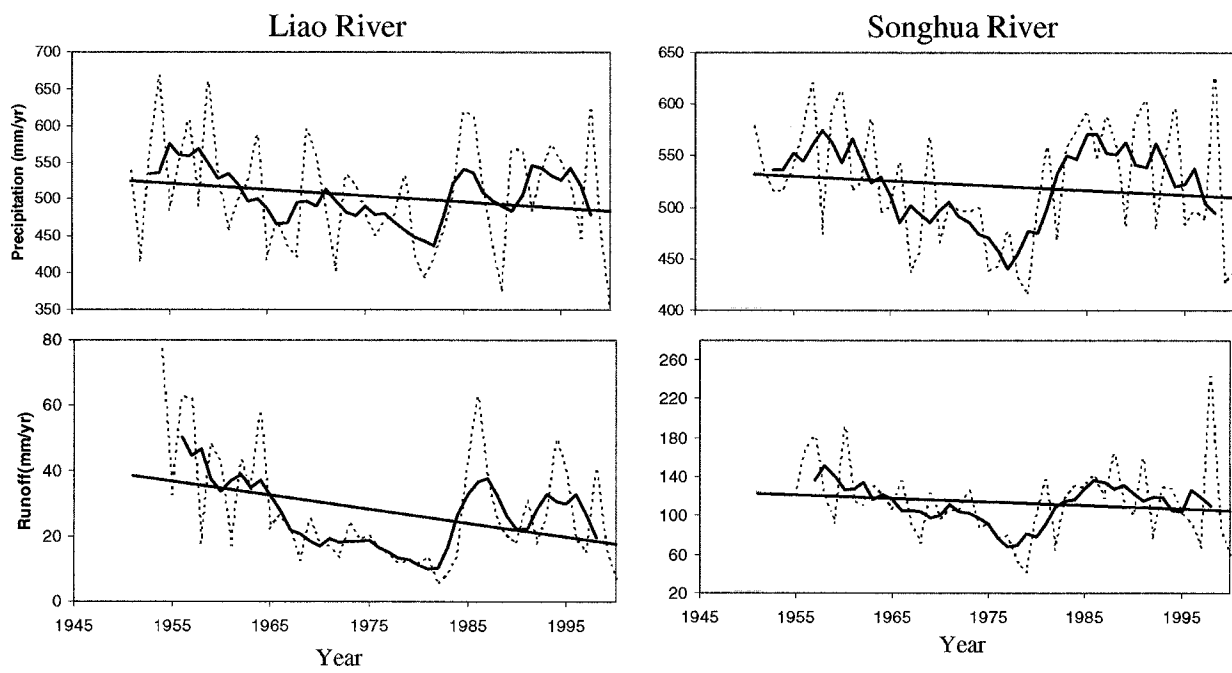


Fig. 6 Individual precipitation and runoff of the Liao River and Songhua River. See explanation in Fig. 3

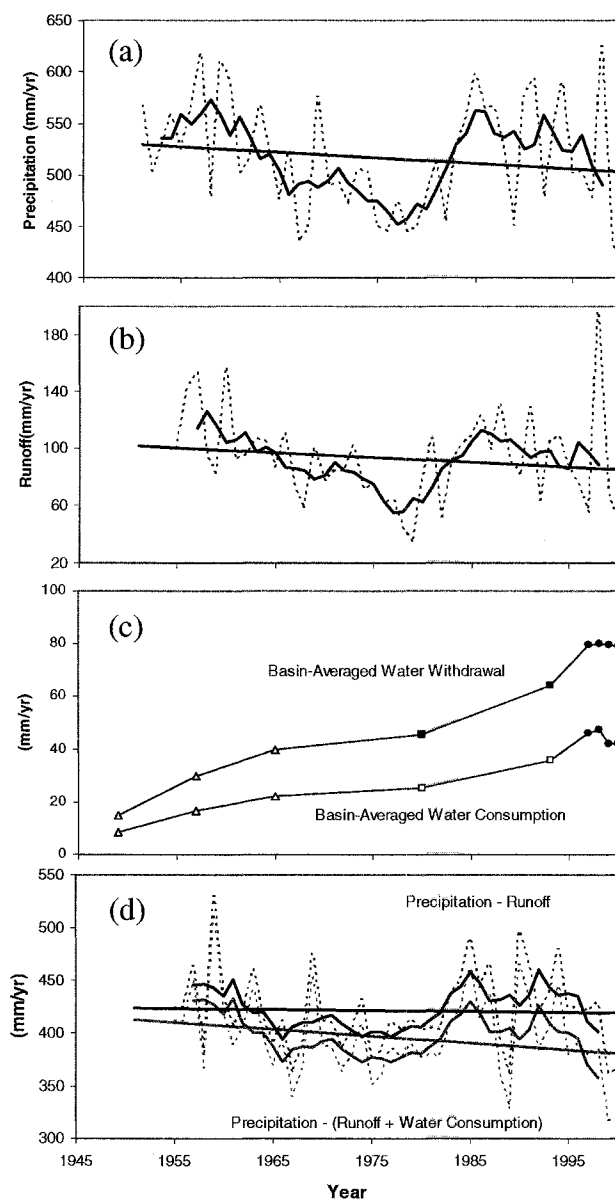


Fig. 7 Precipitation, runoff, and water consumption of the Liao-Songhua rivers
See explanation in Fig. 3

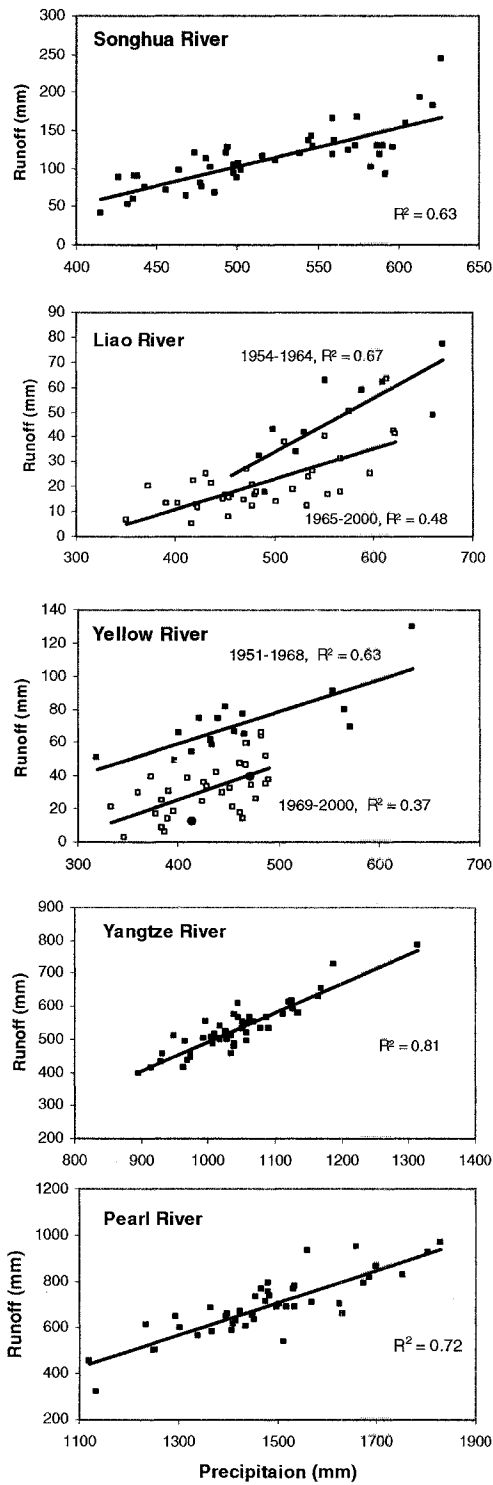


Fig. 8 Relation between precipitation and runoff of Chinese rivers. For the Yellow and Liao rivers, open and solid squares indicate the pre-dam and post-dam periods. Two impounding years (solid circles) of Sanmenxia Dam (1959-60) are excluded from the pre-dam period in the Yellow River.

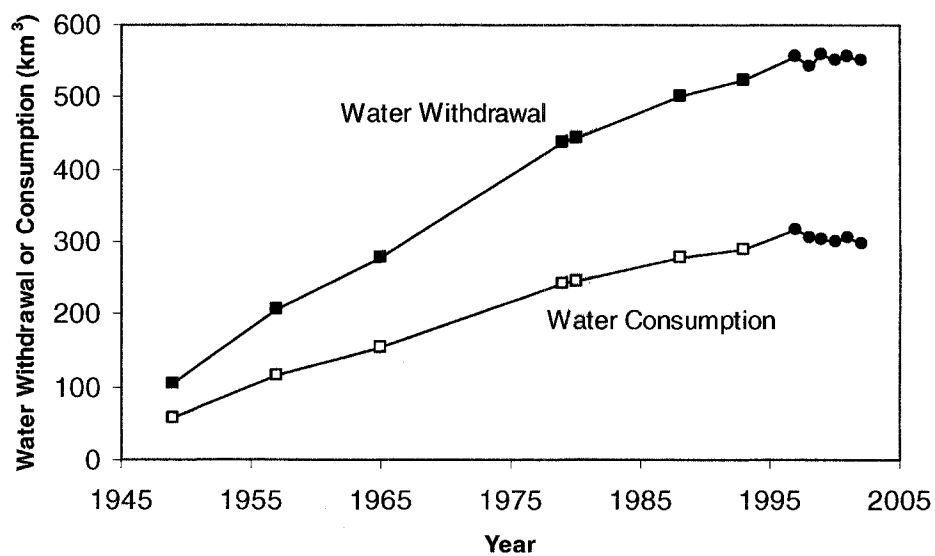


Fig. 9 Total water withdrawal and consumption in China from 1949 to 2002. Solid circles are from Bulletin of Water Resources in China (1997- 2002); solid squares are from Ren et al. (2002). Open squares are calculated assuming a constant ratio of consumption to withdrawal equal to the mean ratio in 1997-2002.

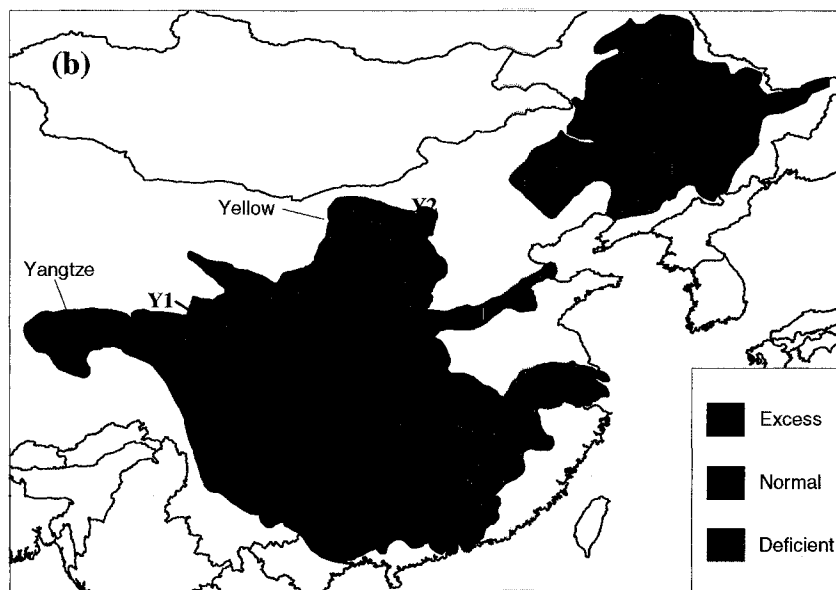
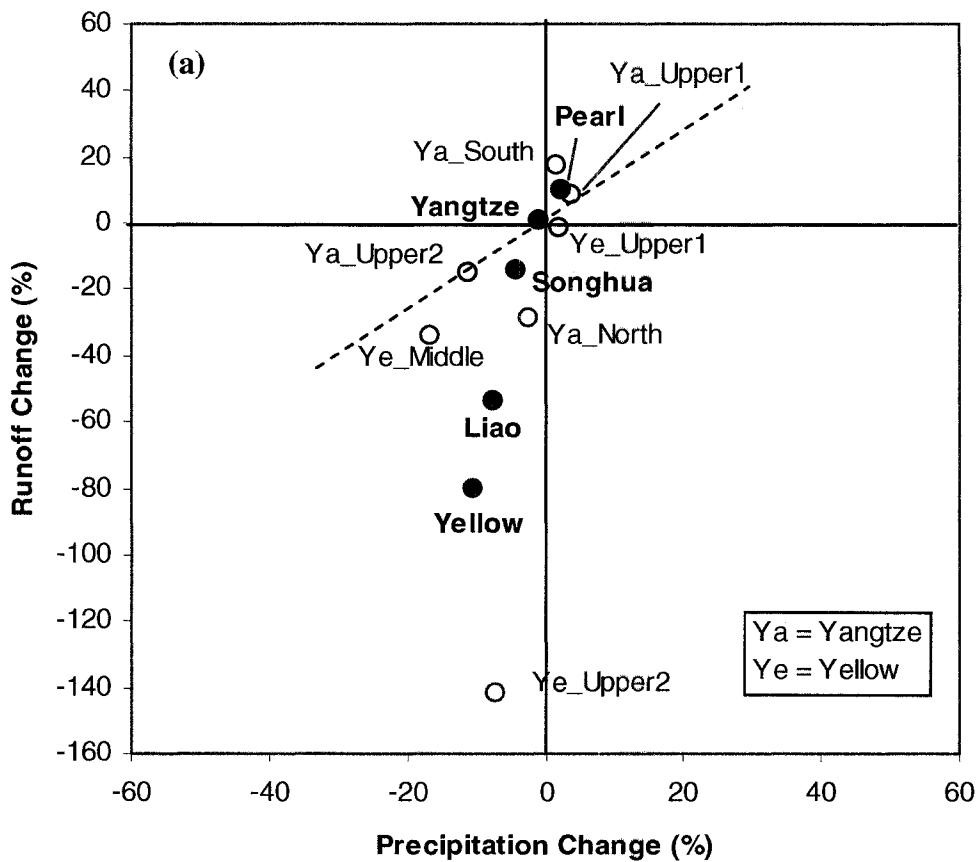


Fig. 10 (a) Comparison of change (%) in precipitation and runoff and (b) classification of major Chinese watersheds. In (a), solid circles are for basins and open circles represent sub-basins. For the sub-basin Upper2 in the Yellow, its exiting water discharge (Y2) is lower than its entering (Y1) in some years after 1980 mainly due to severe water consumption, causing a -140% decrease.

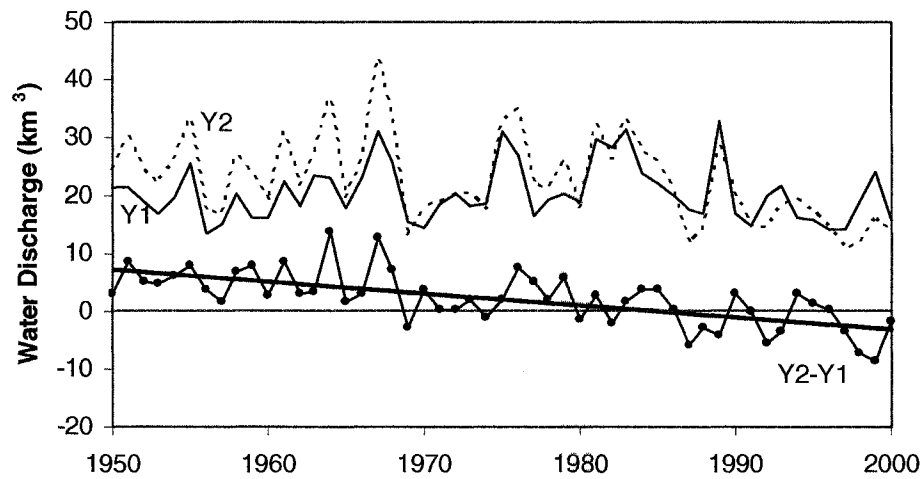


Fig. 11 Water discharges in stations entering and exiting the sub-basin Upper2 in the Yellow. See Fig. 10 for locations and *Section 4* for details

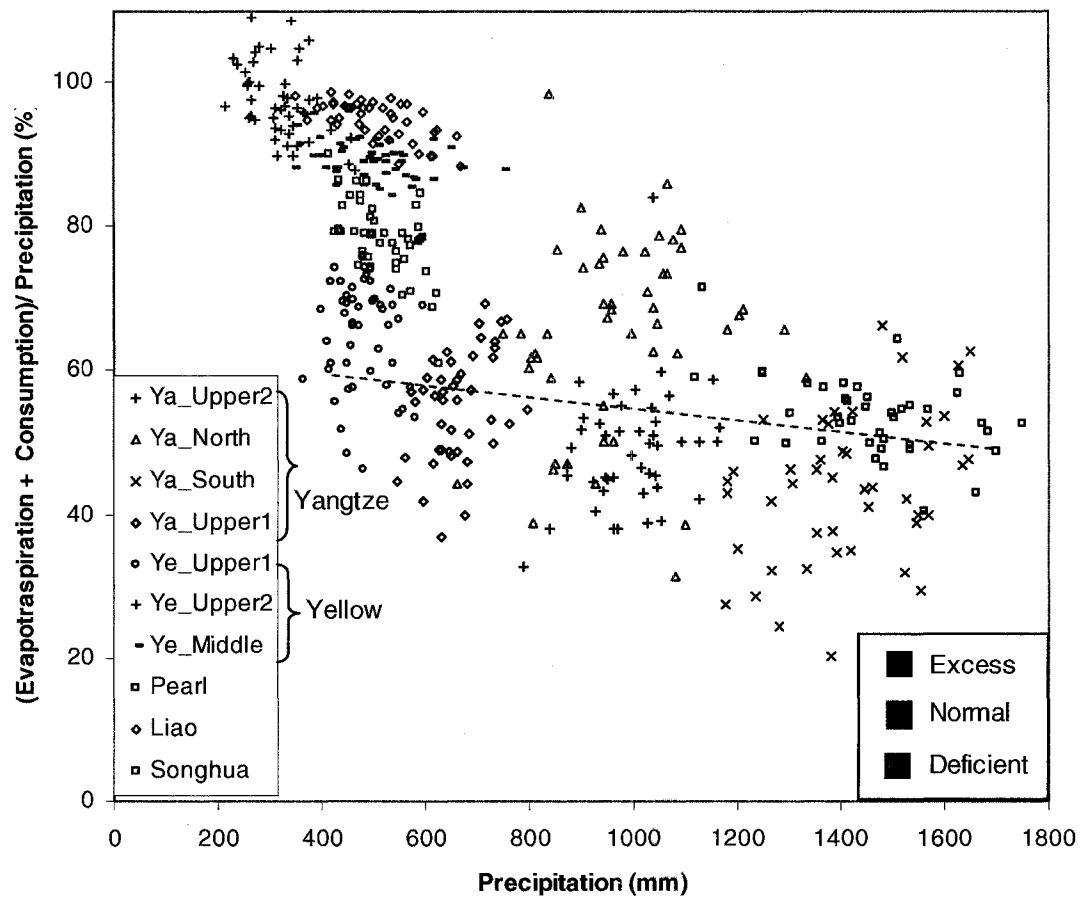


Fig. 12 Comparison of precipitation with the ratio of evapotranspiration and consumption to precipitation in Chinese watersheds. See Fig. 10 for the locations of sub-basins.

CHAPTER 3: Climatic and Anthropogenic Impacts on the Water and Sediment Discharge from the Yangtze River (Changjiang), 1950-2004*

Kehui Xu^{a,†}, John D. Milliman^a, Zuosheng Yang^b and Hui Xu^c

^a 1208 Greate Rd, Virginia Institute of Marine Science, College of William & Mary, Gloucester Point, VA.23062, USA;

^b College of Marine Geosciences, Ocean University of China, Qingdao 266003, People's Republic of China;

^c Institute of Atmospheric Physics, Chinese Academy of Sciences, Beijing 100029, People's Republic of China;

[†] Corresponding author. Tel.: +1-804-684-7739; Fax: +1-804-684-7250; E-mail: kxu@vims.edu

*Prepared for *Journal of Hydrology*

Abstract

Since the 1980s, the Yangtze River (Changjiang) sediment load has declined dramatically, although water discharge has remained relatively constant. Sediment loads in 2004 at Yichang (just below the Three Gorges Dam - TGD) and Datong (lower stream) were only 12% and 33% of those in the 1950s and 60s, primarily reflecting precipitation decline in a high-yield watershed (Jialing), landuse change, and most importantly, construction of >50,000 dams throughout the entire Yangtze watershed. Following impoundment of the TGD, the annual sediment load at Yichang dropped by 164 million tons (mt), but during the preceding 16 years it had decreased by nearly twice as much (~300 mt/yr). Throughout the entire basin, the most significant declines in sediment load (>80%) occurred in two northern tributaries (Jialing and Han), one southern tributary (Zishui), as well as two passages between mainstream and the shrinking Dongting Lake. The role of the Dongting Lake to act as a flood buffer has declined dramatically, putting the middle stream under severe flood pressure. Ongoing and proposed dams (collectively larger than TGD) and North-South river diversions will further impact the Yangtze, probably endangering the Yangtze delta in the near future.

Key Words: Yangtze River, Precipitation, Water, Sediment, Dams

1. Introduction

Rivers form the major link between land and the ocean, particularly through their transfer of water and sediment. Fluvial discharge to the oceans, however, is unevenly

distributed in both space and time, in large part influenced by both climatic (e.g., precipitation) and anthropogenic (e.g., deforestation and dam construction) forcings.

The global water system has been greatly impacted by humans (Vorosmarty et al., 2003), and more than half of the world's large river systems are presently affected by dams or water diversions (Syvitski et al., 2005; Nilsson et al., 2005). Considering projected climate change and growing demographic pressures, freshwater availability and quality have become an increasing concern (Gleick, 1993, 2000; Shiklomanov and Rodda, 2003). Nowhere is water concern more acute than in southern Asia, where water withdrawal increased ~4 times between 1950 and 2000 (Shiklomanov, 1999) in response to accelerating demographic demands. China and India alone account for more than 40% of the global freshwater used for irrigation (Gleick, 2000), and since 1950 China has built almost half of world's large dams (Fuggle et al., 2001).

Historically, terrestrial erosion has accelerated in response to deforestation and land cultivation, but in recent years sediment delivery from many rivers has decreased due to reforestation and dam construction. Construction of Colorado River dams and the Nile's Aswan Dam (together with an extensive irrigation system downstream from the dam) in the 1930s and 1960s resulted in almost total elimination of these rivers' sediment loads, subsequently leading to delta recession (Carriquiry et al., 2001; Stanley and Warne, 1998). In the Yellow River the impact from dam construction has been amplified greatly by decreased precipitation and increased water consumption, such that water and sediment discharges are <~15% of 1950-60s levels, and its once-prograding delta is now eroding (Chu et al., 2006).

The Yangtze River (Changjiang, Fig. 1), home to 400 million inhabitants, has >50,000 dams (Yang et al., 2006) within its watershed, making it one of the most highly regulated rivers in the world (Nilsson et al., 2005). Climate change in the Yangtze has caused rapid snow melt in the headwaters (Wu, 2000; Chen et al., 2001a; Cyranoski, 2005), significant regional precipitation drops (-200 mm) in northern tributaries, as well as more frequent and extreme floods in recent years (e.g., Menon et al., 2002; Xu et al., 2005). Since 1950s, various anthropogenic activities also have impacted the Yangtze. Water withdrawal and consumption of the Yangtze have expanded to ~4 times due to a doubling of population and increased irrigation (Ren et al., 2002). Beginning in 1988, the Project of Yangtze Water and Soil Conservation has decreased the sediment load greatly in the upstream. Presently there are more than 50,000 dams throughout the Yangtze drainage basin, including the world's largest - Three Gorges Dam (TGD), whose impoundment began in June 2003.

Under these diverse climatic and human impacts during the past 55 years, Yangtze water discharge has changed little in both upper and lower streams (at Yichang and Datong stations, respectively; Fig. 1) whereas sediment loads in 2004 at these two stations were only 12% and 33% of their loads in the 1950s-1960s (Fig. 2; Bulletin of Yangtze Sediment, 2000-2004). Considering the full operation of TGD in 2009, the degree to which the TGD will threaten downstream and coastal ecosystems has become an acute concern (Shen and Xie, 2004; Xie, 2003). Plans for future large dams along the mainstream, together with the proposed South-North water diversions to the northern China, almost surely will accentuate any negative impacts.

All of above indicates that the Yangtze has been and will continue to be impacted by anthropogenic activities as well as any future climate change. In this paper we discuss the temporal and spatial variations of water and sediment fluxes along the entire Yangtze watershed from 1950 to 2004, and attempt to quantify the river's responses to these impacts. Specifically, how have local and basin-wide runoff and sediment responded to climatic (e.g., precipitation) as opposed to anthropogenic (e.g., dam construction and reforestation) forcings, how (and why) has the sediment budget changed regionally as well as within the entire Yangtze basin, and finally, given the recent changes within the watershed, what can we expect in the future and what will be the coastal responses to these changes?

2. Physical setting

Draining a watershed of $\sim 1.8 \times 10^6 \text{ km}^2$, the largest in southeastern Asia, the Yangtze River (Fig. 1) is frequently cited as one of the world's largest rivers in terms of both water discharge (5th; $\sim 900 \text{ km}^3/\text{yr}$) and sediment load (4th; ~ 480 million tons per year, mt/yr) (Milliman and Meade, 1983; Milliman and Syvitski, 1992). With headwaters in the Qinghai-Tibet Plateau ($\sim 5400 \text{ m}$ elevation), the Yangtze drains high mountains and cuts steep valleys in its upper reaches (above Yichang, Fig. 1), meanders through low-gradient alluvial plains, before debouching into the East China Sea (ECS) (Chen et al., 2001b). Numerous tributaries connect to the main stream, including four from the north and ten (mostly converging at Dongting and Poyang lakes) from the south (Fig. 1).

Annual precipitation rapidly increases from the northwest (headwaters, $<400 \text{ mm}/\text{yr}$) to the southeast (lower stream, $>1600 \text{ mm}/\text{yr}$), with a basin-wide average of ~ 1050

mm/yr (Fig. 3). The Yangtze has a typical monsoonal regime, with a wet season (March-August in the middle and lower sections; May-September further upstream) when more than 60% of annual precipitation falls (Shi et al., 1985). At Datong Station, the seaward-most gauging station along the river (Fig. 1), about 70% of water and 85% of sediment load are discharged between May and October (Chen et al., 2001b).

3. Data and Methods

Monthly precipitation data (1951-2000) from 47 meteorological stations throughout the Yangtze watershed were extracted from a 160-station precipitation dataset released by Ministry of Meteorology in China (crosses, Fig. 3). After interpolation and gridding in Golden Surfer program, the regional and basin-wide annual average precipitation was determined. Precipitation trends and the correlation coefficients (R^2) between precipitation and runoff were calculated using linear regression analysis.

Water and suspended sediment discharges were obtained primarily from the Bulletin of Yangtze Sediment in 2000-2004 (Website: <http://www.cjh.com.cn/>, in Chinese), Changjiang Water Resources Commission, as well as published papers (Shi et al., 1985; Higgitt and Lu, 1996; Deng and Huang, 1997; Pan, 1997; Lu and Higgitt, 1998; Chen et al., 2001b; Shen et al., 2001; Yang et al., 2002; Zhang and Wen, 2004). Runoff was then calculated by dividing water discharge by its corresponding drainage basin area. Annual water and sediment discharges from 23 gauging stations were collected to analyze their trends from 1951 to 2000. Monthly data from three mainstream stations (Yichang, Hankou and Datong, Fig. 1) since 1950, as well as the stations entering and exiting the TGD in 2003-04, also were gathered. Upstream sediment-yield data were

compiled from Liu and Zhang (1991) and Dai and Tan (1996). Water withdrawal/consumption data were taken from the Bulletin of Water Resources in China (1997-2002), Heilig (1999), Shimokologov (1999), and Ren et al. (2002).

4. Spatial Variations of Water and Sediment

Based on runoff, sediment yield and concentration patterns, the Yangtze drainage basin can be divided into seven distinct sub-basins (Fig. 4); an eighth, upstream from Datong, incorporates 94% of the entire drainage basin (grey region, Fig. 4). Runoff directly reflects precipitation, with the lowest rate in the headwaters (sub-basin Upper 1_a, 200 mm/yr) and highest rates in southern tributaries flowing into Dongting and Poyang lakes (sub-basins South_b and South_c, ~800 mm/yr). In contrast, sediment concentrations are high in the upstream and northern tributaries (e.g., 2300 g/m³ in sub-basin Upper 1_b) due to steep valley and erodible soil, but average only 100 g/m³ in the Poyang tributaries (sub-basin South_c).

Based on long-term means from 37 stations throughout the drainage basin, spatially, the Yangtze's sediment load (Fig. 5a) increases slightly in the headwaters, downstream of which large inputs from tributaries (particularly from the Jialing River, Fig. 1) result in a peak load at Yichang (~500 mt/yr). Trapping in Dongting Lake and lateral escape onto the alluvial plains decrease the load to ~435 mt/yr at Datong. Due to channel aggradation downstream of Datong (600 km from the river mouth), the Yangtze is estimated to export ~370 mt/yr to the East China Sea (Shen et al., 2001).

5. Temporal Variations of Water and Sediment

5.1. Water (*Precipitation and Runoff*)

The 1951-2000 precipitation trend (Fig. 6) show that the southeast became wetter (+100 mm) whereas some upper reaches (mainly in the Jialing and Min tributaries, Fig.1) became drier (-200 mm). To maintain consistency to compare precipitation and runoff (Figs. 4 and 7), two upstream sub-basins (Upper1_a and Upper1_b) were combined into “Upper1” and three southern sub-basins (South_a, South_b and South_c) were combined as “South”. Sub-basins Upper1 and South showed slightly increased precipitation whereas there was a significant drop in Upper2 (-11.3%) and a small decline in North (Fig. 7). Despite these local variations, basin-wide (i.e. above-Datong) precipitation changed little over the 55-yr period.

In correspondence to precipitation, runoff increased in Upper1 and South but decreased in Upper2 and North (Fig. 7). The decrease of runoff (-25.7%, -100 mm) in sub-basin North, however, far exceeded that of precipitation (-2.5%, -24 mm). In contrast, runoff increase (18.6%, 134 mm) in sub-basin South was larger than that of precipitation (1.8%, 25 mm), although correlation between the two was close ($R^2 = 0.82$) (Fig. 7). Above-Datong runoff trend reflected precipitation ($R^2 = 0.83$) but neither showed a significant change.

5.2. Water Impact on Sediment

Occurring in the high sediment-yield (>500 t/km²/yr) area near the Jialing and Min tributaries (Fig. 6), sub-basin Upper2 experienced the greatest decrease in precipitation between 1950 and 2004 (-11.3%; Fig. 7). In Upper2, annual precipitation correlated with runoff ($R^2 = 0.56$) during 1956-2004 (Fig. 8a) as did runoff and sediment load between

1956 and 1985 (Fig. 8b). Since 1986, however, sediment load has declined significantly. Based on the runoff-sediment correlation in 1956-85 (Fig. 8b), post-1986 sediment loads (blue line, Fig. 8c) can be calculated assuming a similar sedimentary setting to 1956-85. Accordingly, the sediment load appeared to have decreased 80 mt, from 220 mt/yr in 1956 to 140 mt/yr in 2004 mainly due to decreased precipitation (dashed line for “climatic impact”, Fig. 8c). The difference between the calculated (blue line) and measured (red line) loads in 1986-2004 (grey region, Fig. 8c) can be regarded as the sediment decline due to dam construction and reforestation, which will be discussed later.

5.3. *Sediment*

Throughout the entire drainage basin, sediment loads have decreased at all stations except for some minor increases in three tributaries discharging into Poyang Lake (open dots, Fig. 9). The most significant sediment drops (>80%, largest solid dots, Fig. 9) occurred in two northern tributaries (Jialing and Han), one southern tributary (Zishui), as well as two passages between Yangtze mainstream and Dongting Lake (see Fig. 1 for locations). Rather than the sharp drops noted on the Jialing (in 1986), Han (1968), and Zishui (1958) tributaries, however, declines at the two passages have been more gradual (Fig. 9). Tributary declines generally have been seen along the mainstem of the river: e.g., an 80-mt reduction at the Han in 1968 corresponded with that in Datong, and 100-mt decrease of the Jialing in 1986 led to corresponding drops in both Yichang and Datong (Fig. 9). Between 1980s and 2002, Yichang sediment has decreased ~300 mt relative to its levels in 1950s-1960s, followed by a 164-mt drop due to the impoundment of TGD in June 2003 (Figs. 2 and 9; Xu et al., 2006).

The 2003-04 Yangtze sediment budget shows the Yangtze has changed dramatically since the 1950s and 60s (Fig. 5). Major sediment inputs, including Jialing and Han, as well as passages entering and exiting the Dongting Lake (big arrows in Fig. 5a), all have been sharply reduced (Fig. 5b). An obvious sediment drop (~240 mt) upstream of the TGD primarily reflects a decline from the Jialing due to decreased precipitation and reforestation, together with a drop along the above-Pingshan (Fig. 1) mainstream mainly caused by dam construction (Xu et al., 2006).

5.4. Monthly Variations of Water and Sediment

Yangtze monthly water and sediment (Fig. 10) show typical seasonal variations: about 70% of water and 85% of sediment are discharged during flood season (May to October) in upper, middle and lower streams (at Yichang, Hankou and Datong, respectively; Fig. 1). Seasonal variations in sediment discharge are particularly extreme, January loads generally being less than 5% of the peak loads in July.

From 1950 to 2002, monthly water discharge showed no dramatic changes along the main stream of the Yangtze. In 2003-04, the Three Gorges Dam (TGD) impoundment dropped water discharges in the upper and middle streams in August, but there was minor change in the lower stream (Datong, 1200 km downstream of TGD) (Fig. 10). Monthly sediment loads in 1986-2000 at all three stations were slightly smaller than these in 1950-85, but they decreased dramatically in 2001-02 and 2003-04 (Fig. 10). Primarily due to TGD trapping, Yichang (downstream of TGD) sediment load in August of 2003-04 was only <10% of its natural load in 1950-85.

Two additional gauging stations, immediately downstream and upstream of the 500-km-long reservoir above TGD, can be used to delineate the amount of water and

sediment lost by the dam. Differences between these two monitoring stations indicate a seasonal pattern in sediment trapping in TGD since June 2003 (Fig. 11), during which the TGD trapped 124 and 102 mt sediment in 2003 and 2004, respectively, with sediment trapping ratios (trapped/entered) of ~60%.

6. Discussion

6.1. Climatic Impacts

In a natural hydrological regime, runoff is the difference between precipitation and the sum of evapotranspiration and storage. Comparing precipitation with runoff, southern Yangtze (sub-basin South, Fig. 7) shows a much greater increase in runoff (134 mm) than in precipitation (25 mm), inferring that evapotranspiration must have decreased. This generally agrees with both measured pan evaporation (Liu et al., 2004) and calculated potential evapotranspiration (Thomas, 2000) in China. The decrease in runoff (-100 mm) in northern Yangtze (sub-basin North, Fig. 7), in contrast, was ~4 times the decrease in precipitation (-24 mm), reflecting increased water consumption, presumably by the ways of dam impoundment and water diversion.

Precipitation, especially heavy rains, plays a key role in sediment yield in the upper Yangtze (Zhang and Wen, 2002; Ma et al., 2002). In four extremely dry years (1994-97), decreased precipitation resulted in a 40% decline in runoff, and thereby leading to the decreased sediment fluxes from the Jialing River (EGRSTGP, 2002a; Xu, 2005). Longer-term (1956-2004) decreased precipitation has resulted in an 80-mt decline in sediment load from the high-sediment yield area in the upper Yangtze (Sub-basin Upper 2, Fig. 7; Fig. 8c).

6.2. Anthropogenic Impacts

The best example of anthropogenic impacts on sediment can be seen in the upper reaches of the Yangtze watershed. Steep relief, easily erodible soil, and recurrent earthquakes (Schaff and Richards, 2004) cause frequent landslides (locally as many as 12 per year). At present, there are ~6800 major landslide gullies in the upper Yangtze (Xie et al., 2004), which are particularly sensitive to any human activity. Taking Yichang as an example (Fig. 2), temporal variation in its sediment load reflects three distinctly different periods, 1956-67, 1968-77, and 1978-87, coinciding, respectively, with deforestation for small-scale iron smelting during the Great Leap Forward, conservancy project, and land responsibility reform (Higgitt and Lu, 1996; Lu and Higgitt, 1998). Since the mid 1980s, sediment loads have declined more or less continuously (except for the extreme floods in 1998) due to increased reforestation and dam construction (Fig. 2).

Various kinds of anthropogenic activities, together with the climatic change mentioned above, overlap with one another in both space and time. Therefore, it is challenging to quantify and separate their impacts despite many efforts to analyze the variations throughout the Yangtze (Higgitt and Lu, 1996; Lu and Higgitt, 1998; Yang et al., 2002; Zhang and Wen, 2004; Li et al., 2004; Yang et al., 2005). In general, deforestation and agriculture cultivation increase the sediment load (Dai and Tan, 1996), but they can be counteracted by water diversion, dam construction and reforestation. Four major types of anthropogenic activities are discussed below.

6.2.1. Water Consumption and Diversion

Water consumption has increased from $\sim 15 \text{ km}^3/\text{yr}$ in 1949 to $90 \text{ km}^3/\text{yr}$ in 2000, in large part due to a population expansion from ~ 180 to >400 million (Bulletin of Water Resources in China, 1997-2002; Heilig, 1999; *Chapter 1*). Increasing water diversion (mainly through dam impoundments, discussed below), however, seems to have an insignificant impact on annual and monthly water discharges (Figs. 2 and 10), even though the Yangtze is ranked as a highly-regulated river (Nilsson et al., 2005). One reason is that 90-km^3 water consumption is only $\sim 10\%$ of its annual discharge ($\sim 900 \text{ km}^3/\text{yr}$). The other is that much of the current water use ultimately is recycled back into the Yangtze watershed considering relatively few inter-basin diversions before 1990s. In 2003, about 17 km^3 water was impounded by TGD (the total capacity of TGD will be 39 km^3 when TGD is in full operation in 2009), causing medium declines in discharge at Yichang and Hankou, but no dramatic change at Datong (Fig. 10), underscoring the modulating capacity of a large high-discharge river like the Yangtze. In contrast with High Aswan Dam and downstream irrigation that trap and divert $>90\%$ of the Nile's discharge, present water diversion and dam impoundments ($>50,000$ dams, including the TGD) along the Yangtze appear to have had little impact on water discharge.

Mainly due to increased water consumption, northern Yangtze runoff has decreased more than that of precipitation (sub-basin North, Fig. 7), similar to the situation in the northern China. Decreased precipitation (upper portion in Fig. 6) and increased consumption have exacerbated the water crisis in northern China, especially in recent decades. The ongoing Project of South-North Water Diversion is scheduled to transfer freshwater from the wet south (mainly the Yangtze) to the dry north (including the Yellow) through three passages (east, middle and west) (Chen et al., 2003). Although

only ~5% (45 km³/yr) of the Yangtze water will be diverted (Chen et al., 2001a), this anthropogenic transfer may fundamentally change the Yangtze water cycle since most of the diverted water will not go back to the Yangtze through the natural hydrological processes.

6.2.2. Dam Construction

The number of Yangtze dams increased dramatically from only a few in 1950s, to ~46,000 in 1995, and >50,000 at present (Yang et al., 2006). Considering this large number and the dramatic reservoir-trapping, dams in the Yangtze watershed probably have played the greatest role in decreasing the sediment loads throughout the entire drainage basin.

Three dramatic declines (>80%) in tributary sediment loads illustrate the impact of dams (Fig. 9). 1) Sediment decline in the Zishui, a southern tributary with low-yield and high-runoff, seems to have been initiated by construction of the Zhexi Dam in 1958 (Fig. 9). Presently there are more than 13,300 dams in the four southern tributaries merging at the Dongting Lake (Li et al., 2005). 2) On the Han River, Danjiangkou Dam decreased sediment sharply in 1968, with a trapping ratio of >95% (Fig. 9). The reservoir behind Danjiangkou Dam will be one of the major freshwater sources for the middle passage of South-North Diversion (Chen et al., 2001a; Chen et al., 2003), delivering water to Beijing. This diversion will certainly further lower both water and sediment discharges of the Han. 3) The sediment drop in the Jialing (Fig. 9), once the major supplier of sediment upstream of Yichang, was initiated by the decreased precipitation in

1986 (Fig. 8), but more importantly is related to the ~12,000 dams on this tributary, which have trapped ~70 mt/yr since 1986 (EGRSTGP, 2002b).

6.2.3. Reforestation

Between 1988 and 2000, the Project of Yangtze Upstream Water and Soil Conservation reforested 63,000 km² of land (Bulletin of Yangtze Sediment, 2000), increasing forest cover (Zhang and Wen, 2002; Zhang and Wen, 2004), leading to a significant sediment reduction in the upper and middle streams (60 mt/yr) (Bulletin of Yangtze Sediment, 2004). Taking the Jialing tributary as an example, reforestation has decreased its sediment load by 30 mt/yr (Mao and Pei, 2002; EGRSTGP, 2002b). Dams and reforestation, combined with decreased rainfall, are the major forcings leading to the sediment reduction in the Jialing since 1980s (Fig. 9); its load should continue to decline in response to continuing water-soil conservancy.

6.2.4. Lake Reclamation

Since the 1950s, reclamation has greatly impacted the lakes along the Yangtze, especially near the Dongting Lake. Five braided passages (labelled 1 to 5, Fig. 12 a) carry a large amount of sediment from mainstream to the Dongting Lake. Four southern tributaries flow northward (labelled 6 to 9), merge with the lake, and then flow back to mainstream through Chenglingji Station (Fig. 12a). The differences between the loads of five passages and Chenglingji ([1 to 5] - Chenglingji) indicate that less and less net sediment has escaped from the mainstream since 1956 (dashed line, Fig. 12b). Similarly,

sediment budget for the Dongting Lake ([1 to 9] - Chenglingji) shows that net trapped sediment into the lake also has declined dramatically (solid line, Fig. 12b).

This trapping Dongting budget, together with extensive lake reclamations, has led to a dramatically decreased lake area (Shi et al., 1985; Du et al., 2001), decreasing from 4,350 km² in 1949 to 2,623 km² in 1995 (Bulletin of Yangtze Sediment, 2000). Historically the Dongting Lake has been critical in buffering the impact of floods along the mainstream and nearby alluvial plains. In 1950s, five passages transported ~35% of water and sediment passing Yichang Station (Li et al., 2000), but in recent years they have carried only ~15% of these from Yichang, indicating the Dongting's declining role in flood modulation. The construction of TGD led to active channel erosion downstream of Yichang in 2003-04 (Xu et al., 2006). Thus, the elevation of mainstream channel has become lower than those of three passages, causing further decreased discharges entering the lake (Zhang, 1995). Although TGD can modulate the water upstream of Yichang, four high-runoff southern tributaries (Fig. 4) can discharge massive water directly into the shrinking Dongting, an unsolved flood problem for the Yangtze middle stream. How to maximize the longevity of the Dongting, the freshwater source for tens of millions of inhabitants, has become a serious issue.

6.3. Future Variations

With 430 mt/yr in 1950s-60s, Datong sediment load is predicted to drop to 170 mt in 2020s and then revert back to ~310 mt (Yang et al., 2002; Fig. 13). However, after several major drops, Datong load has already declined to 140 mt in 2004, only 33% of its natural loads in 1950s-60s.

Various impacts make it difficult to predict future Yangtze sediment entering the East China Sea. The first challenge is to understand the impact of upstream dam construction. Except the TGD and Gezhouba Dam, few dams have been constructed on the mainstream, mainly to avoid sediment trapping and facilitate navigation. However, ongoing or planned dams, such as Wudongde, Baihetan, Xiluodu and Xiangjiaba dams, all located along the mainstream above TGD with tributaries showing particularly high sediment yield (Fig. 5), will add an additional 41 km³ of total water-storage capacity. Their total installed hydropower capacity alone will be 38,500 MW, about double that of the TGD. One of the purposes to build these four dams is to minimize the trapping in TGD, which is difficult to include in the prediction. The second challenge is that trapping in Dongting Lake has decreased from 180 mt in 1950s to nearly zero at present (solid line, Fig. 12b). This decline has fundamentally changed the correlation between Yichang and Datong stations; the sites used by Yang et al. (2002) for predictions. The third challenge is channel erosion downstream of dams. There is usually a time-lag between impoundment and erosion, and channel erosion may counteract with dam trapping. Channel erosion has happened behind the Danjiangkou Dam (Xu, 2005) and the TGD, and will happen downstream of four future major dams. All those above uncertainties elude the sediment prediction.

However, it is probable that Datong sediment load will decrease to ~100 mt/yr because of future dams, ongoing conservancy and water diversions. As such, the lower reaches of the river (downstream of Datong) and coastal region will be under varied environmental pressures. The Yangtze River used to be river-tide dominated, with a large sediment supply (430 mt/yr) and a spring tide range of 3 m. After the dramatic sediment

decline, however, the estuary may shift to tide-dominated (triangle plot, Fig. 13). The sediment threshold to sustain the geometry of modern Yangtze Delta has been estimated to be 263 mt/yr (Yang et al., 2005) (dash horizontal line, Fig. 13), but the load has been below this level since 2000, and will presumably stay below the threshold for at least 50-yr.

Since the Yangtze has contributed ~90% of the nutrient supplied to the ECS, a decrease in sediment will decrease the nutrient supply rapidly. From 1998 to 2003, the ecosystem in the ECS responded quickly to the decreased Yangtze nutrients; ECS primary production has decreased 86% and Si:N ratios has declined from 1.5 to 0.6 (Gong et al., 2006), therefore endangering the fishery resources. Declining sediment loads will also probably cause severe shoreline retreat (Yang et al., 2002), saltwater intrusion (Chen et al., 2001a), and various other serious environmental problems.

7. Conclusions

Over the past 55 years, runoff in the northern Yangtze has declined much more than has precipitation, reflecting increased water consumption. In contrast, runoff increase in the southern Yangtze watershed was more than that of precipitation, presumably reflecting decreased evapotranspiration. Although 50,000 dams and 90 km³ water consumption led to minor variations in runoff, sediment loads have decreased dramatically, and in 2004 at Yichang and Datong in 2004 transported only 12% and 33% of their natural loads. Throughout the basin, the most significant sediment drops (>80%) occurred in Jialing, Han, Zishui tributaries (mainly due to dam construction and reforestation), as well as two passages between mainstream and the Dongting Lake (due

to lake reclamation). The Impoundment behind the Three Gorges Dam drastically decreased sediment loads at Yichang by 164 mt in 2003-04, but during the previous 15 years it decreased by ~300 mt. The shrinking Dongting Lake now carries a much smaller percentage (~15%) of the discharge passing Yichang, such that the middle mainstream is under increased flood pressure. Considering the future major dams and water diversion, it is very probable that sediment load at Datong will decrease to ~100 mt/yr so that both downstream and coast areas could be severely impacted in the near future.

Acknowledgements

This research was supported by the US National Science Foundation (NSF) and Office of Naval Research (ONR). This paper is Contribution No.xxxx of the Virginia Institute of Marine Science, the College of William and Mary.

References

- Bulletin of Yangtze River Sediment (2000-2004), Press of Ministry of Water Resources of the People's Republic of China (in Chinese).
- Bulletin of Water Resources in China, 1997-2002, Ministry of Water Resources of the People's Republic of China, website: <http://sdinfo.chinawater.net.cn/index.asp> (in Chinese).
- Carriquiry, J.D., Sanchez, A. and Camacho-Ibar, V.F., 2001. Sedimentation in the northern Gulf of California after cessation of the Colorado River discharge. *Sedimentary Geology*, 144(1-2): 37-62.

- Chen, J., Chen, X. and Chen, M., 2003. Impacts and countermeasurements of the South-to-North water diversion projects on the ecosystem and environment of the Yangtze estuary. East China Normal University Press, Shanghai, 277pp.
- Chen, X., Zong, Y., Zhang, E., Xu, J. and Li, S., 2001a. Human impacts on the Changjiang (Yangtze) River basin, China, with special reference to the impacts on the dry season water discharges into the sea. *Geomorphology*, 41(2-3): 111-123.
- Chen, Z., Li, J., Shen, H. and Wang, Z., 2001b. Yangtze River of China: historical analysis of discharge variability and sediment flux. *Geomorphology*, 41(2-3): 77-91.
- Chu, Z.X., Sun, X.G., Zhai, S.K. and Xu, K.H., 2006. Changing pattern of accretion/erosion of the modern Yellow River (Huanghe) subaerial delta, China: Based on remote sensing images. *Marine Geology*, 227(1-2), 13-30.
- Cyranoski, D., 2005. Climate change: The long-range forecast. *Nature*, 438(7066): 275-276.
- Dai, D. and Tan, Y., 1996. Soil erosion and sediment yield in the Upper Yangtze River basin. In: D.E. Walling and B.W. Webb (Editors), *Erosion and Sediment Yield: Global and Regional Perspectives in the IAHS Series of Proceedings and Reports*. IAHS Publication, pp. 191-203.
- Deng, X. and Huang, C., 1997. Analysis of transport characteristics and influence of human activities in the Jingsha River. *Journal of Sediment Research*, 4: 37-41 (in Chinese).

- Du, Y., Cai, S., Zhang, X. and Zhao, Y., 2001. Interpretation of the environmental change of Dongting Lake, middle reach of Yangtze River, China, by ^{210}Pb measurement and satellite image analysis. *Geomorphology*, 41(2-3): 171-181.
- EGRSTGP (Expert Group on River-borne Sediment of the Three Gorges Project), 2002a. Study on sediment of the Three Gorges Engineering Project (Book 4). Intellectual Property Press, Beijing (in Chinese).
- EGRSTGP, 2002b. Study on sediment of the Three Gorges Engineering Project (Book 8). Intellectual Property Press, Beijing (in Chinese).
- Fuggle, R., Smith, W., Inc., H.C. and Inc., A.C., 2000. Large Dams in Water and Energy Resource Development in The People's Republic of China (PRC). Country review paper prepared as an input to the World Commission on Dams, Cape Town, www.dams.org.
- Gleick, P.H., 1993. *Water in Crisis: A Guide to the World's Fresh Water Resources*. Oxford University Press, 504pp.
- Gleick, P.H., 2000. *The World's Water 2000-2001: The Biennial Report on Freshwater Resources*. Island Press, Washington, D.C.
- Gong, G., J. Chang, K. Chiang, T. Hsiung, C. Hung, S. Duan, and L. A. Codispoti, 2006. Reduction of primary production and changing of nutrient ratio in the East China Sea: Effect of the Three Gorges Dam?, *Geophys. Res. Lett.*, 33, L07610, doi:10.1029/2006GL025800.
- Heilig, G.K., 1999. *China Food. Can China Feed Itself?* International Institute for Applied Systems Analysis (IIASA), Laxenburg.

- Higgitt, D.L. and Lu, X., 1996. Patterns of sediment yield in the upper Yangtze basin, China. In: D.E. Walling and B.W. Webb (Editors), *Erosion and Sediment Yield: Global and Regional Perspectives in the IAHS Series of Proceedings and Reports*. IAHS Publication, pp. 205-214.
- Li, C., Yang, S., Fan, D. and Zhao, J., 2004. The change in Changjiang suspended load and its impact on the delta after completion of Three Gorges Dam. *Quaternary Sciences*, 24(5): 495-550 (in Chinese).
- Li, J., Wang, K., Qin, J., Xiao, H. and Chao, L., 2005. The evolution of annual runoff and sediment in the Dongting Lake and their driving forces. *Acta Geographica Sinica*, 60(3): 503-510 (in Chinese).
- Li, Y., Li, R. and Deng, J., 2000. A study on sediment transport and flood control in the middle reach of Yangtze River. *Journal of Sediment Research*(3): 12-20 (in Chinese).
- Liu, B., M. Xu, M. Henderson, and W. Gong, 2004. A spatial analysis of pan evaporation trends in China, 1955-2000. *Journal of Geophysical Research*, Vol. 109, D15102.
- Liu, Y. and Zhang, P., 1991. Soil erosion and sediment characters of the high sediment yield regions in the upper Yangtze River. *Hydrology*, 3: 6-12 (in Chinese).
- Lu, X.X. and Higgitt, D.L., 1998. Recent changes of sediment yield in the Upper Yangtze, China. *Environmental Management*, 22(5): 697-709.
- Ma, L., Zhang, M., Guo, H. and Shen, Y., 2002. Research on the change of runoff-sediment relationship due to soil and water conservation in Jialingjiang River basin. *Hydrology*, 22(1): 27-31 (in Chinese).

- Mao, H. and Pei, M., 2002. Influence of human activities on runoff and sediment transmitting in Jialingjiang Valley. *Journal of Soil and Water Conservation*, 16(5): 101-104 (in Chinese).
- Menon, S., Hansen, J., Nazarenko, L. and Luo, Y., 2002. Climate Effects of Black Carbon Aerosols in China and India. *Science*, 297(5590): 2250-2253.
- Milliman, J.D. and Meade, R.H., 1983. World-wide delivery of sediment to the oceans. *Journal of Geology*, 91(1): 1-21.
- Milliman, J.D. and Syvitski, J.P.M., 1992. Geomorphic/tectonic control of sediment discharge to the ocean: the importance of small mountainous rivers. *Journal of Geology*, 100(5): 525-544.
- Nilsson, C., Reidy, C.A., Dynesius, M. and Revenga, C., 2005. Fragmentation and Flow Regulation of the World's Large River Systems. *Science*, 308(5720): 405-408.
- Pan, J., 1997. Study on sediment transport characteristics in Jinsha River basin. *Bulletin of Soil and Water Conservation*, 17(5): 35-39 (in Chinese).
- Ren, L., Wang, M., Li, C. and Zhang, W., 2002. Impacts of human activity on river runoff in the northern area of China. *Journal of Hydrology*, 261(1-4): 204-217.
- Schaff, D.P. and Richards, P.G., 2004. Repeating Seismic Events in China. *Science*, 303(5661): 1176-1178.
- Shen, G. and Xie, Z., 2004. Three Gorges Project: Chance and Challenge. *Science*, 304(5671): 681b.
- Shen, H., 2001. Material flux of the Changjiang Estuary. China Ocean Press, Beijing (in Chinese).

- Shi, Y.-L., Yang, W. and Ren, M.-e., 1985. Hydrological characteristics of the Changjiang and its relation to sediment transport to the sea. *Continental Shelf Research*, 4(1-2): 5-15.
- Shiklomanov, I.A., 1999. *World Water Resources and Their Use*. State Hydrological Institute (SHI), Russia, St. Petersburg.
- Shiklomanov, I.A. and Rodda, J.C., 2003. *World Water Resources at the Beginning of the Twenty-First Century (International Hydrology Series)*. Cambridge University Press, 435pp.
- Stanley, D.J. and Warne, A.G., 1998. Nile Delta in its destructional phase. *Journal of Coastal Research*, 14: 794-825.
- Syvitski, J.P.M., Vorosmarty, C.J., Kettner, A.J. and Green, P., 2005. Impact of Humans on the Flux of Terrestrial Sediment to the Global Coastal Ocean. *Science*, 308(5720): 376-380.
- Thomas, A., 2000. Spatial and temporal characteristics of potential evapotranspiration trends in China. *International Journal of Climatology*, 20, 381-396.
- Vorosmarty, C.J. et al., 2003. Anthropogenic sediment retention: major global impact from registered river impoundments. *Global and Planetary Change*, 39(1-2): 169-190.
- Wu, S., 2000. Counter-proposals for the environmental administration and sustainable development of the main source and upper reaches of the Changjiang River. *Yunnan Geographic Environment Research*, 12(2): 25-30 (in Chinese).

- Xie, H., Zhong, D., Li, Y. and Wei, F., 2004. Features of debris flows in the upper reaches of the Changjiang River. *Resources and Environment in the Yangtze Basin*, 13(1): 94-99 (in Chinese).
- Xie, P., Wu, J., Huang, J. and Han, X., 2003. Three-Gorges Dam: Risk to Ancient Fish. *Science*, 302(5648): 1149b-1151.
- Xu, J., 2005. Variation in grain size of suspended load in upper Yangtze River and its tributaries by human activities. *Journal of Sediment Research* (3): 8-16.
- Xu, K. et al., 2005. Simulated sediment flux during 1998 big-flood of the Yangtze (Changjiang) River, China. *Journal of Hydrology*, 313(3-4): 221-233.
- Xu, K.H., Milliman, J.D., Yang, Z.S., Wang, H.J., 2006. Yangtze sediment Decline Partly from Three Gorges Dam, *EOS Transactions, AGU*, 87(19), 185,190.
- Yang, S.L. et al., 2005. Impact of dams on Yangtze River sediment supply to the sea and delta intertidal wetland response. *J. Geophys. Res.*, 110, F03006, doi: 10.1029/2004JF000271.
- Yang, S.-l., Zhao, Q.-y. and Belkin, I.M., 2002. Temporal variation in the sediment load of the Yangtze river and the influences of human activities. *Journal of Hydrology*, 263(1-4): 56-71.
- Yang, Z.-s. et al., 2006. Dam impacts on the Changjiang (Yangtze River) sediment discharge to the sea: the past 55 years and after the Three Gorges Dam. *Water Resource Research*. 42, W04407, doi:10.1029/2005WR003970.
- Zhang, R., 1995. Problems about sedimentation in Three Gorges Reservoir and its countermeasures. *China Three Gorges Construction*, 3: 18-19, 47 (in Chinese).

Zhang, X. and Wen, A., 2002. Variation of sediment in upper stream of Yangtze River and its tributary. *Shuili Xuebao*, 4: 56-59 (in Chinese).

Zhang, X. and Wen, A., 2004. Current changes of sediment yields in the upper Yangtze River and its two biggest tributaries, China. *Global and Planetary Change*, 41(3-4): 221-227.

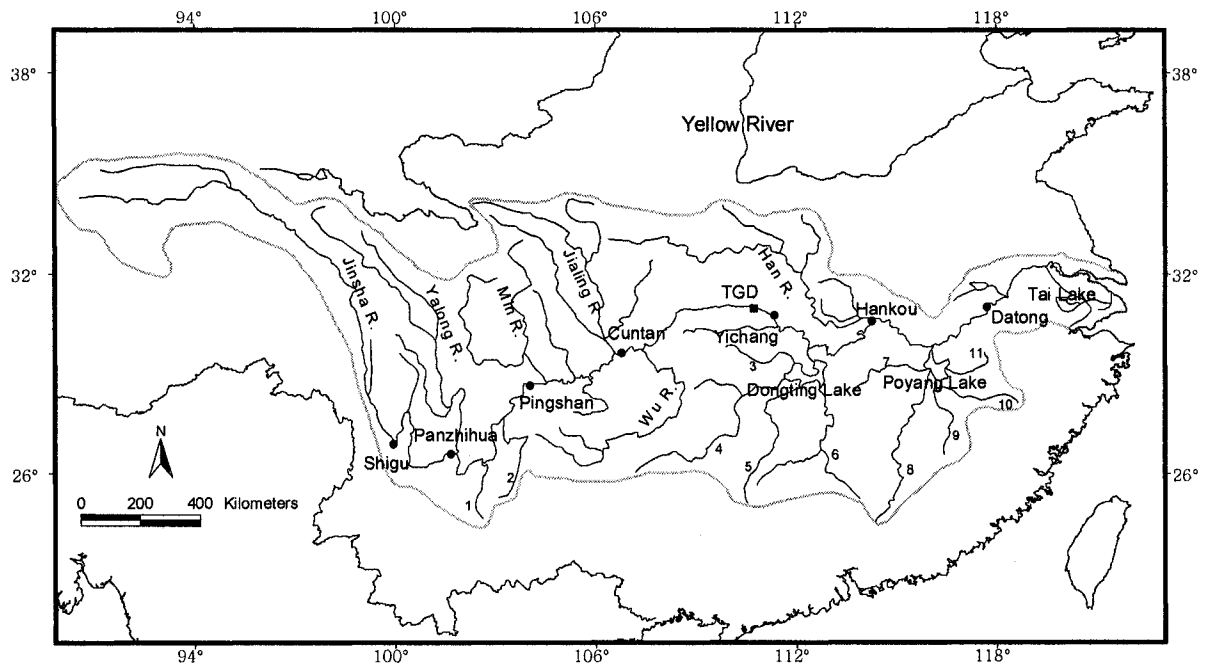


Fig. 1. Yangtze River drainage basin. Black dots are gauging stations along the main stream. TGD: Three Gorges Dam. 1: Pudu River, 2: Niulan River, 3: Lishui River, 4: Yuan River, 5: Zishui River, 6: Xiang River, 7: Xiushui River, 8: Gan River, 9: Fu River 10: Xin River, 11: Rao River.

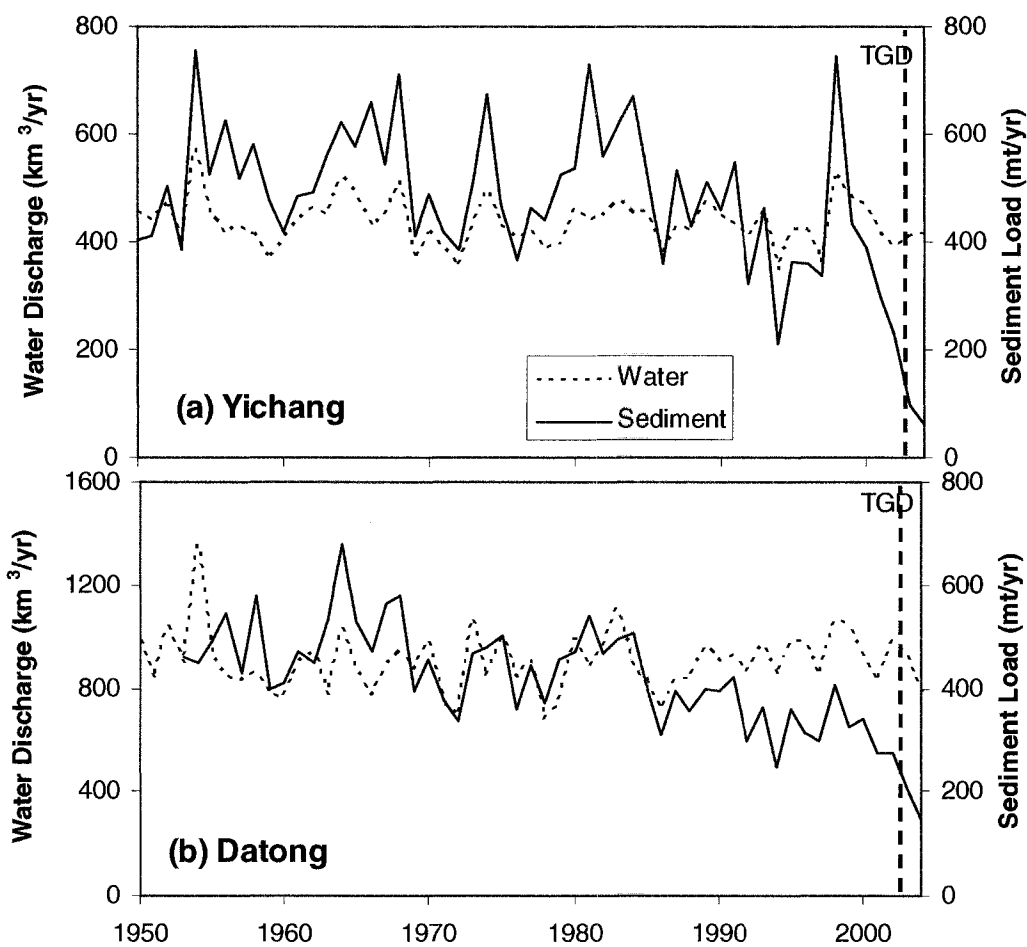


Fig. 2. Water discharge and sediment load at Yichang (upstream) and Datong (lower stream) gauging stations. TGD, Three Gorges Dam, whose impoundment began in June 2003, marked as vertical dash line. mt = million tons. Water and sediment discharges were obtained from the Bulletin of Yangtze Sediment, 2000-2004.

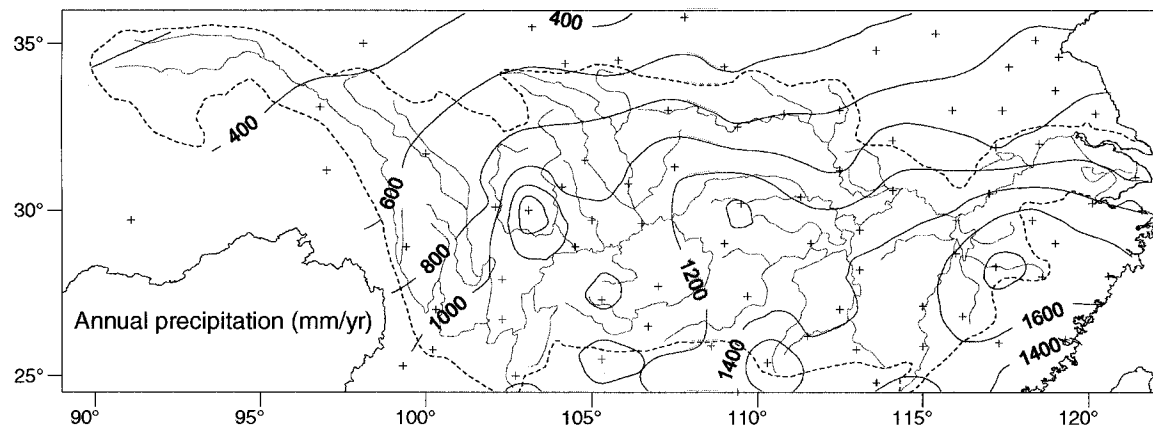


Fig. 3. Mean annual precipitation (mm/yr) in Yangtze drainage basin, 1951- 2000. Crosses represent locations of meteorological stations.

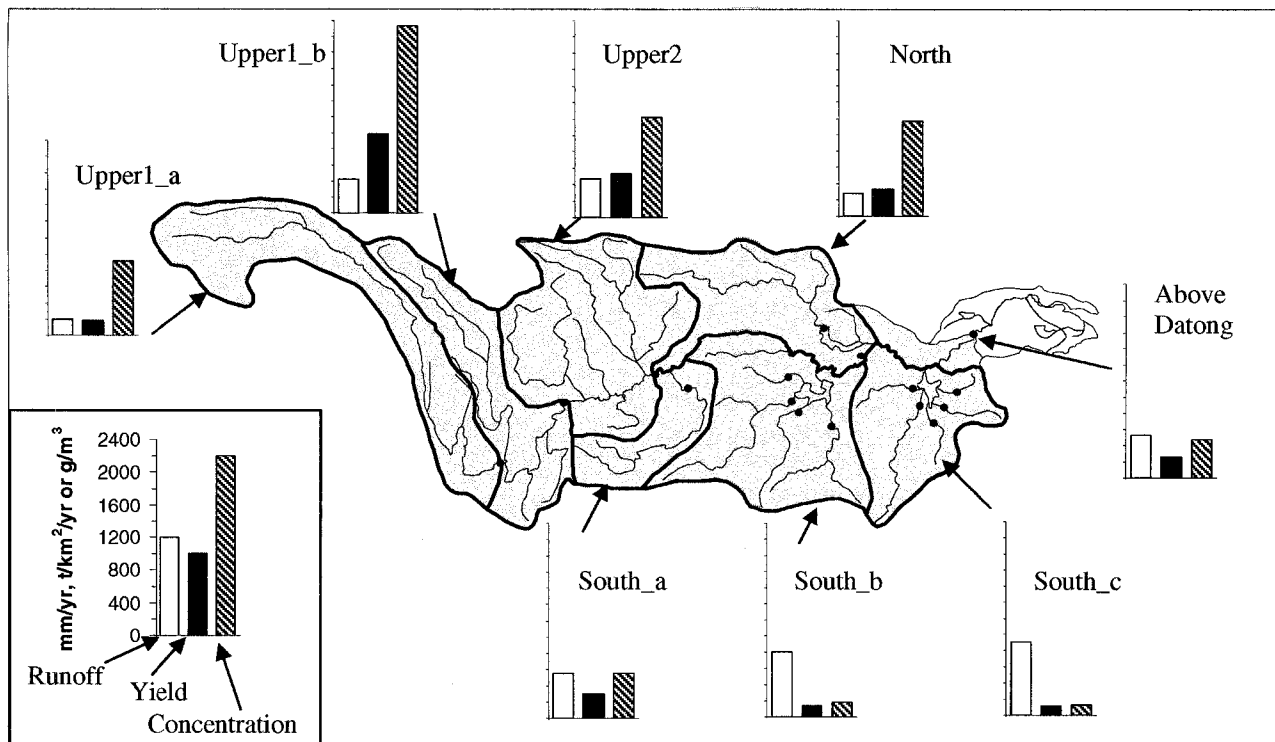


Fig. 4. Runoff, sediment yield and concentration along the Yangtze River. Each histogram represents the average runoff, sediment yield and concentration for the sub-basins. Black dots are hydrological stations used for the calculations: Panzhihua for sub-basin Upper1_a, the difference between Panzhihua and Pingshan for Upper1_b, the difference between Cuntan and Pingshan in Upper2, Huangzhuang in the North and 9 stations (Wulong, Xiangtan, Taojiang, Taoyuan, Shimen, Waizhou, Lijiadu, Meigang, Hushan, Wanjiabu, from west to east) in South_a, South_b and South_c, respectively. Datong (all the light grey region) station covers 94% the total Yangtze drainage basin. Most data are from Bulletin of Yangtze Sediments (2000-04), Pan (1997), Higgitt and Lu (1996) and Lu and Higgitt (1998). See Fig.1 for the locations of the stations and Fig. 7 for comparison.

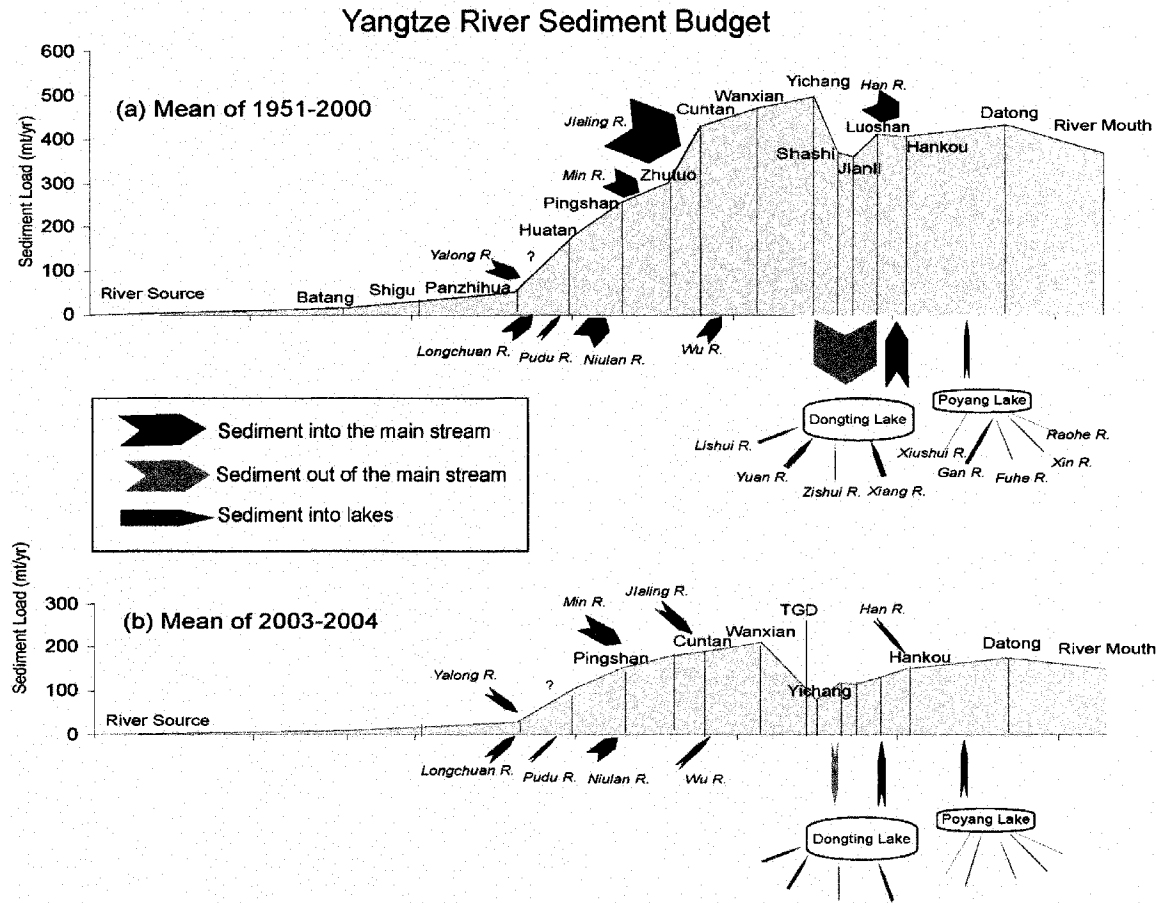


Fig. 5. Yangtze River sediment budget. The x-axis is the distance from river source and y-axis is the sediment load (in million tons per year, mt/yr). The names above the lines are gauging stations along the main stream. The width of arrows corresponds to the scale of y-axis. TGD: Three Gorges Dam. Question mark between Panzhihua and Pingshan indicates possible ungauged inputs from small tributaries. Means of 2003-04 at above-Pingshan stations, Shashi, Jianli, Luoshan and river mouth are calculated assuming proportional variations to nearby upper or lower stations. Most data come from Bulletin of Yangtze Sediments (2000-04), Deng and Huang (1997), Pan (1997), Higgitt and Lu (1996) and Shen et al. (2001).

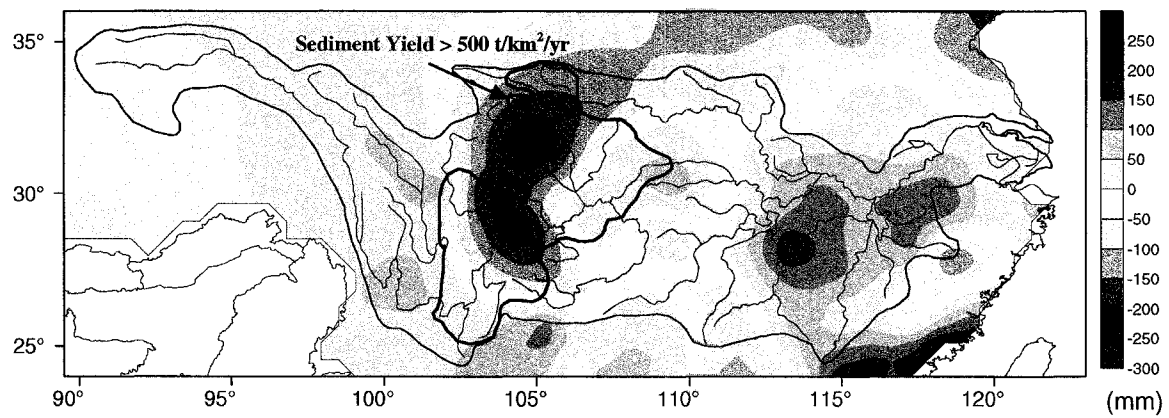


Fig. 6. Precipitation change (mm) in 1951-2000. Blue regions indicate increased precipitation and red regions represent decreased. The area marked with bold black curve is the region with sediment yield greater than 500 t/km²/yr (modified after Liu and Zhang, 1991; Dai and Tang, 1996; Shi et al., 2001).

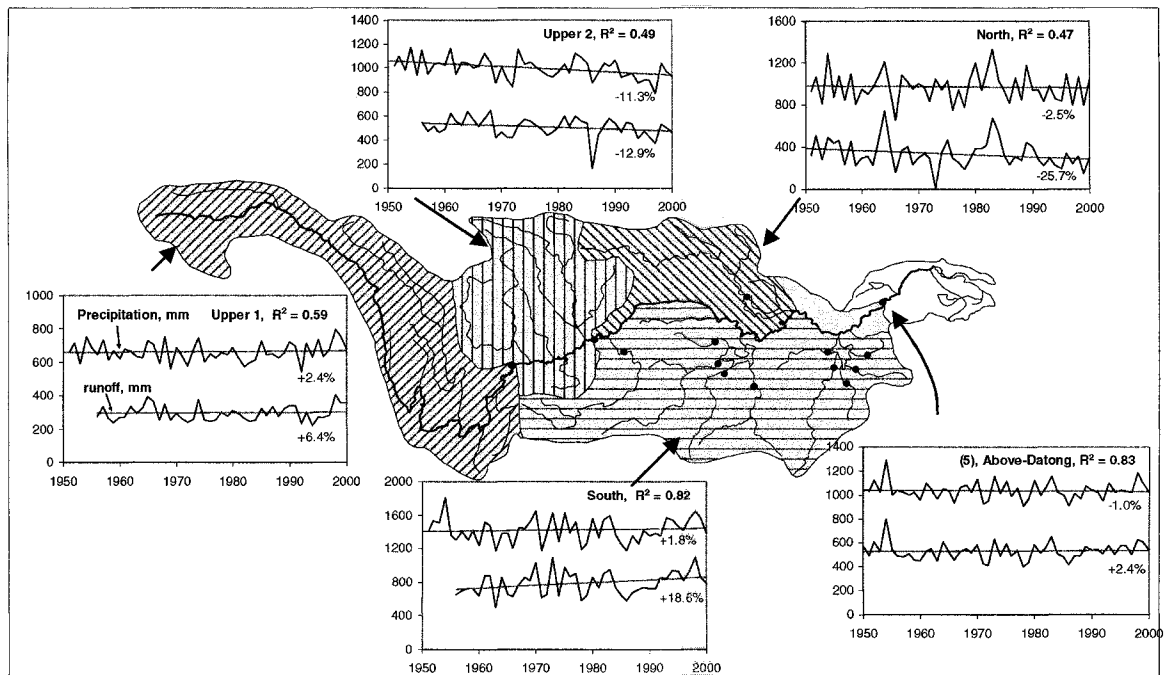


Fig. 7. Spatial and temporal variation of precipitation and runoff in the Yangtze. Upper and lower lines are average annual precipitation and runoff (in mm) for sub-basins, respectively, along with their trends in percentages. Correlation coefficient (R^2) between precipitation and runoff is marked in each panel. Black dots are gauging stations used for the calculations of cumulative runoff. Datong (all the grey region) covers 94% the total Yangtze drainage basin. See Fig. 4 for stations explanation and comparison.

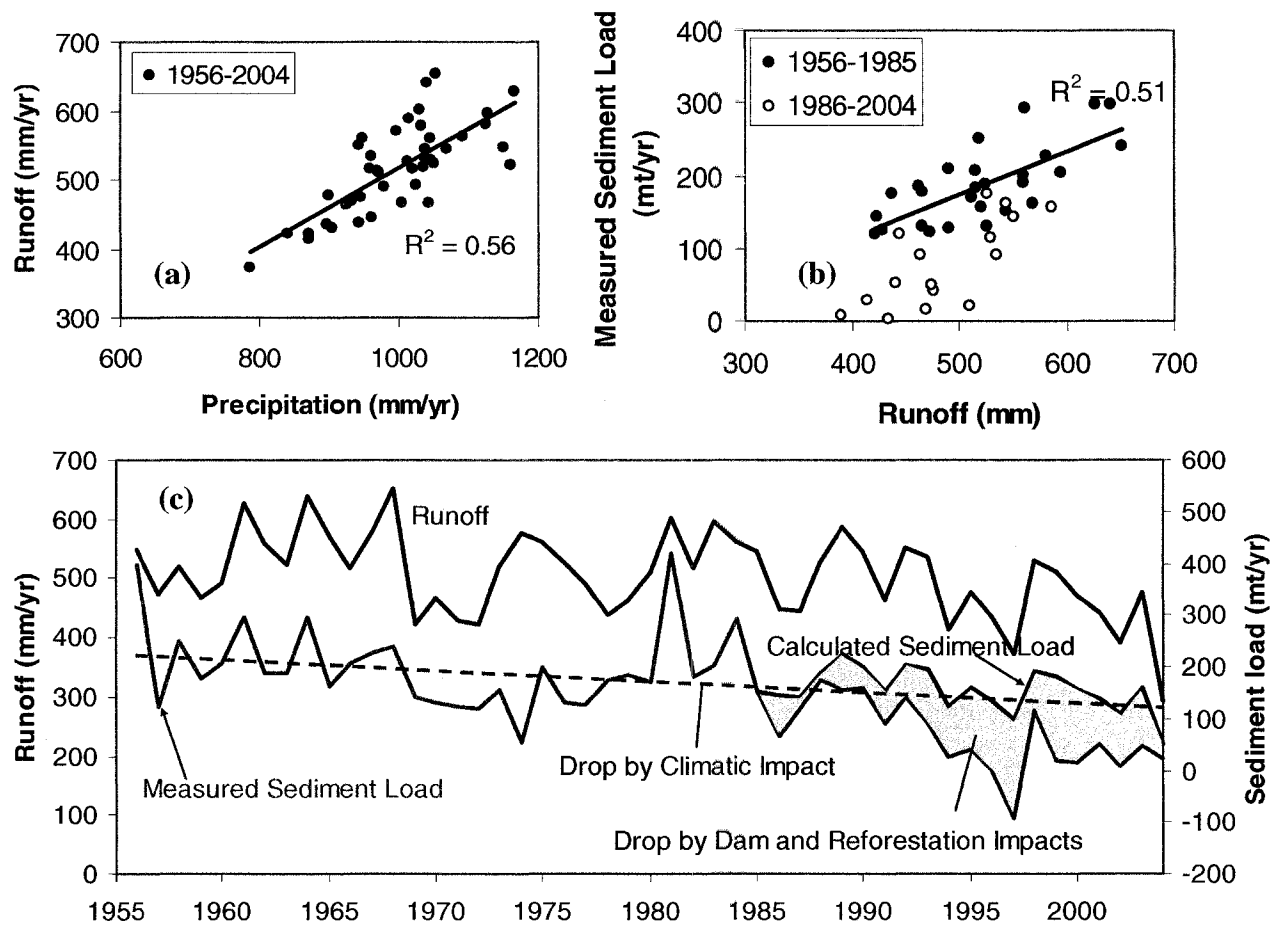


Fig. 8. Precipitation, runoff and sediment loads between Pingshan and Cuntan gauging stations. Runoff and sediment discharge is determined by subtracting discharge of Pingshan from that of Cuntan, see Fig. 3 for explanation. Correlation analysis of 1956-2004 in (a) excludes the abnormal year 1986 due to extensive dam impoundments. In (b), the 1956-1985 runoff-sediment correlation excludes three abnormal years (1956, 74 and 81). In (c), the negative measured load of 1997 indicates possible channel siltation. Runoff in 1986 shown as a dot in (c) is calculated by precipitation-runoff correlation. The dash trend line indicate the sediment drop due to decreased precipitation, and the difference between measured and calculated sediment (grey region) in 1986-2004 is caused by anthropogenic activities, such as dam construction and reforestation.

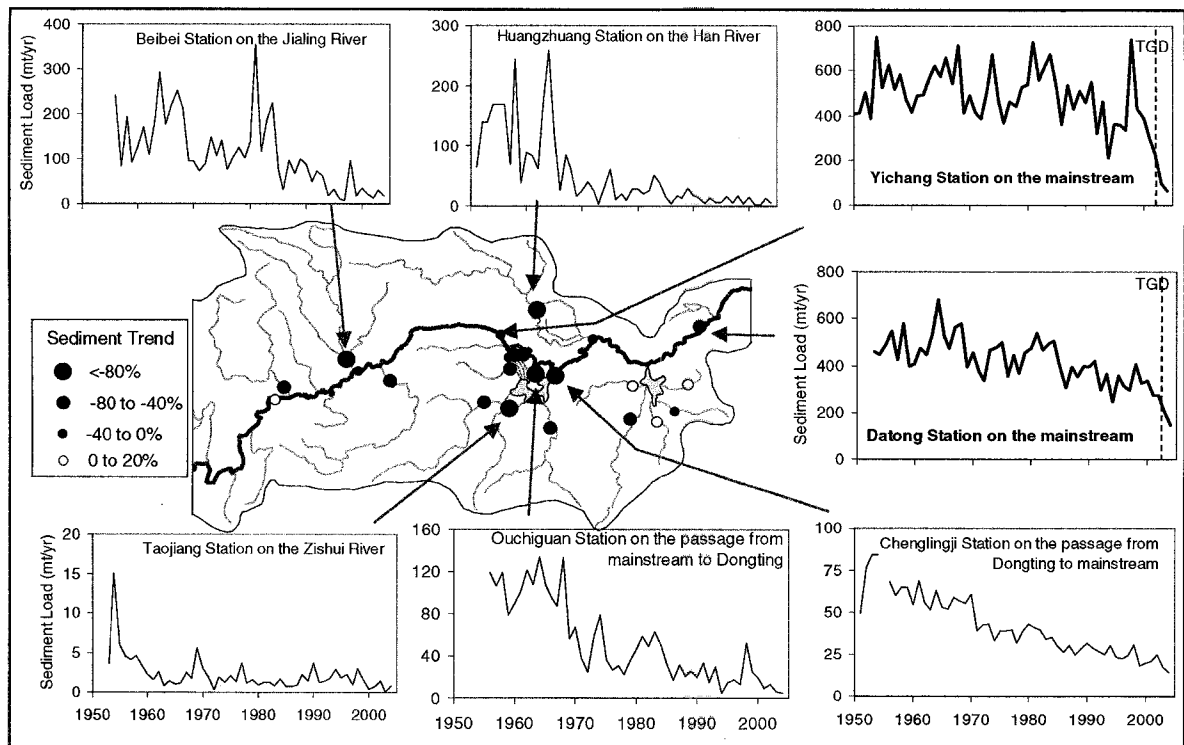


Fig. 9. Temporal Sediment Trends of the Yangtze River. Temporal sediment variations at the five most significant drops (>80%) as well as Yichang and Datong stations on the mainstream are shown in company with their trends. TGD, Three Gorges Dam. See Fig. 12 for the details of the Dongting Lake.

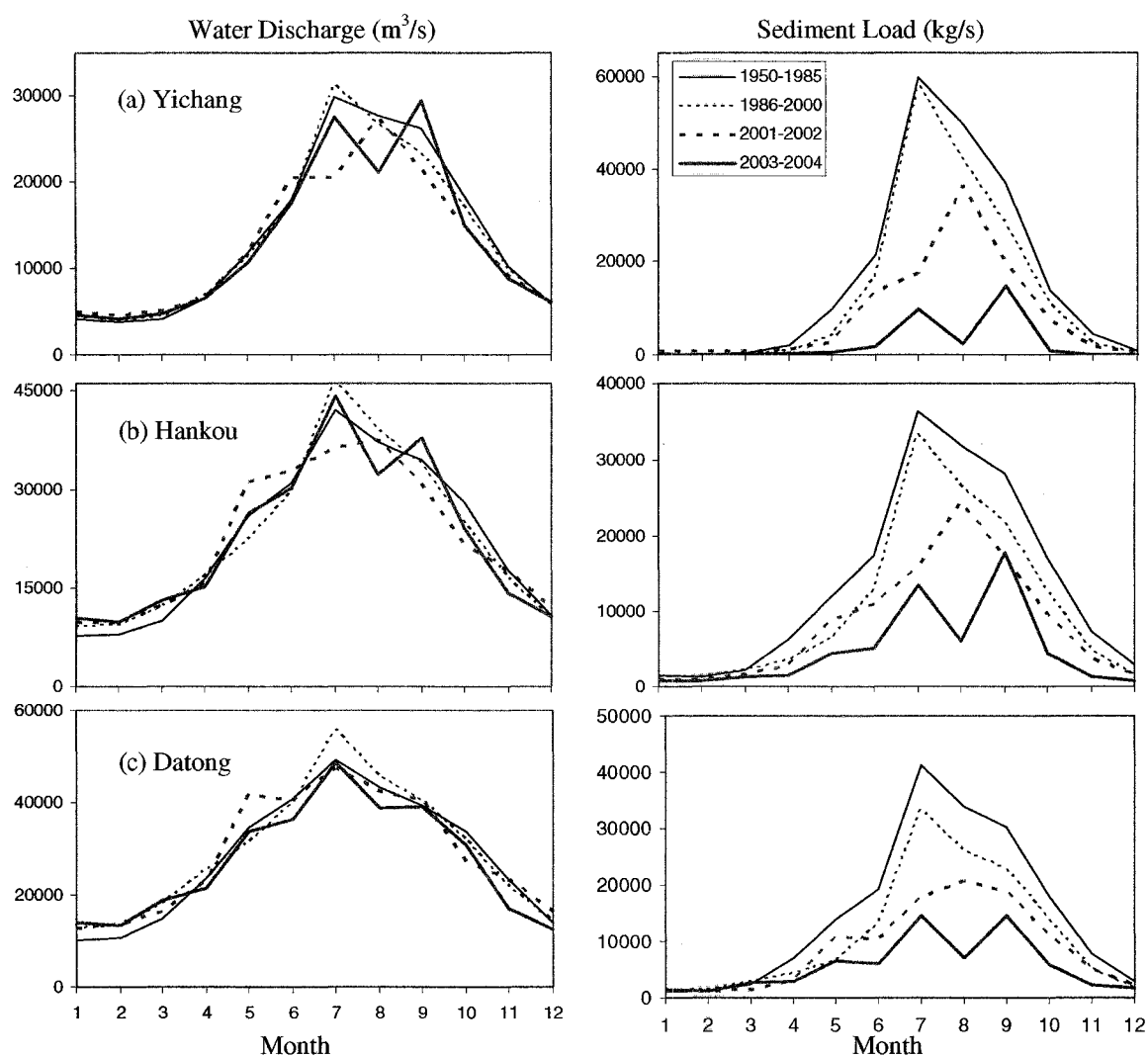


Fig. 10. Monthly water discharge and sediment loads at Yichang, Hankou and Datong. Datong 1950-1985 average is actually from 1953 to 1985, lacking 1970-71 and 1974-75.

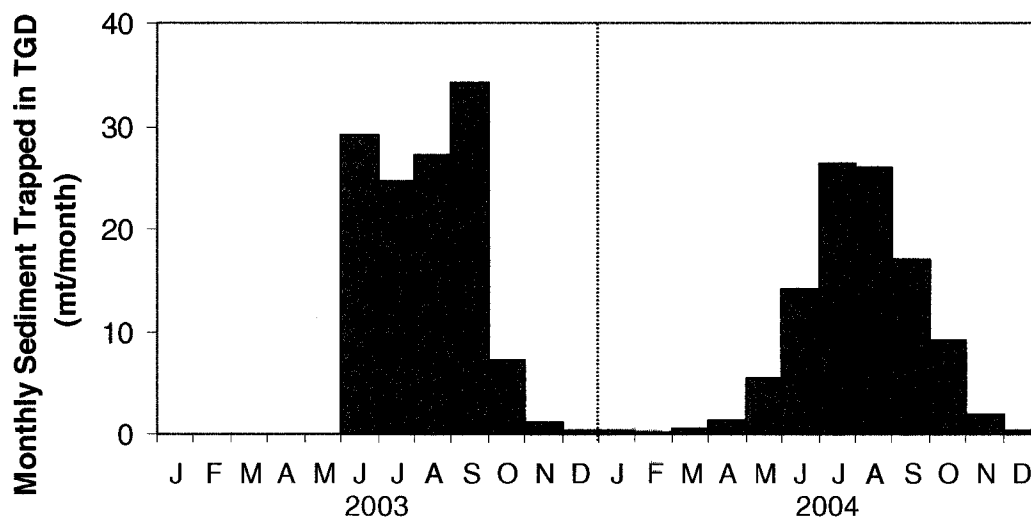


Fig. 11. Monthly sediment trapped in the Three Gorges Dam (TGD) in 2003-04. The trapped sediment is determined by subtracting the load of entering (Qingxichang) from that of exiting (Huanglingmiao) gauging stations.

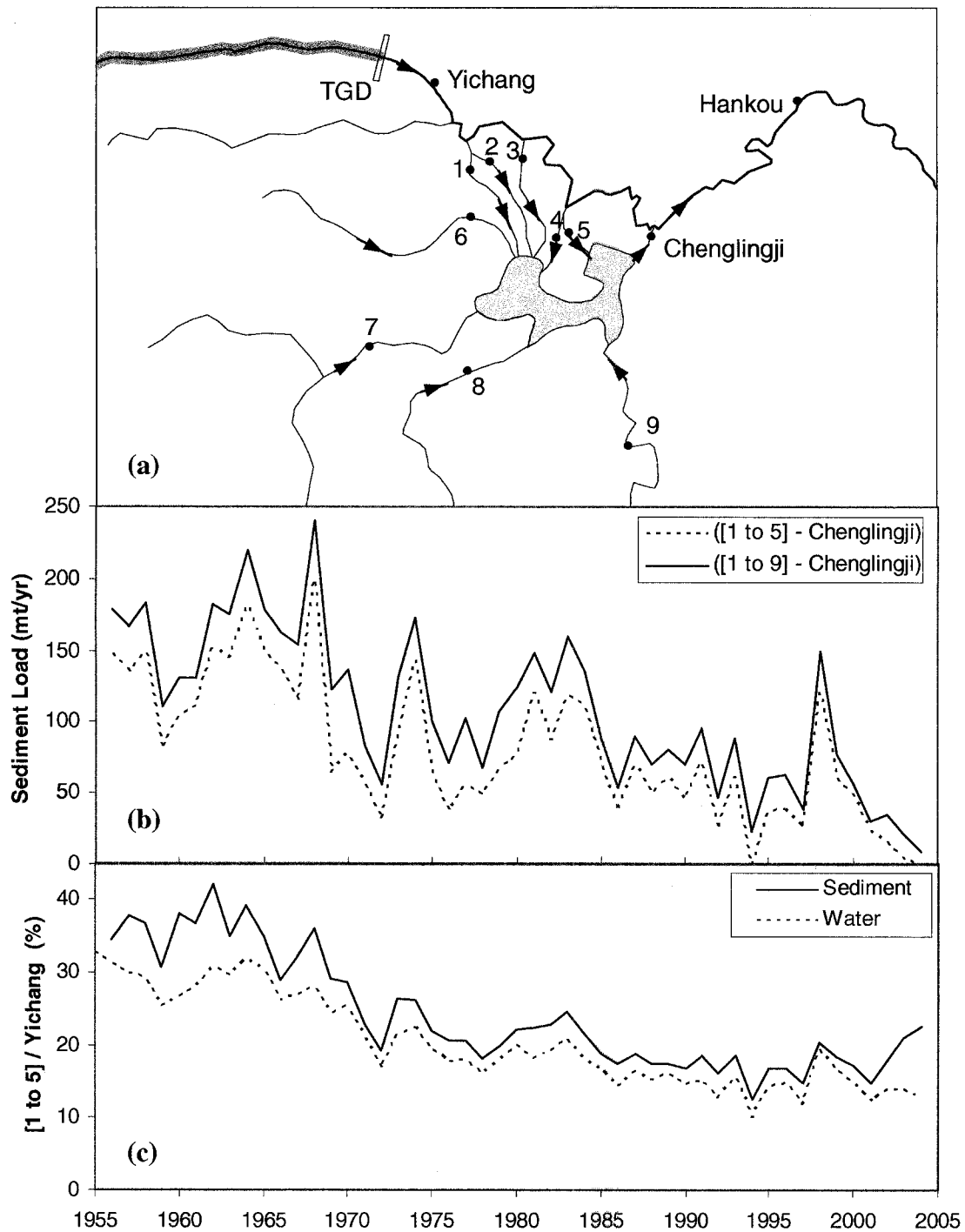


Fig. 12. Temporal sediment budget in the Dongting Lake. TGD, Three Gorges Dam. The bold grey line is the channel section impounded by TGD. 1, Xinjiangkou; 2, Shadaoguan; 3, Taipingkou; 4, Ouchikang; 5, Ouchiguan; 6, Shimen; 7, Taoyuan; 8, Taojiang; 9, Xiangtan. See Fig. 1 for the location of (a).

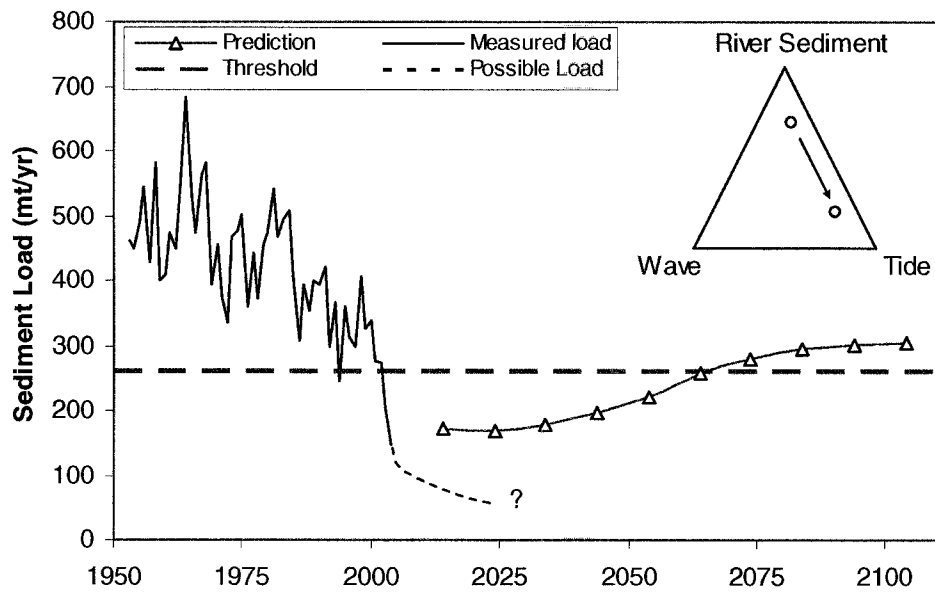


Fig. 13. Measured and future sediment loads at Datong Station. The prediction is from Yang et al. (2002). The grey horizontal dash line is the threshold sediment supply (263 mt/yr) to sustain the Yangtze River Delta (Yang et al., 2005). Black dashed curve and question mark indicate the possible future sediment load. The triangle plot shows the Yangtze is shifting from river-tide dominated to a tide-dominated river.

CHAPTER 4: Yangtze Sediment Decline Partly From Three Gorges Dam*

By K.H. Xu, J.D. Milliman, Z.S. Yang and H.J. Hou

*Published as: Xu, K.H., Milliman, J.D., Yang, Z.S., Wang, H.J., 2006. Yangtze sediment Decline Partly from Three Gorges Dam, *EOS Transactions, AGU*, 87(19), 185, 190.

Introduction

It could be argued that nowhere has the impact of dams on rivers been more important than in China, where since 1950 almost half of the world's large dams (higher than 15 meters) have been built [Fuggle and Smith, 2000]. China's Yangtze River (Changjiang)—the largest river in south Asia (1.8 million square kilometers) and home to more than 400 million inhabitants—alone has more than 50,000 dams within its watershed, including the world's largest, the Three Gorges Dam (TGD) (Figure 1a).

Water and sediment began being impounded behind the TGD in June 2003, and two years after impoundment, river sediment discharge downstream (at Datong Station) had decreased by nearly half of its 2002 load (Figure 1c). However, the decrease in Yangtze sediment load did not begin with TGD impoundment. Rather, the sediment load at Datong has declined continually since 1987 despite a slight increase in river discharge (Figure 1c). The change in pre-TGD loads at Yichang, just downstream from the TGD, has been even more extreme, decreasing by ~300 million tons in 1986–2002, before declining another 130 million tons after 2002 (Figure 1b). All of this suggests that collective changes on the Yangtze upstream (above Yichang) have been more important in decreasing the river's sediment load than the TGD.

Seven stations present the temporal and spatial variations in sediment transport throughout the Yangtze (Figure 2a). (Most data come from the *Bulletin of Yangtze River Sediment* (BYRS), 2000–2004, and from the Changjiang Water Resources Commission in China.) Between 1950 and 1986, the sediment discharge increased sharply downstream, reaching maximum levels at Yichang, downstream of which sediment trapping in Dongting Lake (Figure 1a), floodplain deposition, and channel aggradation decreased the

sediment by approximately 100 million tons per year at Hankou and Datong (Figure 2a).

Changes in Yangtze Sediment Transport

The first dramatic decline in sediment load occurred in 1987, the result of a sharp decrease (~100 million tons per year) in sediment load of the Jialing River, which enters the Yangtze at Beibei Station (Figures 1a and 2c). Low precipitation (60% below normal) and approximately 4500 dams decreased the Beibei sediment load by ~68 million tons per year [Mao and Pei, 2002]. The Project of Yangtze Upstream Water and Soil Conservation, begun in 1988, trapped an additional 30 million tons per year in the Jialing. At the same time, however, increased deforestation upstream led to a marked increase in mean annual suspended sediment concentrations at Pingshan (Figure 2b). The sharp decrease in sediment concentrations at Pingshan after 1997 was presumably related to increased reforestation.

By 2001, a number of small- and medium-sized tributary dams and reforestation efforts, particularly along the steep slopes above Pingshan (Figure 1a), had resulted in a second decrease, leading to declines of 46 and 137 million tons in sediment loads at Pingshan and Yichang, respectively, and further declines of 56 and 71 million tons in 2002 (Figure 2a).

The TGD impoundment in 2003 initiated the third severe decrease along the middle and lower reaches. In 2003–2004, sediment loads at Yichang declined by 164 million tons relative to 2002. At Datong, the 2003–2004 decline was less dramatic (128 million tons), and for the first time sediment loads were actually greater than at Yichang. By 2004, at Yichang and Datong, the Yangtze transported only 12 percent and 33 percent,

respectively, of its 1950–1986 loads. More than half of this decrease (65% and 60%) occurred prior to the TGD impoundment.

Prior to 2000, the middle and lower reaches were primarily depositional. By 2001, however, sediment loads downstream of Yichang increased, first gradually and then markedly after 2002, suggesting active erosion (Figure 2a). This marked change can be assumed to have been due to both decreased sediment storage in Dongting Lake [Du *et al.*, 2001] and channel erosion downstream of Yichang (Figure 3). Erosion along a 55-kilometer stretch between Yichang and Zhicheng (a station downstream of Yichang), for instance, amounted to 30 million cubic meters from September 2002 to October 2003 and 18 million cubic meters from October 2003 to November 2004. Assuming a bulk density of 1.3 tons per cubic meter, the eroded sediment would have been 39 and 23 million tons, representing ~30–35 percent of the increased sediment load noted between Yichang and Datong.

Between 1988 and 2000, the Project of Yangtze Upstream Water and Soil Conservation had reforested 63,000 square kilometers of the watershed [BYRS, 2000] and reduced the sediment yield extensively, especially in two high-yield regions: the Jialing River and the steep slopes above Pingshan. Moreover, a subsequent 1999–2003 conservation effort has reforested an additional 13,100 square kilometers, leading to increasing forest cover and a significant reduction (60 million tons per year) in sediment load [BYRS, 2004].

Future Changes to the Yangtze Watershed

The number of dams along the Yangtze upper reaches above Yichang, increased

from a handful in the early 1950s to approximately 12,000 by the late 1980s, and since then has increased continuously. The water storage capacity of major upstream dams totaled 27 cubic kilometers in 2000, and TGD added another 39 cubic kilometers in 2003. Ongoing or planned dams, such as Wudongde, Baihetan, Xiluodu, and Xiangjiaba, all located along the high-yield mainstream Yangtze River above Pingshan, will add another 41 cubic kilometers of total water-storage capacity. The total installed hydropower capacity of these four dams alone will be 38,500 megawatts, about double that of the TGD.

Between 1950 and 1986, sediment passing Pingshan accounted for about half of sediment passing Yichang, but in 2002 it carried about 90 percent of Yichang sediment (Figure 2a). Since these four future dams will probably trap about 70 percent of sediment passing Pingshan, sediment entering and exiting the TGD should decline quickly, leading to further decreases in the sediment loads at Yichang and Datong.

In addition to increased channel erosion and (presumably) less lateral escape of sediment-laden waters onto broad floodplains near Dongting Lake, the lower part of the Yangtze watershed should undergo increased environmental pressure. Since Datong Station is located 600 kilometers upstream from the East China Sea, very little river-borne sediment may actually reach the coastal ocean. Although the Yangtze developed slowly in its funnel-shaped estuary from 7000 to 2000 years B.P., since then it has prograded eastward rapidly (>50–100 kilometers) in response to increased sediment supply due to deforestation and agriculture. With the recent dramatic sediment decline, however, accretion in the subaqueous delta has slowed and erosion has occurred on the outer side of the delta front [Yang *et al.*, 2002]. Coastal erosion may be a particularly

troubling prospect for the Shanghai region, considering that as recently as 2000 years ago it was coastal marsh. Since the Yangtze contributes about 90 percent of the fluvially derived nutrient supply to the East China Sea, a change in the ecological character and productivity in western East China Sea waters can be anticipated.

Acknowledgments

K. Xu and J. Milliman receive support from the U.S. National Science Foundation (NSF) and Office of Naval Research (ONR). Z. Yang and H. Wang are funded through NFNSC project 90211022 in China.

References

- Bulletin of Yangtze River Sediment (2000–2004), Minist. of Water Resour. of the People's Republic of China.
- Du, Y., S. Cai, X. Zhang, and Y. Zhao (2001), Interpretation of the environmental change of Dongting Lake, middle reach of Yangtze River, China, by ^{210}Pb measurement and satellite image analysis, *Geomorphology*, 41(2-3), 171–181.
- Fuggle, R., and W. T. Smith (2000), Large dams in water and energy resource development in the People's Republic of China, Country Review Paper, Cape Town. (Available at <http://www.dams.org>)
- Mao, H., and M. Pei (2002), Influence of human activities on runoff and sediment transmitting in Jialingjiang Valley (in Chinese), *J. Soil Water Conserv.*, 16(5), 101–104.
- Yang, S.-L., Q.-Y. Zhao, and I. M. Belkin (2002), Temporal variation in the sediment

load of the Yangtze River and the influences of human activities, *J. Hydrol.*, 263(1-4), 56–71.

Author Information

Kehui Xu and John D. Milliman, School of Marine Science, College of William and Mary, Gloucester Point, Va.; E-mail: kxu@vims.edu; Zuosheng Yang and Houjie Wang, College of Marine Geosciences/Key Lab of Seafloor Science & Exploration Technology, Ocean University of China, Qingdao, Peoples Republic of China.

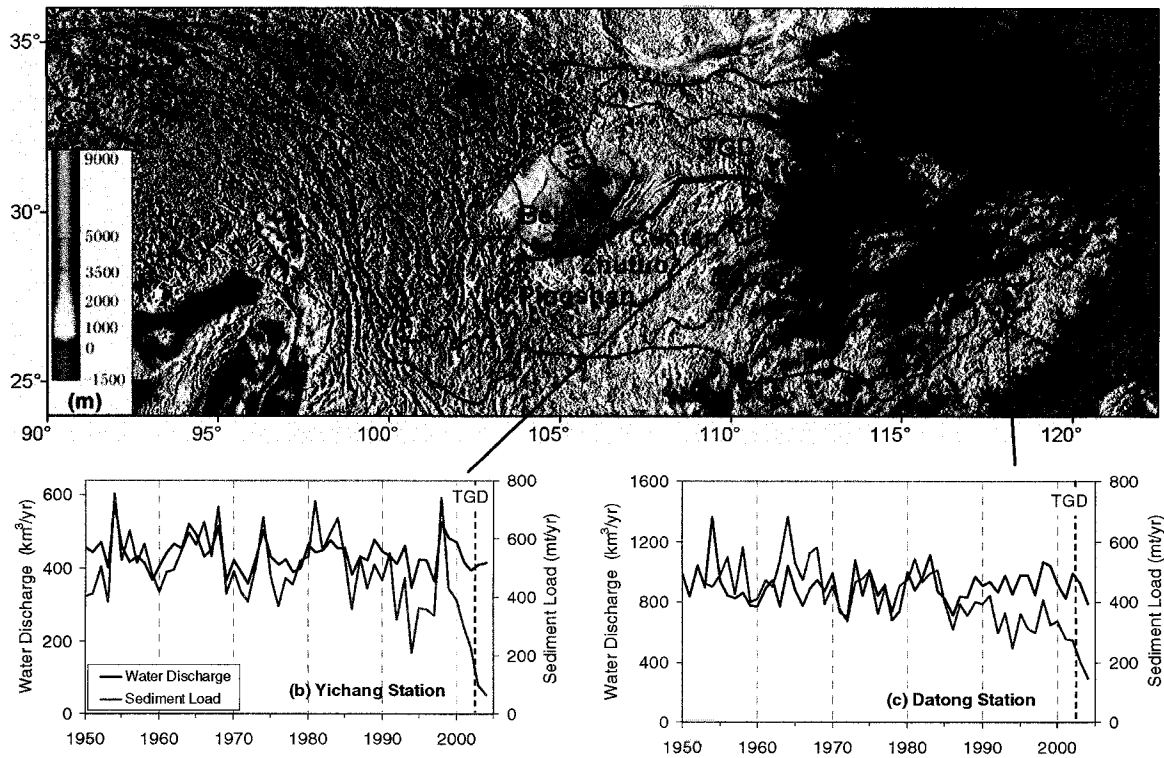


Fig. 1. (a) Yangtze River drainage basin. (b and c) Water discharge and sediment load at Yichang and Datong stations, respectively. TGD indicates Three Gorges Dam, ECS is East China Sea and mt/yr represents million tons per year. In Figure 1a, bold black curve upstream of the TGD is the impounded river channel with a length of 500 kilometers; topographic base map is modified from <http://www.ngdc.noaa.gov/mgg/image/2minrelief.html>; left color bar corresponds to elevation (in meters).

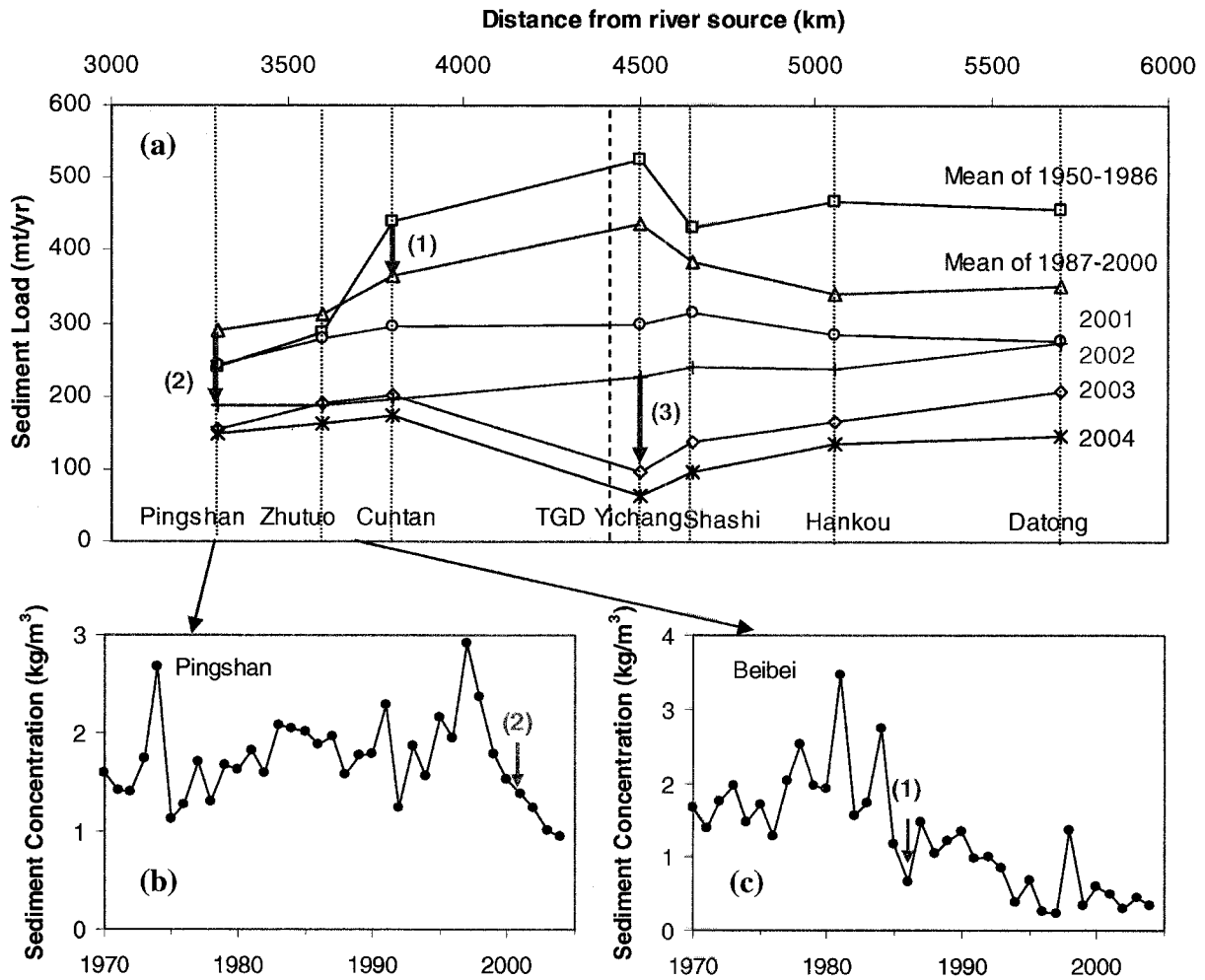


Fig. 2. (a) Sediment load at seven stations along the mainstream of the Yangtze River (locations shown in Figure 1). (b and c) Mean annual sediment concentrations at Pingshan and Beibei, respectively. mt/yr represents million tons per year. Three major sediment decreases (purple numerals 1, 2, and 3 and down arrows) correspond to the decreases at Beibei (1987), Pingshan (2001–2002), and Yichang (2003), respectively. Decreases 1, 2, and 3 are shown in greater detail in Figures 2c, 2b, and 1b, respectively. For the Pingshan, Hankou, and Datong stations, the 1950–1986 records are shorter but longer than 31 years. Means for 1950–1986 and 1987–2000 at Zhutuo Station were calculated by deducting annual loads at Beibei from those at Cuntan. Similarly, loads for these two periods at Shashi were determined by subtracting Yichang from three passages entering Dongting Lake between Yichang and Shashi.

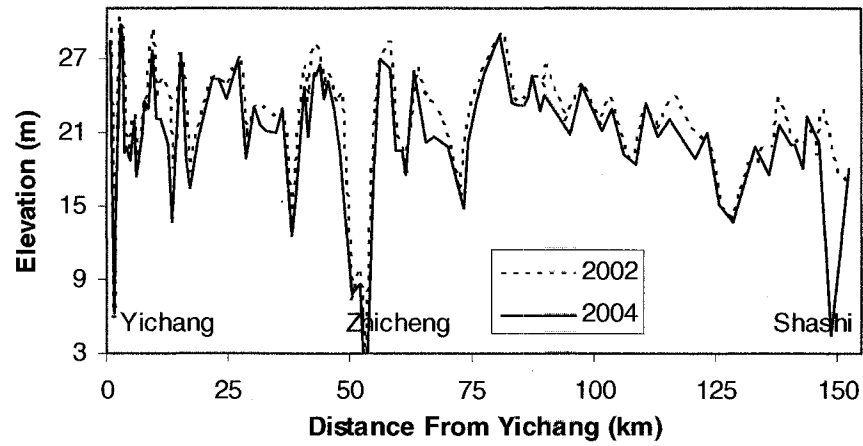


Fig. 3. Comparison of 2002 and 2004 thalweg profiles between Yichang and Shashi, connecting the lowest points of the river valley. Elevation is relative to the mean sea level. The measured dates are September 2002 and November 2004 for profiles from Yichang to Zhicheng, and October 2002 and October 2004 from Zhicheng to Shashi.

CHAPTER 5: Yangtze- and Taiwan-Derived Sediments in the Inner Shelf of East China Sea*

K.H. Xu^{a,†}, J.D. Milliman^a, A.C. Li^b, J. P. Liu^c and S.M. Wan^b

^a School of Marine Science, College of William & Mary, Gloucester Pt, VA 23062, USA,

^b Institute of Oceanology, Chinese Academy of Sciences, Qingdao, 266071, People's Republic of China;

^c Dept. of MEAS, North Carolina State University, Raleigh, NC, 27695, USA;

[†]Corresponding Author. Tel.: 1-804-684-7739; Fax: 1-804-684-7250. *E-mail address:* kxu@vims.edu.

*Prepared for *Marine Geology*

Abstract

Sediments on the inner shelf of the East China Sea reflect the mud mainly from the Yangtze River in the north as well as sandy silt and fine sand from small Taiwanese mountainous rivers in the south. X-Ray Diffraction (XRD) mineralogical analyses show that illite-dominated fine-grained sediments from the Yangtze River are transported more than 800 km southward into northern Taiwan Strait. Illite crystallinity of clay from the Choshui River draining western Taiwan Island is distinctly better than that of clays collected from Yangtze River and Taiwan Strait. Fine sands in the northern Taiwan Strait (south of 26°N), in contrast, are characterized by low feldspar/quartz and low K-feldspar/plagioclase derived primarily from the Choshui River. Both sediments are significantly different from smectite-rich mud derived from the Yellow River as well as kaolinite-dominated mud and high K-feldspar/plagioclase sand from the Min River. Grain-size distribution further confirms that ~25% of sediments (mainly sandy silt and fine sand) in northern Taiwan Strait are Taiwan-derived.

Keywords: Sediment; Mineralogy; X-Ray Diffraction; Yangtze River; East China Sea; Taiwan;

1. Introduction

Rivers provide the major route for the transport of land-derived sediments to the ocean, and mineralogical analyses have been successfully used in identifying both sediment provenances and transfer pathways. Sediments on the Amazon continental shelf, for example, consist primarily of subarkosic sand, unstable heavy minerals, and illite-rich

clay, indicating a derivation from the Andes Mountains (Gibbs, 1967; Milliman et al., 1975a and 1975b), which can be followed northwestward 1400 km to the northern Venezuelan shelf (Milliman et al., 1982; Clayton et al., 1999). Mineralogical analyses also have been used to delineate the fate of sediments delivered by other major rivers, such as the Murray-Darling (Gingele et al., 2004), Indonesian rivers (Gingele et al., 2001) and Ebro (Yuste et al., 2004).

Such mineralogical studies are particularly relevant on the continental margin in southern Asia, where more than half of global fluvial sediment discharges (Meade, 1996), derived primarily from the Himalayas. On the Bangladesh shelf, for example, epidote to garnet heavy mineral suites and high kaolinite+illite clays distinguish Brahmaputra-derived sediments from those discharged by the Ganges River (Heroy et al., 2003). Smectite/kaolinite and kaolinite/quartz ratios are effectively used as the indices of chemical weathering and physical erosion rate in the eastern Tibet Plateau and Mekong drainage basin (Liu et al., 2005).

2. Sediments in the East China Sea

This paper discusses sediments on the East China Sea (ECS) off eastern China, where the Yangtze (480 million tons per year, mt/yr) and Yellow (~1,000 mt/yr) rivers (both derived from or nearby the Himalayas) have been cited to collectively discharge ~10% of the sediments to the global oceans (Milliman and Meade, 1983; Milliman and Syvitski, 1992). Delta development and sediment dispersal of these two large rivers are quite different. During the past 7000 years, the Yangtze River mainly discharged into the ECS with continuous delta progradation southeastward (Saito et al., 2001). In contrast,

the Yellow River has emptied primarily into the Gulf of Bohai, but as recently as 1128-1855 AD it discharged into the southern Yellow Sea, ~400 km north of the Yangtze River mouth (Liu et al., 2004) (Fig. 1).

Because of the counterclockwise circulation in the ECS and Yellow Sea, with cold and brackish China Coastal Current (CCC) flowing southward along the shelf, both Yangtze- and Yellow-derived sediments are transported primarily along shelf rather than directly offshore (Fig. 1). Concentrations of total suspended solids are high close to the river mouths (>50 mg/L) and along the inner shelf (>5 mg/L), but decrease rapidly to <1 mg/L seaward in the central part of the ECS and southern Yellow Sea (Figs. 2 and 3). In the southern ECS and close to Taiwan Strait, however, sediment dispersal is more complex as mainland and Taiwanese small rivers also are potential contributors. Across the northern Taiwan Strait, concentrations decrease from 5 mg/L on the mainland side to 1 mg/L in the middle Strait, and then increase to 5 mg/L near the Taiwan Island (Fig. 3).

During the summer monsoon, the northward-flowing Kuroshio Warm Current (KWC) and Taiwan Warm Current (TWC) dominate the circulation in the eastern ECS. In contrast, the southward-flowing CCC prevails in winter in response to arctic outbreaks of cold-air masses from northern China. Sediment dispersal reflects this seasonal circulation pattern. During the summer, the Yangtze discharges the bulk of its sediment, but the TWC prevents offshore transport. As the CCC intensifies in the late autumn, the summer sediment is resuspended and transported mainly southward (DeMaster et al., 1985; Milliman et al., 1985a), although a small portion occasionally may escape eastward to the middle shelf (Yang et al., 1992; Guo et al., 2002). This dispersal pattern has been confirmed by remote sensing images, which show the sediment-rich surface plume

contracts westward towards the Yangtze mouth in September but a sediment-rich tongue extends eastward to the middle shelf in the winter and early spring (Sun et al., 2000) (Fig. 2).

Extensive mineralogical analyses have been used to identify the sediment provenances in the ECS (Fan et al., 2001; Xiong et al., 2003; Yang et al., 2003; Liu et al., 2006a). Offshore of the Yangtze mouth and along the border between Yellow and East China seas (dashed line, Fig. 1), northern Yellow-derived sediments show significantly higher smectite and Ca concentrations than do southern Yangtze-derived sediments, indicating that the fine-grained sediments in that area are derived primarily from the Yellow River (Yang and Milliman, 1983).

A number of studies also looked at the southern dispersal of Yangtze sediment into ECS. An inner-shelf mud wedge extending from the Yangtze's mouth 800 km southward has long been considered a single-source mud deposit (Liu et al., 2006b and references therein) (Fig. 4). Clay minerals in this mud belt are dominated by illite (60-75%), with low chlorite and kaolinite (10-15%, respectively) and lower smectite (5-10%), similar to the mud off the Yangtze mouth (Yang, 1988; Yang and Milliman, 1983; Aoki et al., 1983; Xu, 1983; Zhou et al., 2003). This simplistic picture, however, has several complications. Of the 480 mt/yr load measured at Datong gauging station (black dot in Fig. 4) which is 600 km upstream from the Yangtze mouth, channel aggradation and delta progradation trap about 70% of the sediment before reaching the East China Sea, leaving ~150 mt/yr sediments transported southward (Milliman et al., 1985a). Second, the 480 mt/yr sediment load cited for the Yangtze reflects neither its post-LGM (Last Glacial Maximum) mean nor its present-day discharge. Prior to 2,000

BP the river's sediment load was 215 mt/yr, increasing to 330 mt/yr in response to deforestation and agriculture on the watershed (*Chapter 5*). Since the 1980s, however, the sediment load has declined dramatically to 147 mt/yr (at Datong) in 2004 due to more than 50,000 dams (including the Three Gorges Dam) and reforestation throughout the watershed (Xu et al., 2006).

To complicate the picture further, the Yangtze may not be the only sediment source. Along the mainland side south of the Yangtze, the Qiantang, Ou and Min rivers discharge totally ~15 mt/yr to the inner-shelf mud wedge (Fig. 4). More importantly, small mountainous rivers draining Taiwan collectively can discharge ~175 to 380 mt/yr sediment into the ocean, often during typhoon-generated floods (Dadson et al., 2003 and 2004; Kao et al., 2005). A super-typhoon in 1996, for example, resulted in nine Taiwanese rivers discharging 217 mt of sediment (Milliman and Kao, 2005), more than the total Yangtze load in 2004. Total western Taiwanese river can deliver ~70 mt/yr into the Taiwan Strait, of which the Choshui River contributes 50 mt/yr (Fig. 4). Although the drainage basin of the Yangtze is >500 times larger than Choshui basin (Table 1), Choshui sediment during several typhoon events between 1995 and 2002 exceeded the load of Yangtze (Fig. 5). The mode of delivery also differs between these two rivers: with a sediment concentration of 0.5 g/L and a diluted plume off the river mouth, Yangtze sediment transport is hypopycnal. In contrast, mean sediment concentration in the Choshui is 8.3 g/L and concentrations can reach 210 g/L (Table 1). Using ~40g/L as a threshold, most of Choshui sediment transports during typhoons in 1996 (130 mt) and 2001 (>200 mt) were essentially hyperpycnal (Milliman and Kao, 2005) (Fig. 4).

Given these circumstances, how can we differentiate the possible sources of sediments to the East China Sea? How far can Yangtze-derived sediment disperse southward and eastward; and what, if any, influence is there from Taiwanese rivers? To answer these questions, we analyzed both clay and sand in samples collected from Yangtze, Qiantang, Ou, Min, and a number of Taiwanese rivers as well as surface sediments throughout the ECS. In this paper, we attempt to identify the sediment provenances, analyze the paths of sediment transport, and discuss the mechanism(s) of sediment dispersal in the inner shelf of ECS. Since both large and small mountainous rivers play major roles in the global sediment delivery (Milliman and Syvitski, 1992; Farnsworth and Milliman, 2003), the ECS provides a unique chance to study the interplay of a large river (Yangtze) and small mountainous rivers (Taiwan).

3. Material and Methods

A total of 84 samples were analyzed, including 49 samples from the mouths of Yangtze, Qiantang, Ou and Min rivers, 14 in the inner shelf of ECS (taken by box or gravity cores), 10 from the Taiwan Strait, and 11 from Taiwanese rivers (including Choshui, Wu, Tanshui and Lanyang rivers) (Fig. 6, left). Most of the samples were surface grabs except three suspended sediment samples from the Choshui River (Fig. 6).

Grain size and X-Ray diffraction (XRD) analyses were performed at the Institute of Oceanology, Chinese Academy of Science (IOCAS), Qingdao. Twenty ml of H₂O₂ (10%) were added to ~3 g of sample in a 60°C bath for 30 minutes to oxidize the organic matter. Then 50 ml of acetic acid (20%) were added to the solution in the 60°C bath for one hour to remove any carbonate minerals. After centrifuging and decanting water

several times, samples were split in half for grain size and XRD analyses. One split was dispersed and homogenized using ultrasound before passing through the CILAS Laser Particle Size Analyzer (Model: 940L).

Prior to XRD analysis, the other split was washed using a series of sieves (63, 90, 125 and 180 μm ; corresponding to phi values of 4, 3.5, 3 and 2.5, respectively). Due to differential weathering as well as provenance, the feldspar/quartz (F/Q) ratio in sand from the source is strongly size-dependent (Gibbs, 1967 and 1977; Milliman, 1972; Weaver, 1989). The F/Q of Yangtze, for example, increases from 1.1 to 1.3 as grain size decreases from 180 to 63 μm (Fig. 7, discussed later). In order to minimize this size-dependency, our sand-sized XRD analysis focused on the 63-90 μm range, the most common fraction throughout the study area; coarser sands (particularly $>180 \mu\text{m}$) were gradually absent from much of the mud wedge sediments. Sand samples were ground into fine powder in a mortar and mounted on a sample holder. One XRD run from 2θ of 4 to 31° was performed on each fine-sand fraction.

The $<63 \mu\text{m}$ fraction was washed with distilled water after each centrifugation. Samples were then dispersed in ultrasound and resuspended with 500 ml of distilled water in a glass beaker. Particles less than 2 μm in size were separated according to the Stokes Law and oriented slides were prepared (Moore and Reynolds, 1989). XRD diagrams were obtained using a Germany Bruker XRD at IOCAS with $\text{CuK}\alpha$ radiation and Ni filter, under a voltage of 40 kV and an intensity of 20 m \AA . Three XRD runs through the 2θ range of $3-30^\circ$ were performed with a 2θ scan step of 0.02° : air-dried, glycolated, and high-temperature (550°C). Identification of clay minerals was made for smectite (17 \AA), illite (10 \AA) and kaolinite/chlorite (7 \AA) on the glycolated curve using the

MacDiff software (Petschick, 2000). Kaolinite and chlorite were separated by relative proportions according to their area ratios of 3.57/3.54 Å. Semi-quantitative analysis of clay minerals followed the calculation of intensity factors provided by Biscaye (1965). Identification of fine sands were made for quartz (3.34Å), K-feldspar (3.24Å), plagioclase (3.18Å) and kaolinite+chlorite (7 Å) on the XRD curves and the calculating intensity factors were taken from Cook et al. (1975).

In addition to 84 clay samples in this paper, large amounts of clay data were collected from the literature for comparison. Clay data in both modern and old Yellow River deltas (Fig. 1) are from Xu (1983), Yang (1988), Guo et al. (1995), Xiong et al. (2003), and Yang et al. (2003). Clay data on the continental shelf of the ECS, around the Taiwan Island and near the northern South China Sea also were compiled from Chen (1973), Chen (1978), Aoki et al. (1983), He and Tang (1985), Milliman et al. (1985b), You and Tang (1992), You et al. (1993), as well as Editorial Board for Marine Atlas in China (1990).

4. Results

4.1. Grain Size

Sediments near the Yangtze mouth are dominated by silt and clay, with 10-20% sand (Fig. 6, right). Southward along the mud wedge, the sediments become finer and more homogenous, sand generally constituting <3 % of the sediment. Approaching the northern Taiwan Strait, however, sediments become somewhat coarser, and in the middle of the Strait they show a distinct peak of fine sand and sandy silt (NT2 in the right of Fig. 6). On a closer inspection, this sand-silt peak corresponds well with the grain-size

fraction of suspended sediments coming from the Choshui. In contrast, sediments from the nearshore muds off the mainland (NT1) appear similar in texture to those from the mud wedge to the north. As confirmed by the mineralogy reported below, the fine sand and sandy silt peaks in middle northern Taiwan Strait (south of 26 °N) suggest that 25% of the sediments is derived from the Choshui River (grey region in NT2; Fig. 6).

4.2. *Clays*

Glycolated XRD curves of clay samples from the Yangtze, Qiantang, Ou and the ECS are all dominated by illite (62-74%), with small amounts of chlorite (16-29%) as well as smaller amounts of kaolinite (5-15%) and smectite (4-10%) (Figs. 8 and 9). Taiwan-derived clays are also illite-dominated (71%), but contain only trace amounts of kaolinite and smectite (Figs. 8 and 9). Min clays are kaolinite-dominated (59-71%) with essentially no smectite or chlorite. The ratios of smectite to the sum of illite and chlorite in Min and Taiwan clays are much smaller than the others (Fig. 10b).

Different to all the rest, Choshui-derived clays from Taiwan show sharp peaks and an obvious hump in the 2θ range of 18-28° which apparently reflect the presence of amorphous materials (Fig. 8). Further calculations on the Full Widths at Half Maximum (FWHM) of illite peaks at 10 Å indicate that illite peaks in the Choshui clays (~0.23°) are much narrower than these from the Yangtze Delta, ECS and Taiwan Strait (0.33-0.36°) (Figs. 10a and 11).

These mineralogical differences can be discriminated in a ternary diagram of smectite, illite, and the sum of chlorite and kaolinite (Fig. 12, upper left). When only smectite, kaolinite and chlorite are considered, the ternary diagram shows the unique

nature of Taiwanese clays with the notable exception of two samples southwest of the Tanshui River mouth, which have slightly higher percentages of smectite (3%) and kaolinite (4-5%) (Figs. 9 and 12).

Clay minerals in the inner shelf of ECS thus can be divided into three types: Yangtze-like, Min-like and Taiwan-like (blue, green, and red colors, respectively, Fig. 12). From the Yangtze mouth to the northern Taiwan Strait (800 km distance), inner-shelf clay mainly is Yangtze-like (19% chlorite and 5% smectite). Taiwan-like clay displays 27% of chlorite and ~1% of smectite (Table 2). Min clay contain only of kaolinite (63%) and illite (37%). All these three types are quite different from the Yellow River-derived clays, which contain higher amounts of smectite (21%) and lesser illite (56%) than Yangtze-derived clays (Table 2; black squares on the left of Fig. 12).

4.3. Fine Sand

XRD curves of fine sands (63-90 μm) show that the Yangtze is characterized by high feldspar (including both K-feldspar and plagioclase) to quartz ratios (1.0); plagioclase is generally more abundant than k-feldspar (Figs. 13 and 14; Table 3). The Min river fine sands have a lower F/Q ratio (0.5), the feldspar being primarily K-feldspar. Choshui and Taiwan Strait also exhibit low F/Q ratios (0.5) but unlike the other rivers, contain considerable kaolinite+chlorite, recognized under the binocular microscope as mica-like minerals (Figs. 13 and 14; Table 3). The general absence of sand in the Yangtze mud wedge (Fig. 6) and the low F/Q ratios in the Taiwan Strait sands suggest that sands in the Strait must be derived from either the Min or Taiwanese rivers. However, the presence of kaolinite+chlorite and low K-feldspar/plagioclase ratio (0.8) in

Taiwan Strait strongly suggests that these sands come from Taiwan, not from the Min River (Fig. 14; Table 3).

5. Discussion and Conclusions

5.1. Clay Provenance

Yangtze clay can be followed from the Yangtze River mouth 800 km southward to the northern Taiwan Strait. It contains much lower smectite (5%) and higher illite (66%) than those of the Yellow River (21% and 56%, respectively), indicating the lack of Yellow River input to the coastal mud wedge south of the Yangtze estuary. Compared with Amazon clay sorting variations during a 1400-km transport (Gibbs, 1977), Yangtze clay shows an extremely stable character. Two small mainland rivers, the Qiantang and Ou, have essentially the same clay character as the Yangtze, a similar finding to those of He (1991) and Yang (1995). However, upstream the Ou shows a distinct local influence of pyrophyllite (Yang, 1995), suggesting that Yangtze-derived clay may overwhelm the much smaller sediment loads of these two rivers in response to energetic tidal mixing. Farther south, the illite-dominated Yangtze clay is distinctly different from the kaolinite-dominated Min clay.

Distinguishing Yangtze from Taiwan clays is more challenging. First, Yangtze and Taiwan clays are both illite-dominated and very similar to each other, although Taiwan clays show slightly lower smectite, lower kaolinite and more chlorite (Table 2; Figs. 9 and 12). Second, Taiwan clays themselves reflect input from a number of different rivers. Clays in the middle Taiwan Island (from the Choshui and Wu rivers), for instance, show trace amount of smectite and kaolinite (Figs. 9 and 12), whereas two samples

farther north show intermediate percentages of smectite and kaolinite (Figs. 9 and 12), suggesting derivation from the Tanshui River, whose sediments have slightly different mineralogies from those Choshui and Wu rivers to the south (S.J. Kao, personal communication).

Considering ~10% of inherited error of XRD clay mineralogical analysis, the differences between Yangtze and Taiwan clays (both illite-dominated) seem to be difficult to distinguish. Illite crystallinity, however, can be used to distinguish as least the Yangtze from the Choshui. The Full Width at the Half Maximum (FWHM) is an effective index, indicating the crystallinity; a narrower FWHM reflects better crystallinity (Krumm and Buggisch, 1991). Throughout the ECS, Choshui clays exhibit the narrowest FWHM, reflecting best illite crystallinity (Figs. 10 and 11). Another distinct character of Choshui clay is a hump in the 2θ range of $18-28^\circ$, which can only be found in Choshui samples (Fig. 8). Considering their relatively poor illite crystallinity and lack of any $18-28^\circ$ hump, it seems that clays in northern Taiwan Strait are Yangtze-dominated. Choshui clays may play a smaller role in the northern Strait, and it is possible that they may remain there after individual events, after which they are resuspended and transported elsewhere (discussed below).

5.2. *Fine-Sand Provenance*

Quartz and feldspar, the most ubiquitous minerals in terrigenous sand, differ significantly in their stability and durability. Quartz is exceedingly stable whereas feldspar is more susceptible to mechanical abrasion (Pettijohn, 1957) and chemical weathering. Low F/Q ratios in Taiwanese rivers therefore reflect not only parent rock but also the

climatic conditions (specifically temperature and precipitation) that help control the degree of physical and chemical weathering. Since Yangtze sediment is mainly derived from cooler western tributaries with generally low precipitation, weathering is less intense, probably resulting in a high F/Q ratio.

Because feldspar grains tend to degrade into finer-size particles (as well as into corresponding clay minerals), 180-125 μm fraction in Yangtze sediments has a mean F/Q ratio of 1.1, compared to 1.3 for the 90-63 μm size fraction; these two size fractions in the Taiwan Strait have F/Q ratios of 0.48 and 0.74, respectively (Fig. 7).

5.3. Mechanisms of Sediment Transport

Sediment distributions and provenances reflect the physical oceanographic environment in the ECS. Tides and currents, two major forcings strongly related to the sediment transport, are discussed here.

The ECS is under the control of strong semidiurnal tides and tidal currents (Larsen et al., 1985). The Yangtze mouth is in a meso-tidal regime with a spring tide range of $\sim 3\text{m}$. Based on data collected from the instrumented tripods southeast the Yangtze mouth, tidal currents are a major cause to the fine-sediment resuspension (Sternberg et al., 1983). South to the funnel-shape Qiantang River mouth, energetic tidal flushing prevents fine sediments accumulation and most of sediment disperse southward along the inner shelf (mud wedge in Fig. 4). Surface drifters in Taiwan Strait show trajectories that are strongly affected by the semidiurnal tides, particularly near the northern Taiwan Strait (Tseng and Shen, 2003).

Major inner shelf currents are the Taiwan Warm Current (TWC) and the China Coastal Current (CCC) (Fig. 1), although they show opposed seasonal intensities. In summer when CCC is weak (but the TWC is most intense), the Yangtze delivers most of its annual sediment load to the East China Sea (Fig. 15). Little of Yangtze sediment can escape offshore or southward, however, due to the blocking of TWC (Yang et al., 1992; Guo et al., 2002). Summer typhoons in the south, in contrast, can trigger hyperpycnal discharge from Taiwanese rivers (particularly the Choshui) into Taiwan Strait (Fig. 15) (Milliman and Kao, 2005). Some of this sediment may temporarily reside in the eastern part of Taiwan Strait (Milliman et al., submitted), but within months most of the typhoon-deposited mud has been removed, some perhaps into the southern Okinawa Trough via retroflection of the TWC (Tseng and Shen, 2003). Much, perhaps even most, of the sand, however, appears to remain within the Strait (S.J. Kao, oral communication).

In winter, when river discharge is reduced, energetic winter storms, however, can resuspend Yangtze mud, and the intensified CCC transports it southward along the inner shelf (DeMaster et al., 1985; Milliman et al., 1985b). In this way the Yangtze mud is mixed with Choshui-derived sand in the northern Taiwan Strait to form the multi-source sediment deposit.

5.4. Clay Assemblage in the East China Sea

Based on extensive published clay data (open dots, Fig. 16) as well as data reported in this paper (solid dots), Yellow-, Yangtze- and Taiwan-dominated clay assemblages can be delineated. Yellow-dominated clay shows relatively low illite (<64%), high smectite (>10%) and high Ca content; Yangtze-dominated clay, in contrast, has

relatively high illite (64-70%), low smectite (4-10%), low Ca concentrations, and poor illite crystallinity; Taiwan-dominated clays have the highest (and most crystalline) illite contents (>70%) and trace amounts of smectite. Yellow-River clays dominate in the northern ECS and extend into northern Okinawa Trough. Yangtze-derived clays occupy most of the middle ECS and may reach the middle Okinawa Trough. In the southern Okinawa Trough, around the Taiwan Island and close to the northern South China Sea, sediments are dominated by Taiwan-derived clays (Fig. 16).

Although this clay assemblage is the first attempt to delineate the clay dispersal and provenance throughout the whole ECS, the actual assemblage probably is more dynamic and complicated. Clay sediment transport involves initial deposition, resuspension, mixing, flocculation and interactions with the physical and biological regimes. As such, we do not exclude the possibility that some Yangtze sediment might occasionally disperse northward into the northern ECS or southward into northern South China Sea. Despite extensive mineralogical studies of fine sediments in ECS, most research has focused on the clay fraction; as shown in this paper, there are also some data concerning the sand fraction. The character and distribution of silt-size (4-63 μm) sediments, in contrast, remains unknown.

5.5. Conclusions

Sediments in the southwestern East China Sea (ECS) reflect the unique interplay of Yangtze-derived muds from the north and Taiwan-derived fine sands from Taiwan. Illite-rich Yangtze clays dominate the inner ECS whereas low feldspar/quartz Taiwan-derived fine sands are prominent in northern Taiwan Strait. Winter storms and

the China Coastal Current resuspend and transport the Yangtze mud southward along the coast. The Taiwan Warm Current (TWC) effectively winnows out mud from typhoon-derived Taiwanese sediments in the Strait, leaving primarily sand. Based on textural character, it appears that ~25% of sediment (mainly sandy silt and fine sand) in northern Strait (south of 26°N) is Taiwan-derived. A large portion of the Taiwan-derived mud appears to be transported northeastward into the southern Okinawa Trough, perhaps via the retroflection of the TWC.

Acknowledgements

We thank the crew of R/V Golden Star, P. Huang and N. Jin (IOCAS), Z. Chen and J. Chen (East China Normal University), S. J. Kao (Academia Sinica, Taiwan), as well as Saulwood Lin (National Taiwan University) for collecting many of the samples analyzed in this study. KXU and JDM were funded by the U.S. National Science Foundation (NSF) and Office of Naval Research (ONR). This paper is Contribution No.xxxx of the Virginia Institute of Marine Science, The College of William and Mary.

References

- Aoki, S., Oinema, K., Okuda, K. and Matsuike, K., 1983. Clay mineral composition in surface sediments and the concentration of suspended matter of the East China Sea. Proceedings of international symposium on sedimentation on the continental shelf, with special reference to the East China Sea, 1, Hangzhou, China: 473-482.
- Biscaye, P.E., 1965. Mineralogy and sedimentation of recent deep-sea clay in the Atlantic Ocean and adjacent seas and oceans. Geol Soc Am Bull, 76(7): 803-831.

- Chen, P.Y., 1973. Clay minerals distribution in the sea-bottom sediments neighboring Taiwan Island and northern South China Sea. *Acta Oceanologica Taiwanica*, 3: 75-97.
- Chen, P.Y., 1978. Minerals in bottom sediment of the South China Sea. *Geological Society of America Bulletin*, 89: 211-222.
- Clayton, T., Pearce, R.B. and Peterson, L.C., 1999. Indirect climatic control of the clay mineral composition of Quaternary sediments from the Cariaco basin, northern Venezuela (ODP Site 1002). *Marine Geology*, 161(2-4): 191-206.
- Cook, H.E., Johnson, P.D., Matti, J.C. and Zemmels, I., 1975. Methods of sample preparation and x-ray diffraction analysis in x-ray mineralogy laboratory. In: A.G. Kaneps (Editor), *Init. Rep. DSDP XXVIII*. Printing Office, Washington, DC, pp. 999-1007.
- Dadson, S.J. et al., 2003. Links between erosion, runoff variability and seismicity in the Taiwan orogen. *Nature*, 426(6967): 648-651.
- Dadson, S.J. et al., 2004. Earthquake-triggered increase in sediment delivery from an active mountain belt. *Geology*, 32(8): 733-736.
- DeMaster, D.J., McKee, B.A., Nittrouer, C.A., Qian, J. and Cheng, G., 1985. Rates of sediment accumulation and particle reworking based on radiochemical measurements from continental shelf deposits in the East China Sea. *Continental Shelf Research*, 4(1-2): 143-158.
- Editorial Board for Marine Atlas in China, 1990. *Marine Atlas of Bohai Sea, Yellow Sea and East China Sea (Geology and Geophysics)*, China Ocean Press, Beijing, 99 pp.
- Fan, D., Yang, Z., Mao, D. and Guo, Z., 2001. Clay minerals and geochemistry of the

- sediments from the Yangtze and Yellow rivers (in Chinese, with English abstr.).
Marine Geology & Quaternary Geology, 21(4): 7-12.
- Fang, T.-H., 2004. Phosphorus speciation and budget of the East China Sea. Continental Shelf Research, 24(12): 1285-1299.
- Farnsworth, K.L. and Milliman, J.D., 2003. Effects of climatic and anthropogenic change on small mountainous rivers: the Salinas River example. Global and Planetary Change, 39(1-2): 53-64.
- Gibbs, R.J., 1967. The geochemistry of the Amazon River system; part I, The factors that control the salinity and the composition and concentration of the suspended solids. Geol Soc Am Bull, 78(10): 1203-1232.
- Gibbs, R.J., 1977. Clay mineral segregation in the marine environment. Journal of Sedimentary Petrology, 47(1): 237-243.
- Gingele, F.X., De Deckker, P. and Hillenbrand, C.-D., 2001. Clay mineral distribution in surface sediments between Indonesia and NW Australia -- source and transport by ocean currents. Marine Geology, 179(3-4): 135-146.
- Gingele, F.X., De Deckker, P. and Hillenbrand, C.-D., 2004. Late Quaternary terrigenous sediments from the Murray Canyons area, offshore South Australia and their implications for sea level change, palaeoclimate and palaeodrainage of the Murray-Darling Basin. Marine Geology, 212(1-4): 183-197.
- Guo, Z.G., Yang, Z.S. and Wang, Z.X., 1995. Influence of water masses on the distribution of seafloor sediments in the Huanghai Sea and the East China Sea (in Chinese, with English abstr.). Journal of Ocean University of Qingdao, 25(1): 75-84.
- Guo, Z.G., Yang, Z.S., Zhang, D.Q., Fan, D.J. and Lei, K., 2002. Seasonal distribution of

- suspended matter in the northern East China Sea and barrier effect of current circulation on its transport (in Chinese, with English abstr.). *Acta Oceanologica Sinica*, 24(5): 71-80.
- He, J. and Tang, Z., 1985. Clay minerals on northeastern waters of the South China Sea (in Chinese, with English abstr.). *Tropical Oceanography*, 4(3): 46-51.
- He, S., 1991. Comparative study on terrigenous mineral component of sediment along nearshore area of the East China Sea (in Chinese, with English abstr.). *Journal of East China Normal University (Natural Science)*, 1: 78-86.
- Heroy, D.C., Kuehl, S.A. and Goodbred, S.L., 2003. Mineralogy of the Ganges and Brahmaputra Rivers: implications for river switching and Late Quaternary climate change. *Sedimentary Geology*, 155(3-4): 343-359.
- Kao, S.J., Lin, F.J. and Liu, K.K., 2003. Organic carbon and nitrogen contents and their isotopic compositions in surficial sediments from the East China Sea shelf and the southern Okinawa Trough. *Deep Sea Research Part II: Topical Studies in Oceanography*, 50(6-7): 1203-1217.
- Kao, S.J., Lee, T.Y. and Milliman, J.D., 2005. Calculating highly fluctuated suspended sediment fluxes from mountainous rivers in Taiwan. *Terres. Atmos. Ocean. Sci.*, 16(3): 441-432.
- Krumm, S. and Buggisch, W., 1991. Sample preparation effects on illite crystallinity measurements: grain size gradation and particle orientation. *J. Metam. Geol.* 9, 671-677.
- Larsen, L.H., Cannon, G.A. and Choi, B.H., 1985. East China Sea tide currents. *Continental Shelf Research*, 4(1-2): 77-103.

- Liu, J.P., Milliman, J.D., Gao, S. and Cheng, P., 2004. Holocene development of the Yellow River's subaqueous delta, North Yellow Sea. *Marine Geology*, 209(1-4): 45-67.
- Liu, J.P. et al., 2006a. Sedimentary features of the Yangtze River-derived alongshore clinoform deposit in the East China Sea. *Continental Shelf Research* (In Press).
- Liu, J.P. et al., 2006b. Flux and Fate of Yangtze River Sediment Delivered to the East China Sea. *Geomorphology* (In Press).
- Liu, Z. et al., 2005. Late Quaternary climatic control on erosion and weathering in the eastern Tibetan Plateau and the Mekong Basin. *Quaternary Research*, 63(3): 316-328.
- Meade, R.H., 1996. River-sediment inputs to major deltas. In: J. Milliman and B. Haq (Editors), *Sea-Level Rise and Coastal Subsidence*. Kluwer, London, pp. 63-85.
- Milliman, J.D., 1972. Atlantic continental shelf and slope of the United States - Petrology of the sand fraction of sediments, northern New Jersey to Southern Florida. United States Government Printing Office, Washington, 40 pp.
- Milliman, J.D., Summerhayes, C.P. and Barretto, H.T., 1975a. Oceanography and suspended matter off the Amazon River, February-March 1973. *Journal of Sedimentary Petrology*, 45(1): 189-206.
- Milliman, J., Summerhayes, C.P. and Barretto, H.T., 1975b. Quaternary sedimentation on the Amazon continental margin; a model. *Geol Soc Am Bull*, 86(5): 610-614.
- Milliman, J.D., 1982. Depositional patterns of modern Orinoco/Amazon muds on the northern Venezuelan shelf. *Journal of Marine Research*, 40(3): 643-657.
- Milliman, J.D. and Meade, R.H., 1983. World-wide delivery of sediment to the oceans.

- Journal of Geology, 91(1): 1-21.
- Milliman, J.D., Shen, H.T., Yang, Z.S. and H. Mead, R., 1985a. Transport and deposition of river sediment in the Changjiang estuary and adjacent continental shelf. *Continental Shelf Research*, 4(1-2): 37-45.
- Milliman, J.D., Beardsley, R.C., Yang, Z.S. and Limeburner, R., 1985b. Modern Huanghe-derived muds on the outer shelf of the East China Sea: identification and potential transport mechanisms. *Continental Shelf Research*, 4(1-2): 175-188.
- Milliman, J.D. and Syvitski, J.P.M., 1992. Geomorphic/tectonic control of sediment discharge to the ocean: the importance of small mountainous rivers. *Journal of Geology*, 100(5): 525-544.
- Milliman, J.D. and Kao, S.-J., 2005. Hyperpycnal Discharge of Fluvial Sediment to the Ocean: Impact of Super-Typhoon Herb (1996) on Taiwanese River. *J. of Geology*, 113, 503-516.
- Moore, D.M. and Reynolds, R.C., 1989. X-Ray Diffraction and the Identification and Analysis of Clay Minerals. Oxford University Press, New York, 332 pp.
- Petschick, R., 2000. MacDiff 4.2.5, available at <http://servermac.geologie.uni-frankfurt.de/Rainer.html>.
- Pettijohn, F.J., 1957. *Sedimentary Rocks*. Harper & Brothers, New York, 718 pp.
- Saito, Y., Yang, Z. and Hori, K., 2001. The Huanghe (Yellow River) and Changjiang (Yangtze River) deltas: a review on their characteristics, evolution and sediment discharge during the Holocene. *Geomorphology*, 41(2-3): 219-231.
- Sternberg, R.W., Larsen, L.H. and Miao, Y., 1983. Near bottom flow conditions and associated sediment transport on the East China Sea continental shelf. *Proceedings*

- of international symposium on sedimentation on the continental shelf, with special reference to the East China Sea, 2, Hangzhou, China: 522-535.
- Sun, X.G., Fang, M. and Huang, W., 2000. Spatial and temporal variations in suspended particulate matter transport on the Yellow and East China Sea shelf (in Chinese, with English abstr.). *Oceanologia Et Limnologia Sinica*, 31(6): 581-587.
- Tseng, R.-S. and Shen, Y.-T., 2003. Lagrangian observations of surface flow patterns in the vicinity of Taiwan. *Deep Sea Research Part II: Topical Studies in Oceanography*, 50(6-7): 1107-1115.
- Weaver, C.E., 1989. *Clay, Muds and Shales*. Elsevier Press, 820 pp.
- Xiong, Y., Yang, Z. and Liu, Z., 2003. A review of source study of the Changjiang and Yellow River Sediments (in Chinese, with English abstr.). *Advances in Marine Science*, 21(3): 355-362.
- Xu, D., 1983. Mud Sedimentation on the East China Sea Shelf. *Proceedings of international symposium on sedimentation on the continental shelf, with special reference to the East China Sea*, 2, Hangzhou, China: 544-556.
- Xu, K.H., Milliman, J.D., Yang, Z.S. and Wang, H.J., 2006. Yangtze Sediment Decline Partly from Three Gorges Dam. *EOS Transactions*, 87(19): 185,190.
- Yang, S.Y., Jung, H.S., Lim, D.I. and Li, C.X., 2003. A review on the provenance discrimination of sediments in the Yellow Sea. *Earth-Science Reviews*, 63(1-2): 93-120.
- Yang, X., 1995. Clay minerals of suspended sediments in Oujiang River (in Chinese, with English abstr.). *Marine Science Bulletin*, 14(3): 86-92.
- Yang, Z., Guo, Z., Wang, Z., XU, J. and Gao, W., 1992. The overall pattern of total

- suspended solids dispersal to the Yellow and East China Sea (in Chinese, with English abstr.). *Acta Oceanologica Sinica*, 14(2): 81-90.
- Yang, Z. and Milliman, J.D., 1983. Fine-grained sediment of Changjiang and Huanghe rivers and sediment sources of East China Sea. Proceedings of international symposium on sedimentation on the continental shelf, with special reference to the East China Sea, 1, Hangzhou, China: 436-446.
- Yang, Z.S., 1988. Mineralogical assemblages and chemical characters of clays from sediments of the Yellow, Changjiang and Pearl rivers and their relations to the climate environments in their sediment source areas (in Chinese, with English abstr.). *Oceanologia et Limnologia Sinica*, 19(4): 336-346.
- You, Z. and Tang, J., 1992. Preliminary study on clay minerals of sediments in western Taiwan Strait (in Chinese, with English abstr.). *Acta Sedimentologica Sinica*, 10(4): 129-136.
- You, Z., Tang, J. and Liao, L., 1993. Studies on clay mineral in sediment cores from western Taiwan Strait (in Chinese, with English abstr.). *Journal of Oceanography in Taiwan Strait*, 12(1): 1-7.
- Yuste, A., Luzon, A. and Bauluz, B., 2004. Provenance of Oligocene-Miocene alluvial and fluvial fans of the northern Ebro Basin (NE Spain): an XRD, petrographic and SEM study. *Sedimentary Geology*, 172(3-4): 251-268.
- Zhou, X., Gao, S. and Jia, J., 2003. Preliminary evaluation of the stability of Changjiang clay minerals as fingerprints for material source tracing (in Chinese, with English abstr.). *Oceanologia et Limnologia Sinica*, 34(6): 683-692.

Table 1 Comparison of the Yangtze River with the Choshui River

Type	Yangtze River	Choshui River
Drainage Basin ($\times 1000 \text{ km}^2$)	1900	3.3
Water Discharge (km^3/yr)	874	6
Sediment Load (million tons)	480* (150 southward)	50
Sediment Concentration (g/L)	0.5	8.3 (210 maximum)
Sediment Yield ($\text{t}/\text{km}^2/\text{yr}$)	250	20,000
Type of Sediment Transport	Hypopycnal	Mainly hyperpycnal

*total sediment load from the Yangtze in 2004 was 147 million tons.

Table 2 Clay percentages of smectite, illite, kaolinite and chlorite.

Type	Sample Numbers	Smectite	Illite	Kaolinite	Chlorite
Yangtze-Like	58	5	66	9	19
Min-Like	5	0	37	63	0
Taiwan-Like	11	1	71	1	27
Yellow-Like	13	21	56	10	13

Table 3 Mineral ratios in fine-sand fraction (63-90 μm)

Type	Sample Numbers	Feldspar[*] /Quartz	K-feldspar /Plagioclase	Kaolinite /Quartz
Yangtze ⁺	7	1.0	0.5	0.1
Min	4	0.5	1.8	0.0
Choshui	6	0.5	0.8	0.2
Taiwan Strait	6	0.5	0.8	0.1

⁺ including samples in the inner shelf north of 27 °N

^{*} including both K-feldspar and Plagioclase

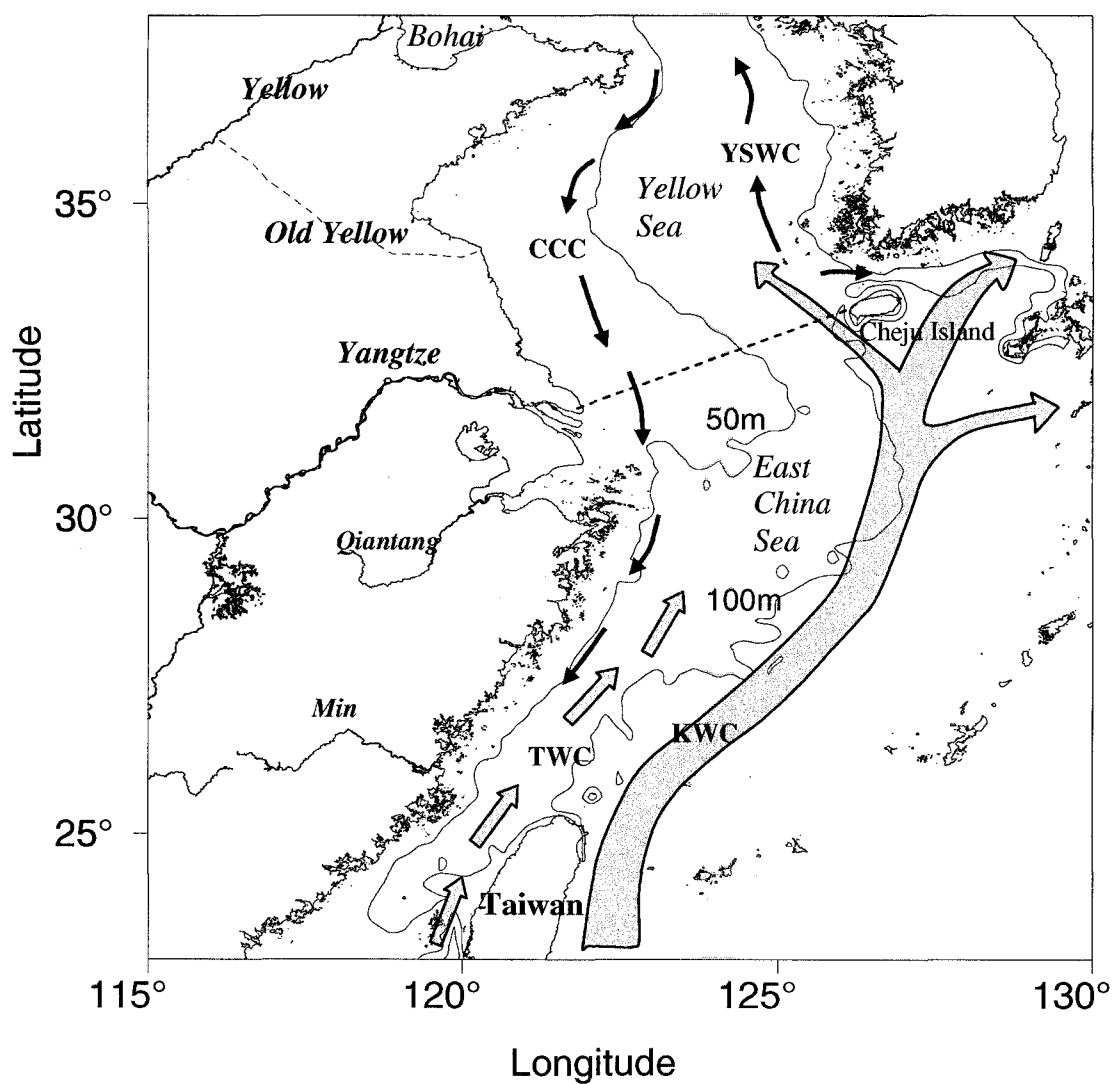


Fig. 1. Bathymetry and major currents in the East China Sea and Yellow Sea. KWC, Kuroshio Warm Current; TWC, Taiwan Warm Current; CCC, China Coastal Current; YSWC, Yellow Sea Warm Current. Dashed line from Yangtze mouth to Cheju Island is the dividing line between East China Sea and Yellow Sea.

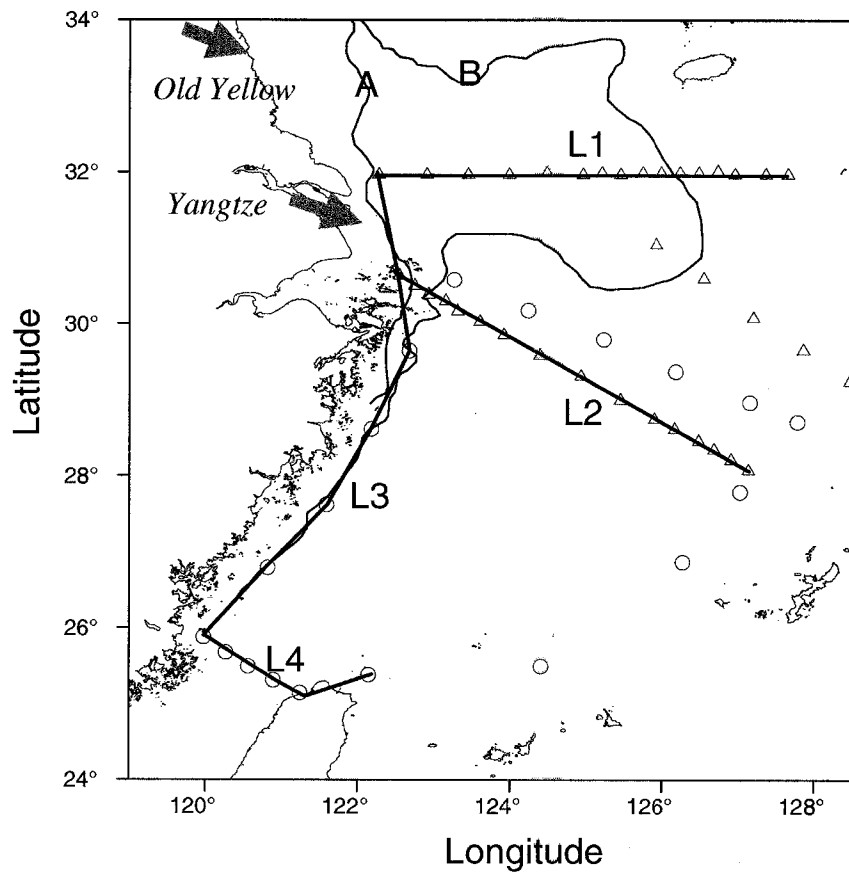


Fig. 2. Dispersal of total suspended solids (TSS) in the surface and water-column of ECS. Based on NOAA AVHRR remote sensing images, Line A and B are the eastern dispersal extents of surface TSS in September and March, respectively (Sun et al., 2000). TSS contracts westward towards the Yangtze mouth in September due to strong northward Taiwan Warm Current whereas it disperses eastward to the middle shelf in March due to weakened Taiwan Warm Current and intensified southward China Coastal Current. Triangles (Guo et al., 2002) and circles (Fang, 2004) are stations to collecting the TSS samples in the water columns and four profiles are shown in Fig. 3.

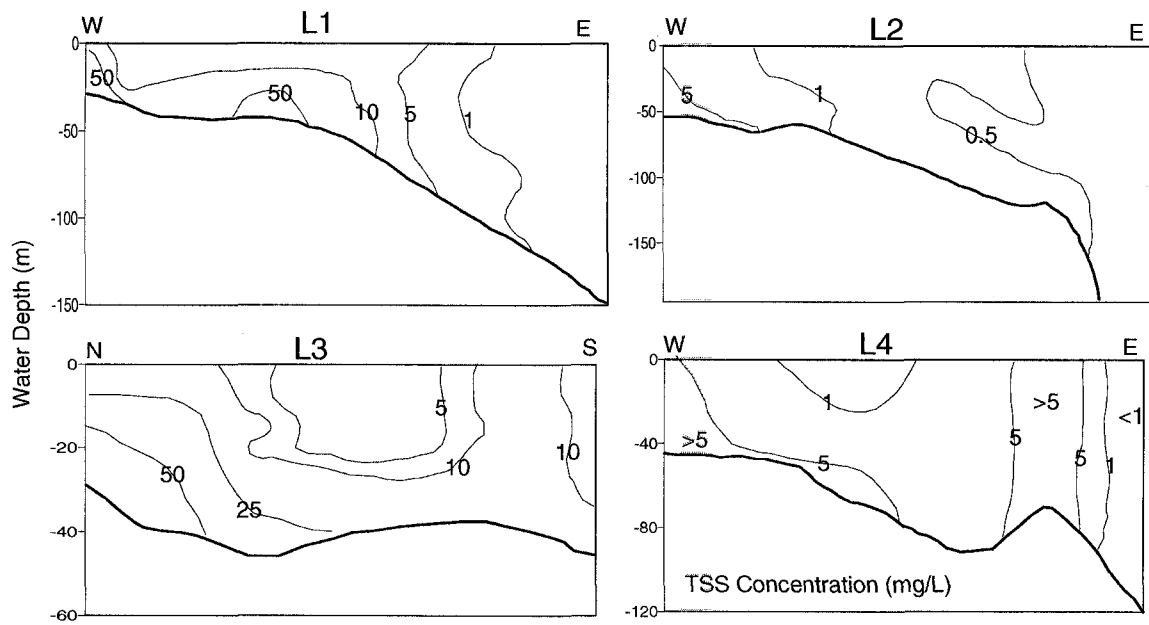


Fig. 3. Total suspended solids (TSS) concentration in profiles of L1, L2, L3 and L4. See Fig. 2 for data sources and the locations of profiles. TSS is generally high close to the Yangtze River mouth and near the inner shelf but low in the middle to outer shelf.

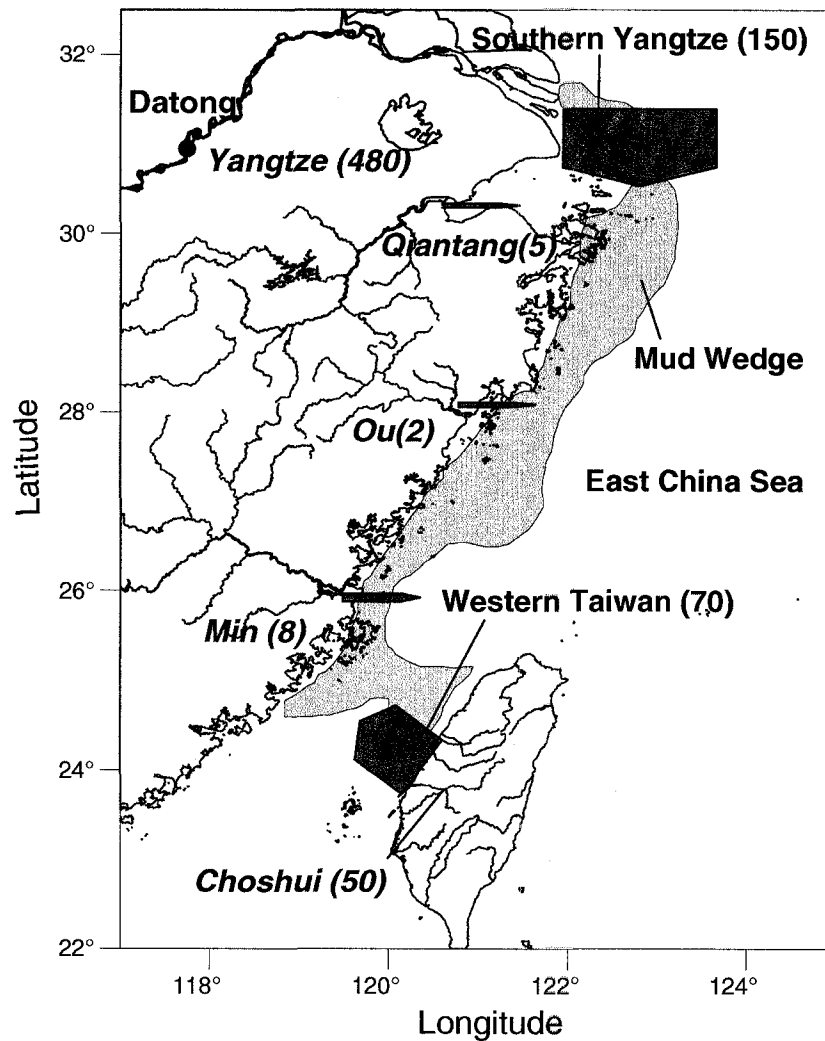


Fig. 4. Relative sediment loads entering the inner shelf of East China Sea. The numbers in parentheses are sediment loads in million tons per year (mt/yr). Yangtze sediment passing Datong Station (black dot) is ~480 mt/yr, of which about 150 mt/yr disperses to the south to facilitate the formation the mud wedge (grey belt) in the inner shelf. In contrast, total western Taiwanese rivers loads are ~70 mt/yr, of which 50 mt/yr are transferred by the Choshui River. The location of mud wedge is from Kao et al. (2003).

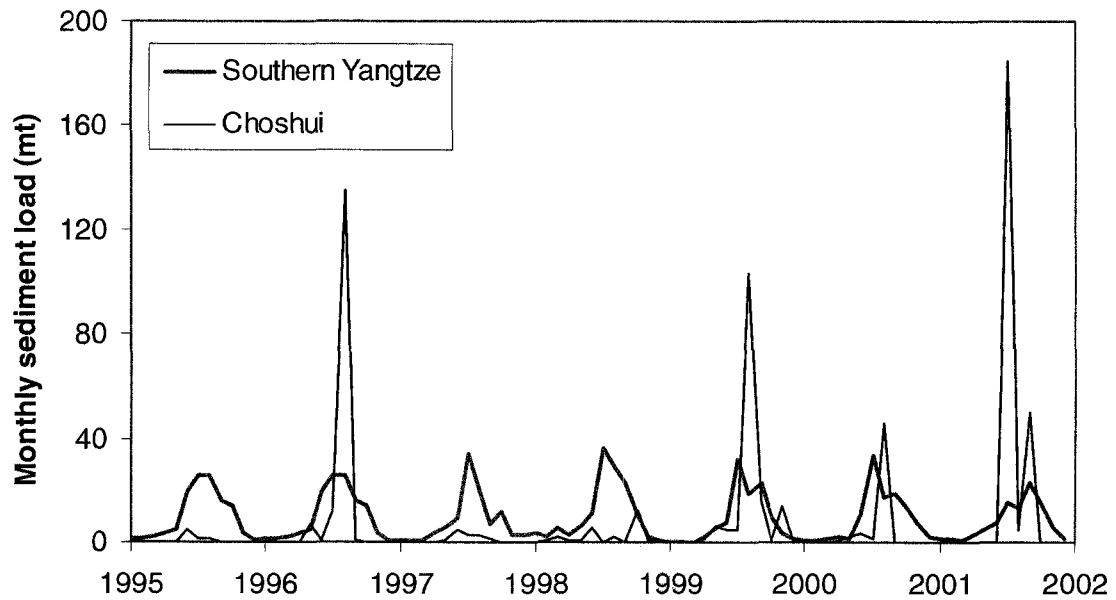


Fig. 5. Comparison of monthly loads of Yangtze sediment (transported southward) with that of Choshui. Yangtze sediment is gradual and continuous whereas Choshui is very spiky and episodic. Choshui peaks were mainly caused by summer typhoons and/or earthquakes.

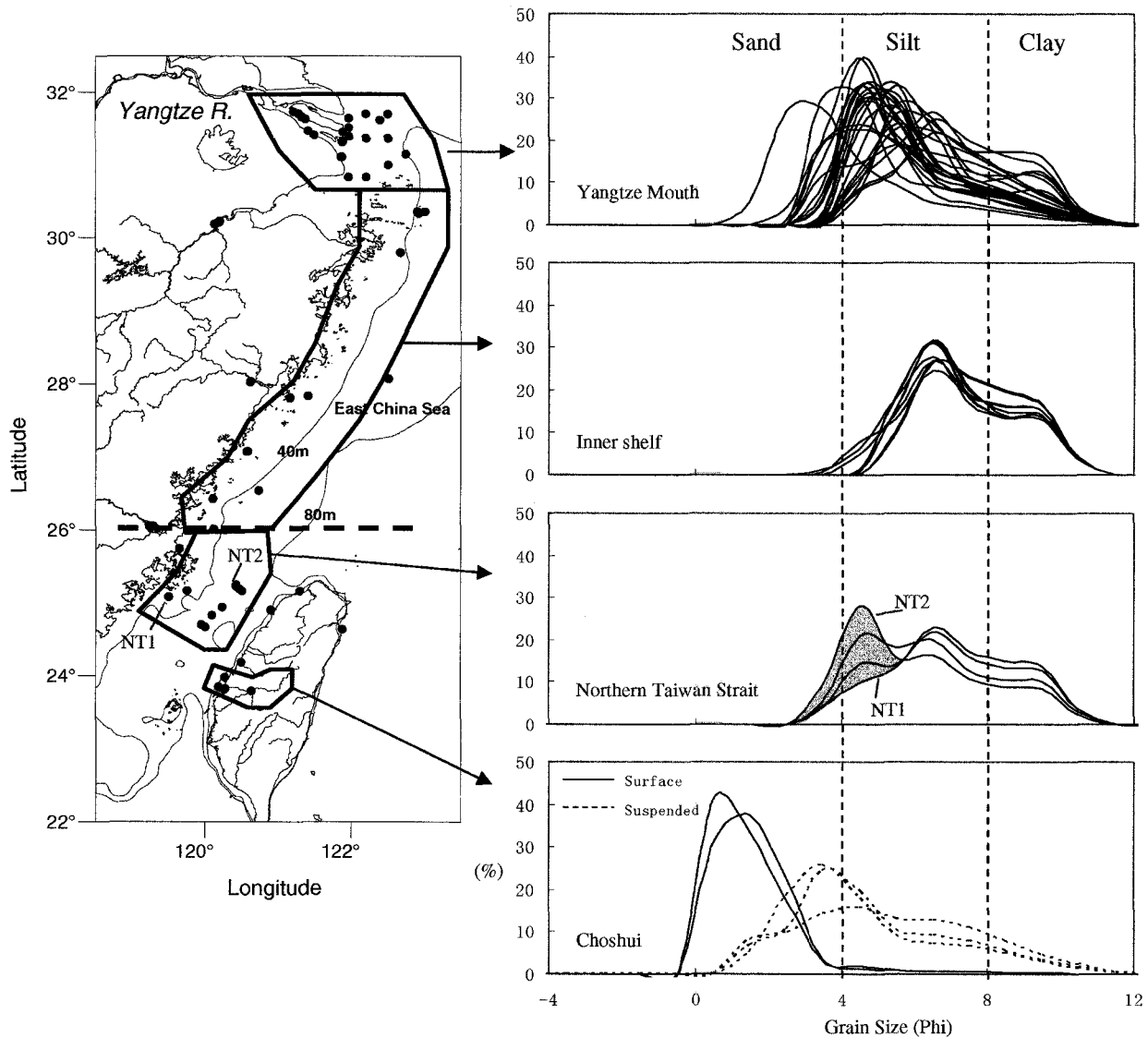


Fig. 6. Samples collected in the inner shelf of East China Sea and nearby rivers (left), and their grain size distributions (right). Most samples are surface type except the suspended ones collected from the Choshui River during a typhoon event in 2004. Sediments near the Yangtze mouth and inner shelf are mainly bimodal, but they become trimodal when entering the northern Taiwan Strait. The new peak (e.g., Sample NT2) indicates that in the northern Strait south of 26°N about 25% of sediments (grey area) come from Taiwan.

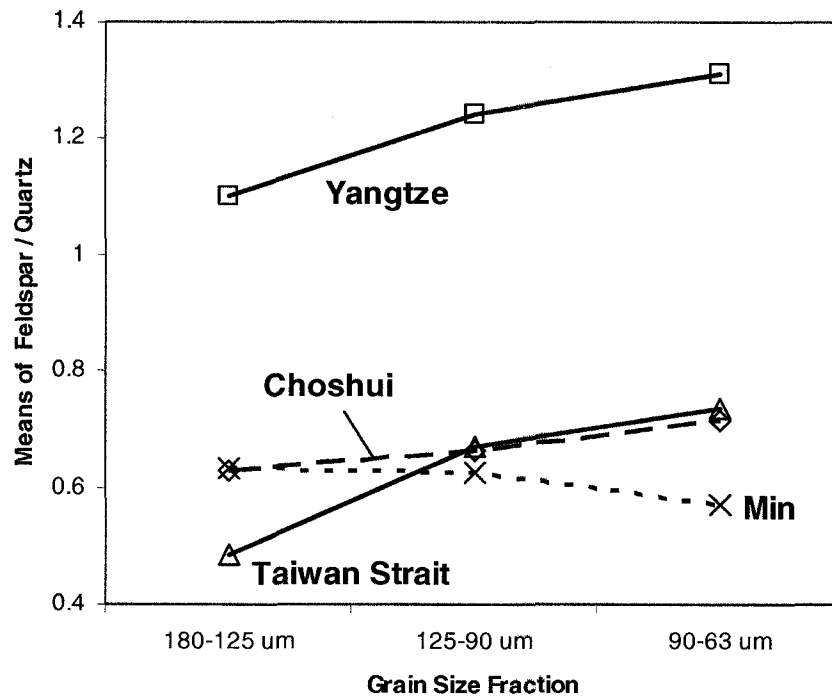


Fig. 7. Feldspar to quartz ratios of sand samples in three grain-size fractions (180-125, 125-90 and 90-63 μm). Due to differential weathering as well as the provenance, the ratios in sand are strongly size-dependent. Ratios in Taiwan Strait are close to those in Choshui and Min, but unlike the Yangtze.

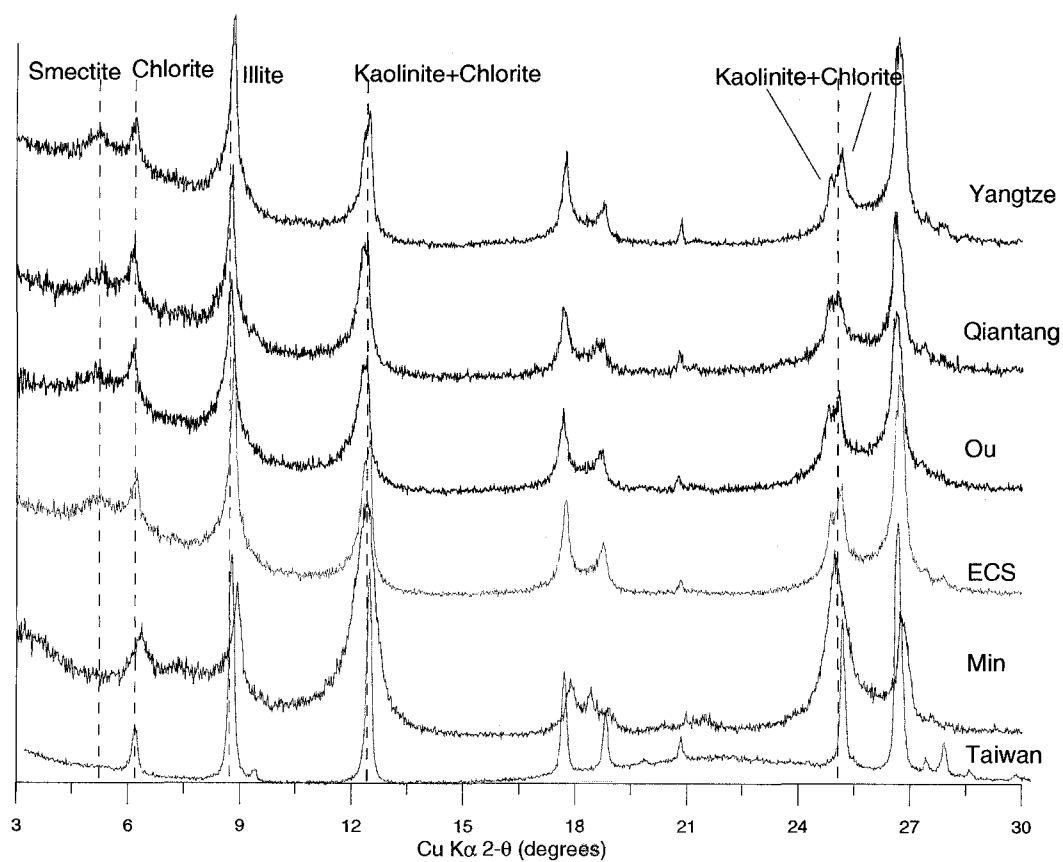


Fig. 8. Glycolated XRD curves of clay samples (<2 μm) from Yangtze, Qiantang, Ou, Min and Choshui (Taiwan) rivers as well as the East Chins Sea.

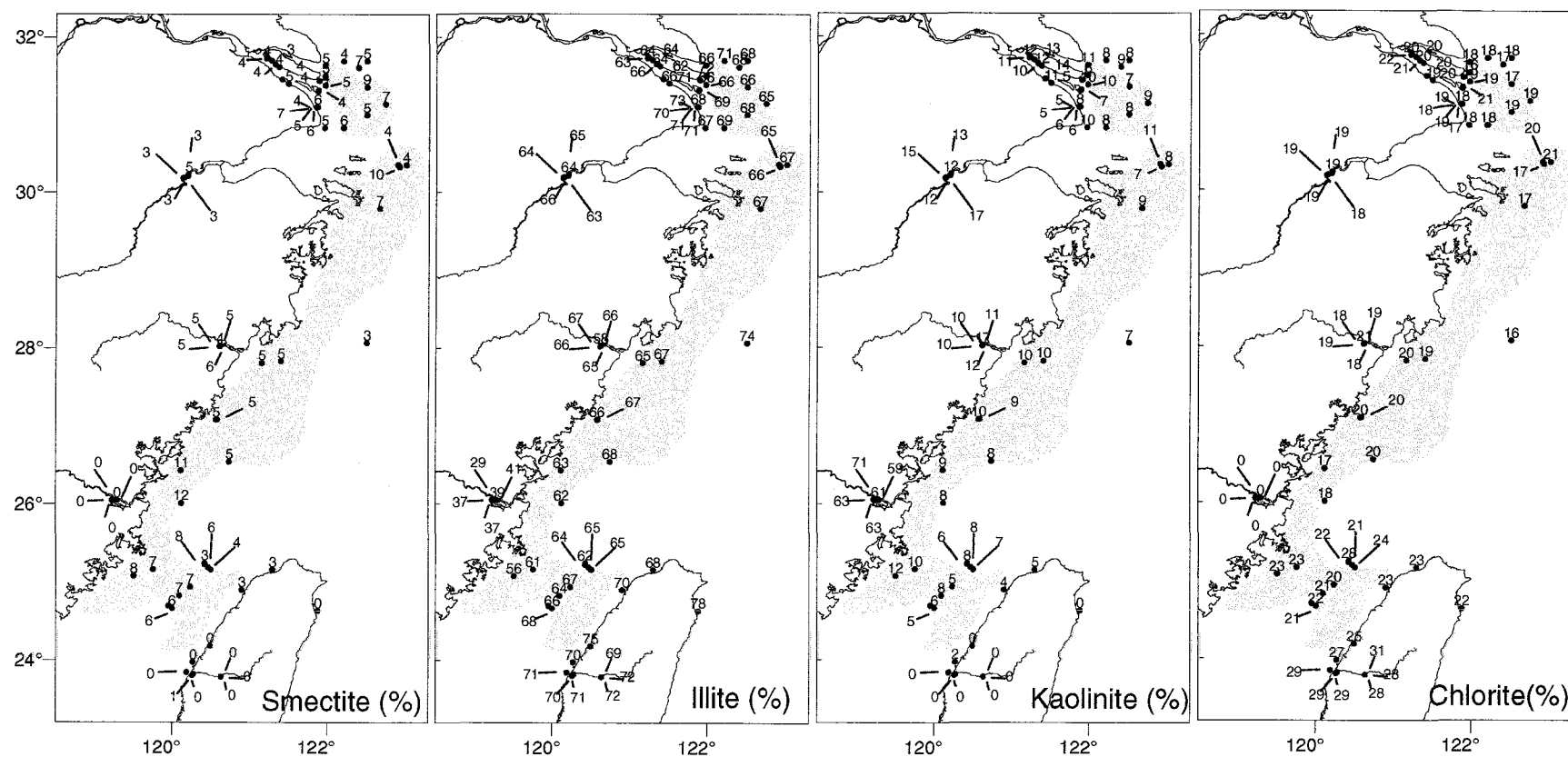


Fig. 9. Clay percentages in the inner East China Sea and nearby rivers. The grey belt is the mud wedge (Kao et al., 2003) along the inner shelf.

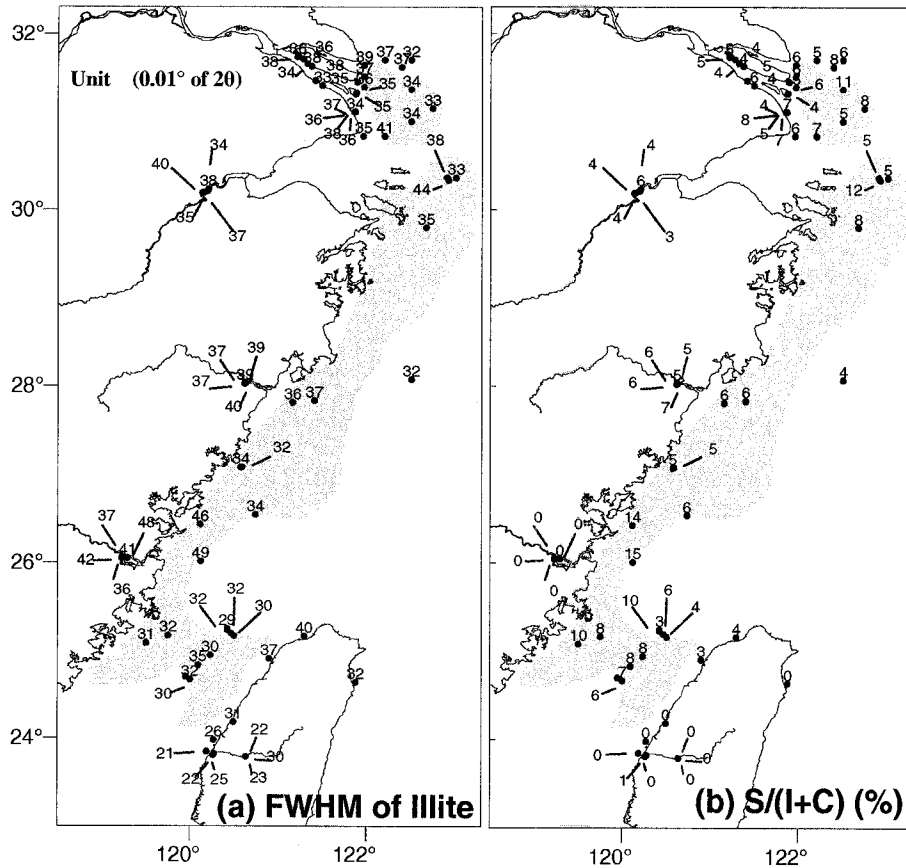


Fig. 10. (a) Full Width at Half Maximum (FWHM) of illite with a unit of 0.01 degree of 2θ. Lower FWHM indicates a better crystallinity. (b) The percentage of smectite (S) to the sum of illite (I) and chlorite (C). The grey belt is the mud wedge (Kao et al., 2003) in the inner shelf.

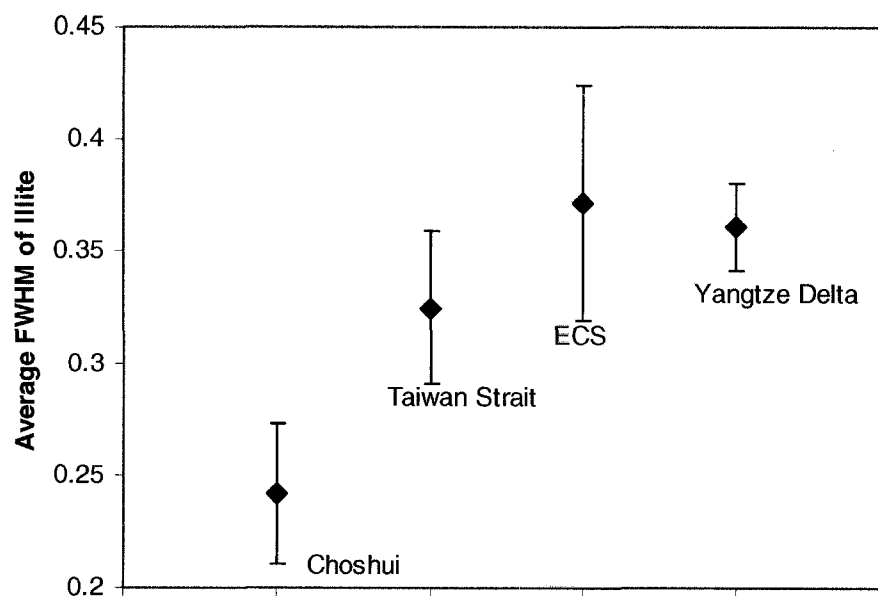


Fig. 11. Average Full Widths at Half Maximum (FWHM) of illite in Choshui River, Taiwan Strait ($<26^{\circ}\text{N}$), East China Sea (ECS, $26-30.5^{\circ}\text{N}$) and Yangtze Delta ($>30.5^{\circ}\text{N}$).

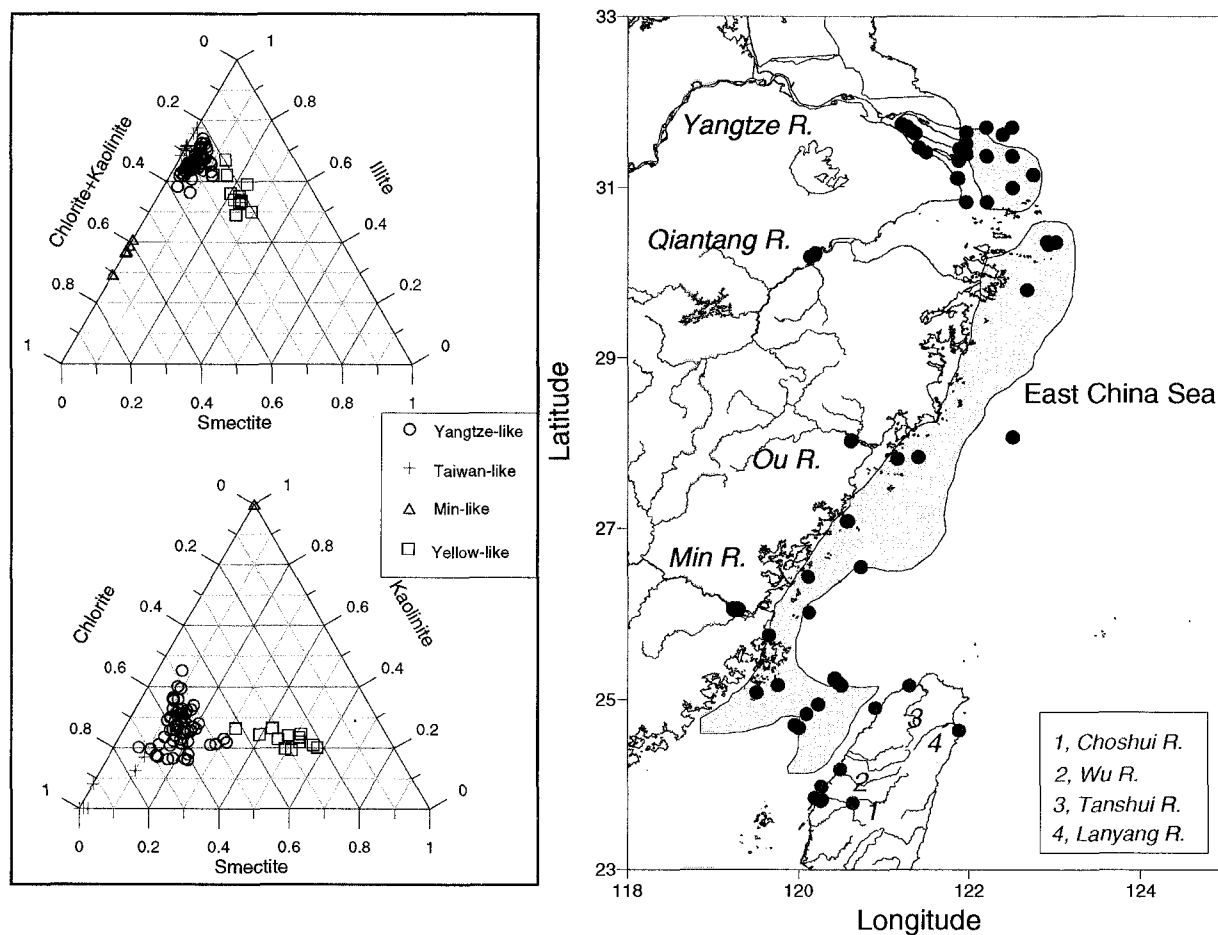


Fig. 12. Classification of clays in the inner shelf of East China Sea. For both left and right panels, blue, green and red colors correspond to Yangtze-, Min- and Taiwan-like clays, respectively. The black squares on the left are clays from Yellow samples collected mainly from old and modern Yellow River deltas (Xu, 1983; Yang, 1988; Guo et al., 1995; Xiong et al., 2003; Yang et al., 2003). The yellow belt on the right is the mud wedge in the inner shelf (Kao et al., 2003).

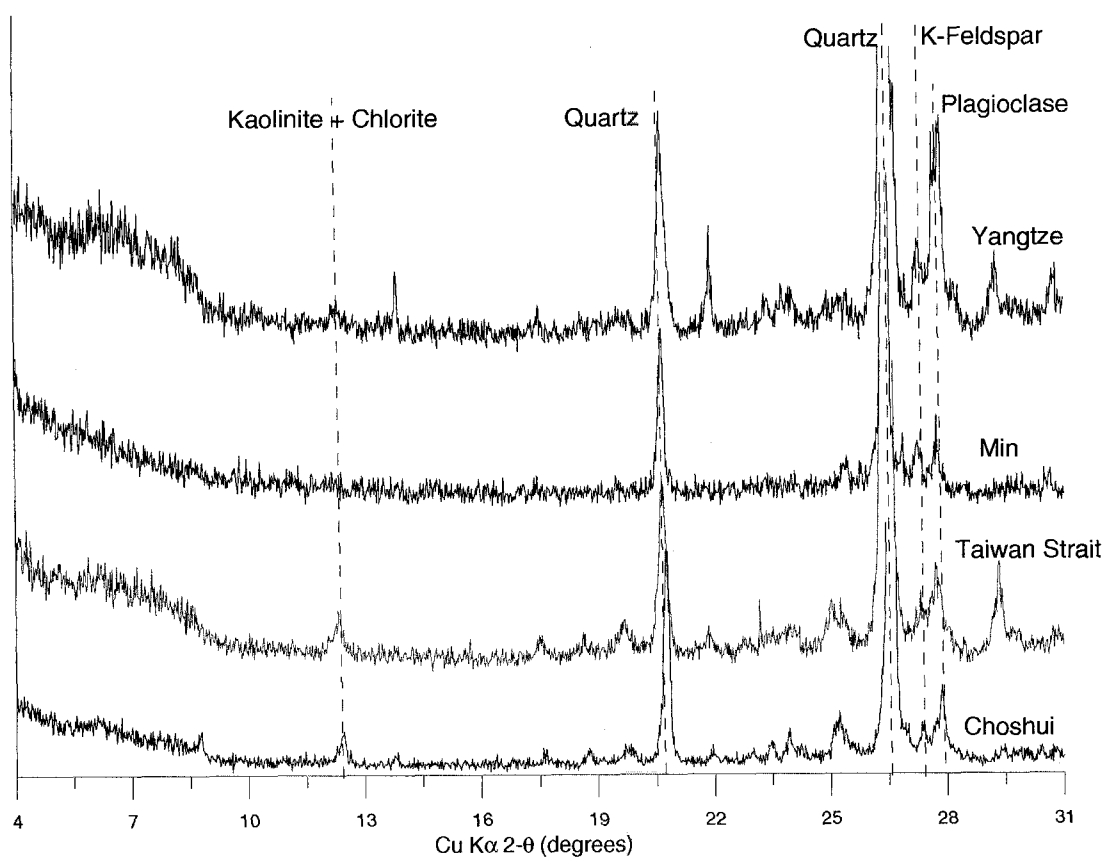


Fig. 13. XRD curves of fine sand (63-90μm) samples from Yangtze, Min and Choshui rivers as well as the Taiwan Strait.

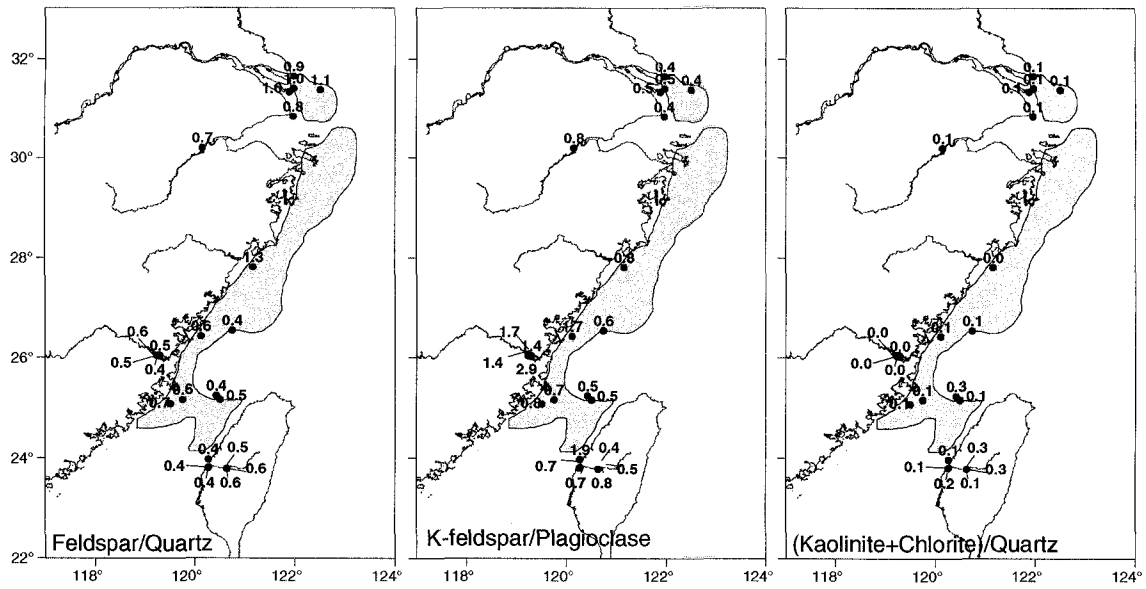


Fig. 14. Mineral ratios of fine-sand (63-90um) samples from ECS and nearby rivers. Quartz, K-feldspar, plagioclase and kaolinite+chlorite are calculated from 20 of 20.8, 24.9, 25.2 and 12.4, respectively. Feldspar includes both K-feldspar and plagioclase. The grey belt is the inner-shelf mud wedge (Kao et al., 2003).

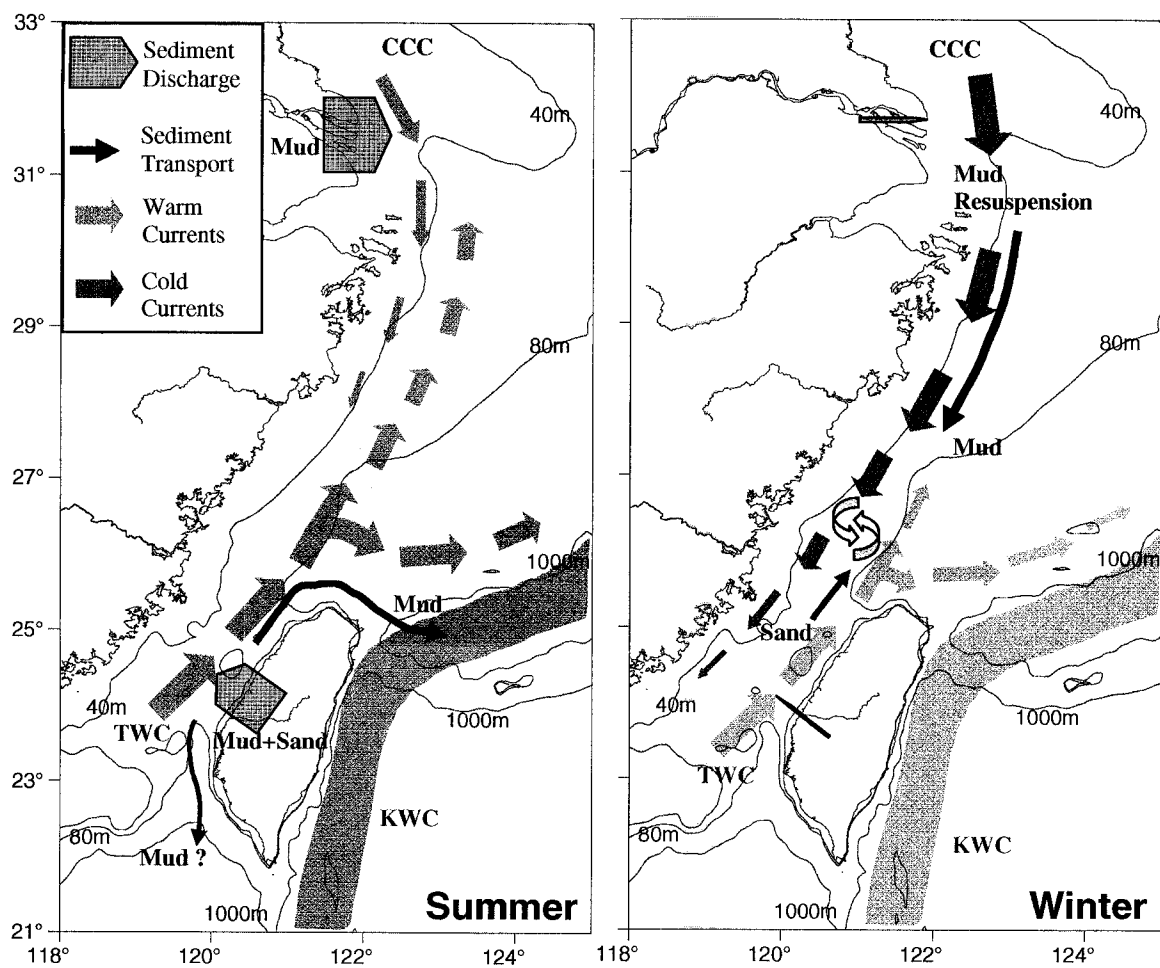


Fig. 15. Summer/winter currents and sediment transports in the inner shelf of East China Sea. KWC, Kuroshio Warm Current, perennially going northward; TWC, Taiwan Warm Current; CCC, China Coastal Current.

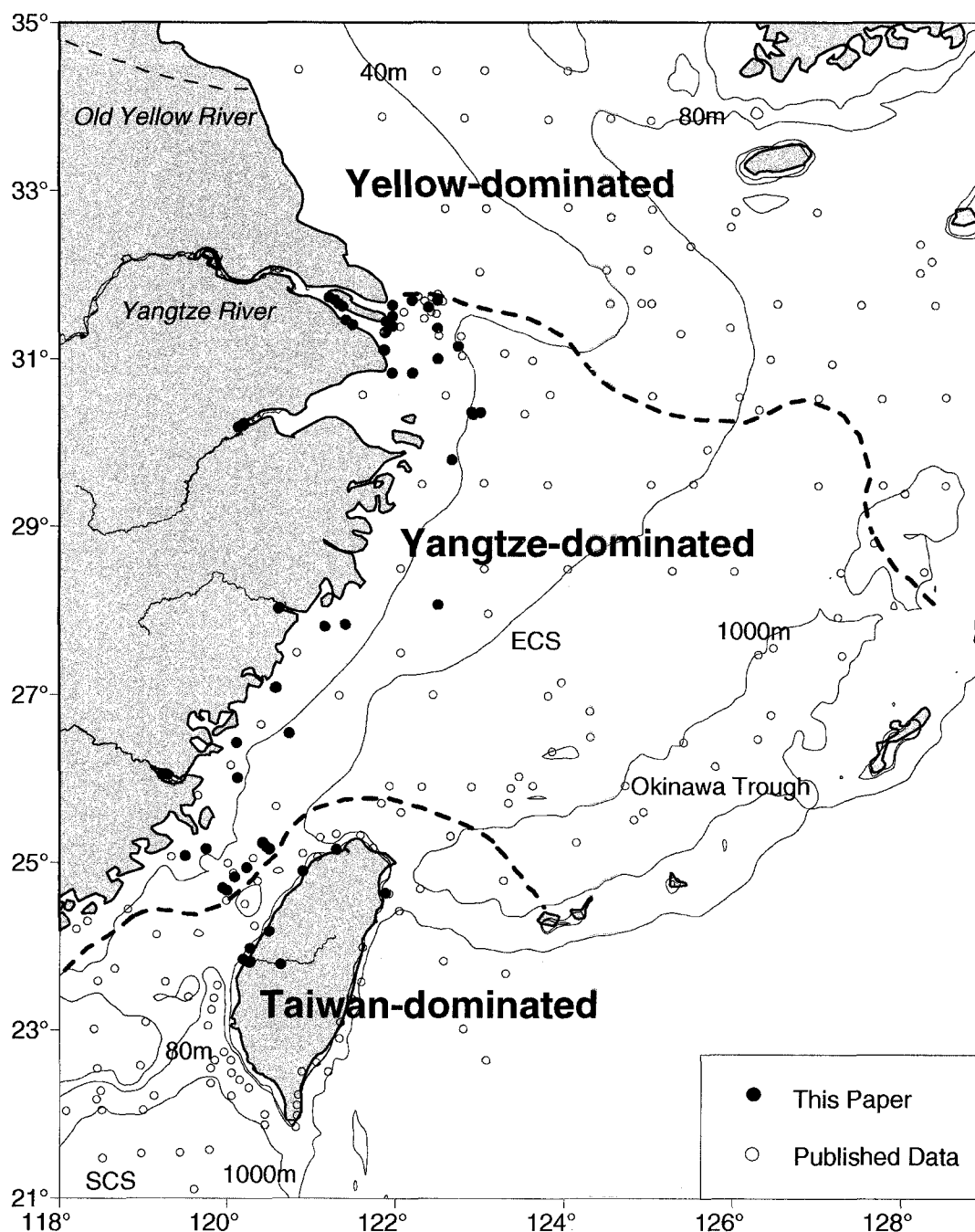


Fig. 16. Preliminary clay assemblage in the East China Sea. Published clay data are from Chen (1973), Chen (1978), Aoki et al. (1983), He and Tang (1985), Milliman et al. (1985b), You and Tang (1992), You et al. (1993), as well as Editorial Board for Marine Atlas in China (1990). ECS, East China Sea. SCS, South China Sea. Yellow-dominated clay shows relatively low illite (<64%), high smectite (>10%) and high content of Ca; Yangtze-dominated clay indicates relatively high illite (64-70%), low smectite (4-10%), low Ca and poor illite crystallinity; Taiwan-dominated clay displays highest illite (>70%), trace amount of smectite and the best illite crystallinity.

CHAPTER 6: Structure and Formation of the Yangtze-derived Holocene Clinoform, Inner Shelf of the East China Sea*

K.H. Xu^{1,a}, J. P. Liu², J.D. Milliman¹, A.C. Li³, Z.S. Yang⁴ and S.B. Xiao⁵

¹ School of Marine Science, College of William & Mary, Gloucester Pt. VA 23062, USA,

^a E-mail: kxu@vims.edu;

² Dept. of MEAS, North Carolina State University, Raleigh, NC 27695, USA;

³ Institute of Oceanology, Chinese Academy of Sciences, Qingdao, 266071, People's Republic of China;

⁴ College of Marine Geosciences, Ocean University of China, Qingdao, 266003, People's Republic of China;

⁵ South China Sea Institute of Oceanology, Chinese Academy of Sciences, Guangzhou, 510301, People's Republic of China;

*Prepared for *Continental Shelf Research*

Abstract

An elongated (800 km) mud wedge extends southward along the inner shelf of the East China Sea from the Yangtze River mouth to the northern Taiwan Strait. Overlying a transgressive sand layer, the lens-like Holocene clinoform thins offshore, from 40-m thickness at the 30-m isobath to <2 m at the 80-m isobath. Four distinct acoustic facies can be delineated in the mud wedge (from bottom to top): late-Pleistocene, Transgressive System Tract (TST), early and late High-Stand System Tracts (HST). The thin (<3 m) and acoustically transparent TST occurs between the 90- and 40-m isobaths south of 30°N. In contrast, early (2-11 ka BP) and late (0-2 ka BP, more acoustically opaque) sigmoidal HSTs are widely distributed in the inner shelf shallower than the 70- and 50-m isobaths, respectively. Clay mineralogy indicates that the mud wedge is primarily Yangtze-derived, although sand mineralogy shows the contribution of coarser Taiwan-derived sediments south of 26°N. Total volume of this Holocene mud wedge is $22 \times 10^{11} \text{ m}^3$, of which the early and late HSTs account for 5.7 and $16.3 \times 10^{11} \text{ m}^3$, respectively. Assuming a density of 1.2 tons/m^3 , the average Yangtze sediment flux in 2-11 ka BP was 215 million tons per year (mt/yr), but increased to 330 mt/yr during 0-2 ka BP, primarily reflecting increased deforestation and agricultural cultivation.

Keywords: Clinoform, Mud Wedge, Sediment, East China Sea, Yangtze River

1. Introduction and Background

Rivers provide the bulk of sediments deposited in the global ocean, presently 15-20 billion tons per year (Milliman and Meade, 1983; Milliman and Syvitski, 1992), but during sea-level highstands, much of the sediment is deposited in coastal and nearshore environments. More than half of the fluvial sediment is delivered by Asian rivers, such as the Indus, Ganges-Brahmaputra, Mekong, Yangtze and Yellow (Meade, 1996). The Yangtze and Yellow rivers transfer 480 and ~1,000 million tons per year (mt/yr) to the China seas, respectively, totally representing ~10% of the total global discharge. The fate of these bulk sediments from the Yellow and Yangtze, however, is largely controlled by the counter-clockwise circulation in the China seas (Fig. 1). The dominating current in the East China Sea (ECS) is the Kuroshio Warm Current (KWC), which flows around the eastern side of Taiwan and along the edge of the Okinawa Trough, pushing the Yellow Sea Warm Current into the eastern part of the sea, off western Korea. A branch of the KWC, the Taiwan Warm Current (TWC) flows through the Taiwan Strait and northward along the western part of the ECS. Completing the circulation, the China Coastal Current (CCC) flows southward along the edge of the ECS, particularly during winter, bringing colder water into the southwestern ECS (Fig. 1).

Debouching onto a wide (> 600 km) epicontinental (<100 m) shelf, the Yangtze and Yellow rivers have formed three distinct mud deposits in the ECS: the inner shelf, a mud patch southwest of the Cheju Island, and the deeper Okinawa Trough (Fig. 2). Perhaps the most extensive river-derived deposit in southern Asia – but relatively unstudied – is an elongated inner-shelf mud wedge that extends from Yangtze mouth 800 km southward to the northern Taiwan Strait (Fig. 2). Based on extensive ^{210}Pb geochronological data,

sediment accumulation rates in this mud wedge are generally high (>0.5 cm/yr, and temporally and regionally as high as 5 cm/yr; e.g., DeMaster et al., 1985), the rates decreasing towards northern Taiwan Strait (Fig. 3). Across the shelf, there also is a trend of decreasing accumulation from 1 cm/yr in the inner shelf to <0.1 cm/yr near Okinawa Trough (Figs. 2 and 3).

There are several possible sediment provenances to facilitate the formation of inner-shelf mud wedge: the Yangtze, Yellow (in the north) and small but highly energetic Taiwanese rivers (in the south). The Yellow has emptied primarily into the Gulf of Bohai, but during 1128-1855 AD it discharged into the southern Yellow Sea, forming a delta about 400 km north of Yangtze mouth (Liu et al., 2002) (Fig. 1). After the northern shift in 1855AD, the abandoned old Yellow delta has served as a source of resuspended sediments, particularly during winter storms (Milliman et al., 1985 and 1989); much of the sediment in the Cheju mud patch has been derived from erosion of Yellow River sediments. South of the Yangtze, there are a number of small mainland rivers (e.g., Qiantang, Ou and Min, Fig. 2) that collectively deliver ~ 15 mt/yr of sediment to the inner shelf of ECS. But the most important sediment sources in the south are the Taiwanese rivers, particularly the Choshui, which in recent years has delivered as much as 130 to 200 mt during single typhoon events (Dadson et al., 2003 and 2004; Kao et al., 2005; Milliman and Kao, 2005).

A large number of geological and geophysical studies have been made in the ECS to understand the fate of Yangtze-derived sediments, especially near the Yangtze mouth (e.g., Milliman et al., 1985; Chen and Stanley, 1993; Hori et al., 2001a; Chen et al, 2003) and on the middle shelf (Liu et al., 2000; Berne et al., 2002). Few geophysical studies,

however, focused on the innermost shelf south of the Yangtze despite the presence of a prominent mud wedge. Using high-resolution chirp seismic profiling and geochronology (^{14}C and ^{210}Pb) as well as textural and mineralogical analyses, in this paper, we document the structure and formation of this inner-shelf mud wedge. Specifically, how much of these sediments come from the Yangtze – as compared, for instance, than from the Yellow (in the north) or Taiwan (in the south)? What has been the Holocene development of this mud wedge? And how has Yangtze sediment flux changed in response to climate change and anthropogenic activities?

2. Material and Methods

About 1200 km seismic data were obtained using a high-resolution Chirp Sonar Sub-bottom Profiler (EdgeTech 0512i) (Fig. 4). Seismic profiles were processed using EdgeTech Discover and Adobe Photoshop, and then loaded into IVS Fledermaus to build the fence diagram; an acoustic velocity of 1500 m/s was assumed to calculate water depth and sediment thickness (Chen et al., 2003). The labels for cross-shelf profiles were labeled 1-8, north to south, whereas along-shelf ones were labeled A-E (Fig. 4). Sediment accumulation on the *subaerial* and *subaqueous* deltas near the Yangtze mouth was based on hundreds of boreholes (Li et al., 2000, 2002 and 2003) and extensive seismic profiling (Chen and Stanley, 1993; Chen et al., 2003), respectively.

Sediment isopachs were plotted as thickness above the maximum flooding surface delineated in the seismic profiles (discussed below). After projection and interpolation, isopachs were converted to volume using Golden Surfer software. Latitude 30°N can be regarded as the dividing line between Yangtze subaqueous delta and southern along-shelf

mud wedge; south of 26°N the mud wedge contains both Yangtze- and Taiwan-derived sediments (*Chapter 4*). Therefore, volumes for each latitude range (>30, 30-26, <26°N) were calculated.

In addition to published conventional radiocarbon dates derived from Yangtze delta to northern Taiwan Strait (Qin et al., 1987; Yu and Li, 1992; Lan et al., 1993; You and Tang, 1992; Huang et al., 1996; Xu, 1996; Ye et al., 2002), two AMS radiocarbon dates were determined through mollusks in two vibrocores (SK3 and SK4) near the Yangtze subaqueous delta (Wang et al., 2005) and seven AMS ages were obtained by testing foraminifera in three gravity cores (DD2, 30 and PC6) further to the south (Xiao et al., 2004a; Xiao et al., 2005; Liu et al., 2006a). Radiocarbon ages are reported in both ^{14}C and calendar year BP (Before Present-1950 AD) calibrated using Calib software (Stuiver et al., 1998; <http://calib.qub.ac.uk/calib/>). Published ^{210}Pb accumulation rates based on gravity and box cores also were collected (DeMaster et al., 1985; Alexander et al., 1991; Chen, 1995; Chung and Chang, 1995; Huh and Su, 1999; Xia et al., 1999 and 2004; Su and Huh, 2002; Oguri et al., 2003; Liu et al., 2006b) (Figs. 3 and 4).

A total of 84 surface samples from the mouths of mainland and Taiwanese rivers as well as the inner ECS were analyzed for this study. Grain-size and clay mineralogy analyses were performed at the Institute of Oceanology, Chinese Academy of Sciences, Qingdao, China. The procedures for grain size analysis and sediment mineralogy are explained in *Chapter 4*. Down-core clay mineral analysis was performed for two gravity cores in the north (DE2) and middle (DE15) of the mud wedge (Fig. 4), respectively, and clay data from a core in the south of mud wedge (northern Taiwan Strait) also were collected (Core 737, You and Tang, 1992; Fig. 4).

3. Results and Analyses

3.1. Acoustic Facies

From bottom up, four distinct acoustic facies (A, B, C and D, delineated by blue, yellow, red and green colors, respectively) were identified in the chirp seismic profiles (Figs. 5-10). In each profile a prominent subsurface reflector truncates the underlying strata at a depth range of 40-90 m (Figs. 5-10). Based on published seismic profiles near the Yangtze subaqueous delta (Chen and Stanley, 1993; Chen et al., 2003), this reflector appears to be the base of the post-glacial sandy transgressive surface (Liu et al., 2004).

Below the transgressive surface is Facies A (Blue), which varies greatly in character between the northern and southern regions of the mud wedge. In the north and near the Yangtze subaqueous delta, three and one ridge-like acoustic units are found in profiles A and 1, respectively (Fig. 5), which have been interpreted as 'relict mud ridges' by Chen et al. (2003); similar relict sand ridges are widely distributed further seaward to the middle shelf (Liu et al., 1998; Fig. 11d), trending more or less parallel the direction of tidal flow (Chen et al., 2003). South of 30 °N, extensive strata accumulate below the transgressive surface in Profiles 3a, D-E, 5, 6, 7a and the thickest (25 m) accumulation can be found in the along-shelf profiles D-E (Figs. 5-10). Although biogenic gas wipes out much of the record shallower than 30 m, cut-and-fill features and paleo-channels can be clearly identified at 30-60 m below some transgressive surfaces (Figs. 5-10 and 11d).

Above the transgressive surface, in some profiles, there is a thin (<3m), subparallel and acoustically transparent layer overlain by the maximum flooding surface. Between transgressive surface and maximum flooding surface is Facies B (Yellow), which is

termed the Transgressive System Tract (TST). On closer inspection, Facies B is seen only south of 30 °N, between the 40- and 90-m isobaths (Fig. 11c).

The strata downlapping onto the maximum flooding surface are the High-stand System Tracts (HST), which can be divided into two facies. The lower part (relatively acoustically transparent, e.g., Profile 5) is termed Facies C (early HST, Red), and its more opaque upper part is Facies D (late HST, Green). Facies C and D are separated either by angular unconformities (profiles A, 1 and 5) or by distinct acoustically opaque strata (borders between blue and red in profiles B-C, 3a, D-E, 7a and 8). After combining all profiles together and comparing the depth and thickness with each other in the fence diagram (Fig. 10), all these divisions were confirmed.

Both early and late HSTs are widely distributed at water depths shallower than 70 and 50 m isobaths, respectively (Figs. 11a and 11b). In the northern mud wedge, starting from core Ch1, HSTs prograde eastward and northward (Fig. 5), whereas in the south they mainly prograde eastward. There are conformities between facies C and D in most profiles, but angular unconformities are found in profiles A, 1 and 5 due to slight truncations in the upper early HST (Figs. 5-10). Interestingly, there are actually two truncations in Profile A, one in the upper early HST and the other in the lower part of the late HST. To the south, there is no late HST in Profile 6, suggesting that its early HST (also with a slight truncation) has not yet been overlaid by late HST (Fig. 8). Biogenic gas is widely found in the early HST in profiles 1, 3a, D, 5 and 6, but locally it penetrates upward into the late HST.

3.2. ^{14}C and ^{210}Pb Geochronology

Radiocarbon dates from five cores (Ch3, Ch1, Dc1, Dc2 and 737) indicate that the time of the transgressive surface is about 11 ka BP (Figs. 5, 6, and 9). Therefore, Facies A (Blue) below the transgressive surface is interpreted as a late-Pleistocene unit. Acoustically transparent Facies B (Yellow) presumably represents strata deposited after rapid transgression, either ~11 ka BP or earlier (discussed below). Although distinguishing Facies C (Red) and D (Green) is difficult, a radiocarbon date in DD2 shows that the dividing time of Facies C and D is about 2 ka BP (Fig. 6). ^{14}C dates younger than 2 ka BP (SK3, SK4, DD2, PC6) and ages older than 2 ka BP (30 and PC6) confirm this division (Figs. 5-7).

Based on ^{210}Pb analysis, short time-scale (100-yr) sediment accumulation rates are generally high (3-5 cm/yr) near the Yangtze subaqueous delta but low (0.2 cm/yr) offshore (Profile A; Fig. 5); a declining trend is noted southward from 0.9 cm/yr in Profile B-C to 0.47 cm/yr in Profile 7a (Figs. 6 and 9). The average ^{210}Pb accumulation rate (~1 cm/yr, Fig. 3), however, is about 5 times of ^{14}C rate (0.2 cm/yr, generally 20 m in 10 ka; Fig. 12).

3.3. Sediment Thicknesses

Extending from the Yangtze River mouth 800 km southward into the northern Taiwan Strait, the elongated and lens-like mud wedge thins offshore, from ~40 m thickness at 30-m isobath to <2 m at 80-m isobath (Fig. 12). Total volume of this isopach (including both early and late HSTs) is $22 \times 10^{11} \text{ m}^3$, of which 14, 6.5 and $1.5 \times 10^{11} \text{ m}^3$ are in >30, 30-26 and <26°N latitude ranges, respectively (Fig. 12). Total volumes of late and early HSTs are 5.7 and $16.3 \times 10^{11} \text{ m}^3$, including 0.8 and $0.7 \times 10^{11} \text{ m}^3$ south of 26°N, respectively (Fig. 11a and 11b).

3.4. Core-based Mineralogy and Geochronology

Surficial mineralogical data show that modern Yangtze-derived clays are illite-dominated, with lesser amounts of kaolinite and chlorite as well as a minor amount of smectite (*Chapter 4*). This mineralogy assemblage extends from the Yangtze mouth 800 km south to the northern Taiwan Strait. Down-core clay mineralogy in the north (Core DE2), middle (DE15) and south (737) of the mud wedge indicate most clays also are illite-dominated (~70%) (Figs. 4 and 13).

Although there has been no dating of Core DE2 (4-m long), its position in Profile 1 suggests that it was probably deposited between 4 and 2 ka BP (Fig. 5). Core DE15, which is sandy throughout, is located in a pinched-out region (60 m isobath) of mud wedge and its age therefore is probably older than 11 ka BP (Fig. 4). Mainly consisting of silty clay, all sediments in Core 737 seem to be younger than ~11 ka BP (Figs. 9 and 13). Despite these variations in age, most clays (except the lower part of Core 737) are similar in character to Yangtze, and different from the Yellow, Min and Taiwan clays (Fig. 14). From top to the bottom in Core 737, smectite increases from 5% to 20%, illite decreasing correspondingly; the ratio in lower Core 737 is similar to the Yellow River clay assemblage (Figs. 13 and 14). Considering the location of 737 (1200 km from the old Yellow) and non-Yellow characters in DE2 and DE15 (both are even closer to the old Yellow), lower part of Core 737 should be Yangtze-derived and its mineral variation is probably due to climatic rather than provenance change (discussed below).

4. Discussion

The development of the post-glacial Clinoform in the inner shelf of ECS has been impacted by both sea-level/climatic and anthropogenic forcings. Changes in accumulation in the mud wedge in the ocean may well reflect the variations of Yangtze sediment flux on the land.

4.1. Sea-level/Climate Changes

Nourished by tremendous sediments and developed on a wide (>600 km) and flat (<100m) epicontinental shelf, the inner-shelf mud wedge is particularly sensitive to any change in sea level. Since the last glacial maximum (LGM, 15-20 ka BP; Wang and Sun, 1994), there were six rapid sea level rises, in two of which sea level rose from -96 to -76 m (Melt Water Pulses, MWP-1A: ~14.3-14.0 ka BP) and from -58 to -45 m (MWP-1B: ~11.5-11.2 ka BP) (Fairbanks, 1989; Liu and Milliman, 2004). Post-LGM sea level reached its highest level at +3 to +5 m around ~7 ka BP (Chen and Stanley, 1998) and fell slowly down to the present level.

During rapid transgressions, late Pleistocene strata were swept and truncated by paleo-tidal currents that may have been stronger than modern ones (Uehara et al., 2002; Uehara and Saito, 2003), and the old Yangtze mouth rapidly retreated landward, presumably northwestward along the relict ridges (Fig. 11d). After the MWP-1B transgression, the shoreline was actually located near the *modern* -20-m isobath, considering the 20-m thickness of mud wedge there. Offshore the wide ECS shelf (particularly in the south) became far away from Yangtze mouth (sediment source) and thereby sediment-starved, receiving a small amount of fine-sediment (acoustically very transparent in yellow TST, Fig. 5-10) accumulation. As a result, TST only is located south of 30°N. Considering the wide depth range of TST from -40 to -90m, these TSTs

were probably formed after the rapid sea level rises in ~14 or ~11 ka BP (Liu et al., 2006a). Another interesting character related to the rapid sea level rises is the disconformities near the pinch-out regions in profiles 3a and D-E (cores DD2 and PC6) (Figs. 6 and 7). The strata directly overlying the 5-6 ka BP sediments show less than 2 ka BP ages, indicating >3 ka accumulation discontinuity due to either strata erosion or more likely sediment starvation.

Near the Yangtze mouth, two series of truncations are found in the late HST of profile A. Similar truncations are located in the profiles 1, 5 and 6 further southward. One possible reason for these disconformities is the change in oceanographic regime and therefore the path of sediment dispersal. Since LGM, the Yangtze sometimes shifted northward into the southern Yellow Sea (Li et al., 2000 and 2002) and merged with the old Yellow so that small amounts of sediments were transported along the inner shelf of ECS, leading to truncated strata. Considering two series of truncations in recent 2 ka in Profile 1, another explanation is sea level regressions. Although post-LGM sea level changes were mainly transgressions, short-period regressions were possible (Chen and Stanley, 1998; Hori et al., 2001b; Xiao et al, 2004b). When sea level retreated seaward, recently formed strata were truncated and washed away, leading to disconformities in the seismic profiles.

Sea level change has been coupled with climate change. After the reintensification of the SW monsoon around 11 ka BP, the climate in southern Asia became increasingly warm and wet (Thompson et al., 1989; Gasse et al., 1991). Palynological studies on long boreholes in the Yangtze delta have revealed that around 10-9 ka BP the Yangtze

climate was warm and wet, preceded and followed by cooler and drier conditions (Yi et al, 2003).

4.2. Mineralogy

Clay mineral variations reflect this climate change. Both gravity cores in the inner shelf of ECS and an ODP long cores in northern South China Sea reveal that smectite increased during interglacials and decreased during glacials, in contrast to illite and chlorite (Zhu, 1985; Liu et al., 2003). In the Ganges-Brahmaputra river system, increased smectite also was found in the early Holocene (10-7 ka BP), reflecting enhance chemical weathering under increasingly warmer and more humid conditions (Heroy et al., 2003). In a similar manner, high smectite levels (~20%) in lower part of Core 737 may indicate warmer and wetter conditions during the early and middle Holocene (Figs. 13 and 14). The low (5%) smectite in upper part of Core 737, as well as in DE2 and DE15, reflect cooler and drier conditions, similar to the modern climate.

Therefore, both modern surficial clays and those cores in the Holocene mud wedge are Yangtze-derived (Fig. 14). Analyses of grain size and fine-sand mineralogy, however, indicate that south of 26°N about 25% of sediments (mainly fine sand and sandy silt) come from Taiwan (*Chapter 4*). Assuming few changes in provenance mineralogy during the Holocene, all the sediments in this inner-shelf mud wedge are considered to be Yangtze-derived - except for 25% of sediments from Taiwan in northern Taiwan Strait south of 26°N.

4.3. Sediment Budget

4.3.1. Budget Assumption and Error Analyses

Since Yangtze sediment budget was mainly based on the data from Yangtze delta and inner-shelf mud wedge, this budget analysis inevitably involved several assumptions. Based on the mineralogy results, we assumed that all fine sediments were Yangtze-derived and 25% of coarse sediments south of 26°N were Taiwan-derived. In other words, no significant amounts of sediments from the Yellow, Qiantang, Ou and Min rivers were transported into the mud wedge. Second, we assumed that there were no escapes of Yangtze sediments outside of the mud wedge (to the north, east or south). Clay mineralogical data showed that few Yangtze clay could reach the southern Yellow Sea (north) and northern South China Sea (south) (*Chapter 4*). Considering the flat continental shelf in ECS and Yangtze hypopycnal flow, eastern escape of Yangtze sediment is very unlikely. Based on the chirp profiles in the fence diagram, most fine-sediment strata pinched out in the eastern edge of mud wedge at 60-80 m isobath (Fig. 10), and fine sediments rarely deposited on the middle shelf (Fig. 2).

Sediment fluxes were calculated by multiplying the volume by density, then dividing the product by time. One major volume error was derived from the calculation of vertical depth. An average acoustic velocity of 1,500 m/s was assumed to calculate the depth of the seismic profiles. Acoustic velocity may change from ~1,400 to ~1,800 m/s when the sound goes through different types of sediments. Due to limitation of research vessel and frequent nearshore fishing activities, the spatial coverage of our nearshore seismic profiles is very limited, leading to another possible volume error. Mainly depending on the grain size and water content, dry bulk density can vary from ~0.9 to ~1.6 t/m³. We assumed an average density to be 1.2 t/m³ considering most sediments were silty clay and clayey silt (Figs. 5-9). Time error depended on dating methods: errors for conventional

radiocarbon dating were ~500a whereas AMS dating errors were only ~50a. Despite these assumptions and errors, our preliminary budget calculation is the first attempt to calculate the Yangtze sediment flux by compiling seismic, grain-size and mineralogical data.

4.3.2. Yangtze Sediment Flux

South of 26°N, the total volume of the Holocene is $1.5 \times 10^{11} \text{ m}^3$ (Fig. 12). Assuming that Taiwan rivers contribution ~25% of the sediment in northern Taiwan Strait, the Yangtze would contribute $\sim 1.1 \times 10^{11} \text{ m}^3$. Combined with the $6.5 \times 10^{11} \text{ m}^3$ of sediment between 30°N and 26°N, accumulation of Yangtze-derived sediment south of 30 °N would be $7.6 \times 10^{11} \text{ m}^3$, representing 35% of total Holocene Yangtze-derived sediment (Fig. 12). This result agrees well with the estimate of 30% southern transport based on studies near the Yangtze delta and estuary (Milliman et al., 1985).

After excluding the Taiwan-derived sediment, Yangtze-derived sediment in late and early HSTs would be 5.5 and $16.1 \times 10^{11} \text{ m}^3$, respectively (Fig. 11a and 11b). Assuming a density of 1.2 tons/m^3 , sediments accumulated in late (0-2 ka BP) and early (2-11 ka BP) HSTs amount to 6.6 and $19.4 \times 10^{11} \text{ tons}$, respectively. Dividing these cumulative loads by the time intervals indicates that average Yangtze sediment flux was 215 mt/yr between 11 and 2 ka BP, about 45% of its modern load (480 mt/yr) (Fig. 15). After 2 ka BP, however, it increased to 330 mt/yr, presumably in response to increased anthropogenic activities (e.g., deforestation, agriculture) in the watershed. This finding matches well with both shoreline changes based on Yangtze Delta chenier record as well as progradation rate of Yangtze delta derived from radiocarbon dating from long cores (Liu et al., 1992; Hori et al., 2001a). It is reported that Yangtze seaward progradation rate was 38 m yr^{-1} between

6-2 ka BP, but increased to 80 m yr^{-1} after 2 ka BP, primarily in response to increased human activities (Hori et al., 2001b). In recent centuries, the stabilizing of river channels and thus less trapping in alluvial plain along the middle and lower reaches of the river (e.g., Dongting Lake; *Chapter 2*), resulted in more sediments transported downstream to the Yangtze mouth.

Since 1987 AD, however, extensive reforestation and the construction more than 50,000 dams, including the world's largest dam – the Three Gorges Dam (TGD), have decreased Yangtze sediment dramatically so that its load in 2004 was only 157 mt/yr (*Chapter 3*) (Fig. 15). Considering the prospectus of a number of major dams upstream from the TGD (Xu et al., 2006) and the ongoing water diversion, it seems likely that in the next few decades the Yangtze load will decline even further, to less than a half of its pre-anthropogenic levels (Fig. 15).

5. Conclusions

The Holocene mud wedge extends along the western edge of the East China Sea stretches from the Yangtze mouth to the northern Taiwan Strait, thinning from ~40 m thickness at 30-m isobath to <2 m at 80-m isobath. An acoustically transparent TST is constrained between 40 and 90 m isobaths south of 30°N , whereas early (2-11 ka BP) and late (0-2 ka BP) HSTs are widely distributed in the inner shelf shallower than 70 and 50 m isobaths, respectively. Rapid sea-level transgressions caused discontinuities in the seaward edge of southern mud wedge, but short-term regression(s) presumably led to angular unconformities between early and late HSTs. Total volume of this Holocene mud wedge is $22 \times 10^{11} \text{ m}^3$, of which early and late HSTs account for 5.7 and $16.3 \times 10^{11} \text{ m}^3$,

respectively. Average Yangtze sediment flux was 215 mt/yr in 2-11 ka BP, but increased to 330 mt/yr in 0-2 ka BP, primarily reflecting increased deforestation and agricultural cultivation. In future decades, however, extensive reforestation and dam construction will probably decrease the Yangtze load to less than half of its pre-anthropogenic level.

Acknowledgement

We thank the crew of R/V Goldern Star II of Institute of Oceanology, Chinese Academy of Sciences. K.H. Xu and J.D. Milliman receive support from the U.S. National Science Foundation (NSF) and Office of Naval Research (ONR). This paper is Contribution No.xxxx of the Virginia Institute of Marine Science, The College of William and Mary.

References

- Alexander, C.R., DeMaster, D.J. and Nittrouer, C.A., 1991. Sediment accumulation in a modern epicontinental-shelf setting: The Yellow Sea. *Marine Geology*, 98(1): 51-72.
- Berne, S. et al., 2002. Pleistocene forced regressions and tidal sand ridges in the East China Sea. *Marine Geology*, 188(3-4): 293-315.
- Chen, S.K., 1995. Sediment accumulation rates and organic carbon deposition in the East China Sea continental margin sediments, Ph.D. Dissertation. National Taiwan University, Taiwan,
- Chen, Z. and Stanley, D.J., 1993. Yangtze delta, eastern China: 2. Late Quaternary subsidence and deformation. *Marine Geology*, 112(1-4): 13-21.

- Chen, Z. and Stanley, D.J., 1998. Sea-level rise on eastern China's Yangtze delta. *Journal of Coastal Research*, 14(1): 360-366.
- Chen, Z., Saito, Y., Hori, K., Zhao, Y. and Kitamura, A., 2003. Early Holocene mud-ridge formation in the Yangtze offshore, China: a tidal-controlled estuarine pattern and sea-level implications. *Marine Geology*, 198(3-4): 245-257.
- Chung, Y. and Chang, W.C., 1995. Pb^{210} fluxes and sedimentation rates on the lower continental slope between Taiwan and the South Okinawa Trough. *Continental Shelf Research*, 15(2-3): 149-164.
- Dadson, S.J. et al., 2003. Links between erosion, runoff variability and seismicity in the Taiwan orogen. *Geology*, 31(6): 648-651.
- Dadson, S.J. et al., 2004. Earthquake-triggered increase in sediment delivery from an active mountain belt. *Geology*, 32(8): 733-736.
- DeMaster, D.J., McKee, B.A., Nittrouer, C.A., Jiangchu, Q. and Guodong, C., 1985. Rates of sediment accumulation and particle reworking based on radiochemical measurements from continental shelf deposits in the East China Sea. *Continental Shelf Research*, 4(1-2): 143-158.
- Fairbanks, R.G., 1989. Glacio-eustatic sea level record 0-17,000 years before present: influence of glacial melting rates on Younger Dryas event and deep ocean circulation. *Nature*, 342(7): 637-642.
- Gasse, F. et al., 1991. A 13,000-year climate record from western Tibet. *Nature*, 353(6346): 742-745.

- Heroy, D.C., Kuehl, S.A. and Goodbred, J., Steven L., 2003. Mineralogy of the Ganges and Brahmaputra Rivers: implications for river switching and Late Quaternary climate change. *Sedimentary Geology*, 155(3-4): 343-359.
- Hori, K. et al., 2001a. Sedimentary facies of the tide-dominated paleo-Changjiang (Yangtze) estuary during the last transgression. *Marine Geology*, 177(3-4): 331-351.
- Hori, K. et al., 2001b. Sedimentary facies and Holocene progradation rates of the Changjiang (Yangtze) delta, China. *Geomorphology*, 41(2-3): 233-248.
- Huang, H. et al., 1996. *Sedimentary Geology of the Yangtze River Delta*. China Geology Press, Beijing, 244 pp (in Chinese).
- Huh, C.-A. and Su, C.-C., 1999. Sedimentation dynamics in the East China Sea elucidated from ^{210}Pb , ^{137}Cs and $^{239,240}\text{Pu}$. *Marine Geology*, 160(1-2): 183-196.
- Kao, S.J., Lee, T.Y. and Milliman, J.D., 2005. Calculating highly fluctuated suspended sediment fluxes from mountainous rivers in Taiwan. *Terres. Atmos. Ocean. Sci.*, 16(3): 441-432.
- Lan, D.Z. et al., 1993. Transgressions and the sea-level changes of the western Taiwan Strait since the Late Pleistocene. *Acta Oceanologica Sinica*, 12(4): 617-627.
- Li, B.H., Li, C.X. and Shen, H.T., 2003. A preliminary study on sediment flux in the Changjiang Delta during the postglacial period. *Science in China Series D*, 46(7): 743-752.
- Li, C.X., Chen, Q., Zhang, J., Yang, S. and Fan, D., 2000. Stratigraphy and paleoenvironmental changes in the Yangtze Delta during the Late Quaternary. *Journal of Asian Earth Sciences*, 18(4): 453-469.

- Li, C.X. et al., 2002. Late Quaternary incised-valley fill of the Yangtze delta (China): its stratigraphic framework and evolution. *Sedimentary Geology*, 152(1-2): 133-158.
- Liu, J.P., Milliman, J. and Gao, S., 2002. The Shandong mud wedge and post-glacial sediment accumulation in the Yellow Sea. *Geo-Marine Letters*, 21(4): 212 - 218.
- Liu, J.P. and Milliman, J.D., 2004. Reconsidering Melt-water Pulses 1A and 1B: Global Impacts of Rapid Sea-level Rise. *Journal of Ocean University of China*, 3(2): 183-190.
- Liu, J.P., Milliman, J.D., Gao, S. and Cheng, P., 2004. Holocene development of the Yellow River's subaqueous delta, North Yellow Sea. *Marine Geology*, 209(1-4): 45-67.
- Liu, J.P. et al., 2006. Flux and Fate of Yangtze River Sediment Delivered to the East China Sea. *Geomorphology* (in press).
- Liu, J.P. et al., 2006. Sedimentary features of the Yangtze River-derived alongshore clinoform deposit in the East China Sea. *Continental Shelf Research* (in press).
- Liu, K.-B., Sun, S. and Jiang, X., 1992. Environmental change in the Yangtze River delta since 12,000 years B.P. *Quaternary Research*, 38(1): 32-45.
- Liu, Z. et al., 2003. Clay mineral assemblages in the northern South China Sea: implications for East Asian monsoon evolution over the past 2 million years. *Marine Geology*, 201(1-3): 133-146.
- Liu, Z.X. et al., 1998. Tidal deposition systems of China's continental shelf, with special reference to the eastern Bohai Sea. *Marine Geology*, 145(3-4): 225-253.

- Liu, Z.X., Berne, S., Saito, Y., Lericolais, G. and Marsset, T., 2000. Quaternary seismic stratigraphy and paleoenvironments on the continental shelf of the East China Sea. *Journal of Asian Earth Sciences*, 18(4): 441-452.
- Meade, R.H., 1996. River-sediment inputs to major deltas. In: J. Milliman and B. Haq (Editors), *Sea-Level Rise and Coastal Subsidence*. Kluwer, London, pp. 63-85.
- Milliman, J.D. and Meade, R.H., 1983. World-wide delivery of sediment to the oceans. *Journal of Geology*, 91(1): 1-21.
- Milliman, J.D., Shen, H.T., Yang, Z.S., and Mead, R.H., 1985. Transport and deposition of river sediment in the Changjiang estuary and adjacent continental shelf. *Continental Shelf Research*, 4(1-2): 37-45.
- Milliman, J. D., Qin, Y. S. and Park Y.A., 1989. Sediments and Sedimentary Processes in the Yellow and East China Seas. In: A. Taira and F. Masuda (Editors), *Sedimentary Facies in the Active Plate Margin*, Terra Scientific Publishing Company, Tokyo, pp 233-249.
- Milliman, J.D. and Syvitski, J.P.M., 1992. Geomorphic/tectonic control of sediment discharge to the ocean: the importance of small mountainous rivers. *Journal of Geology*, 100(5): 525-544.
- Milliman, J.D. and Kao, S.-J., 2005. Hyperpycnal Discharge of Fluvial Sediment to the Ocean: Impact of Super-Typhoon Herb (1996) on Taiwanese River. *J. of Geology* 113, 503-516.
- Oguri, K., Matsumoto, E., Yamada, M., Saito, Y. and Iseki, K., 2003. Sediment accumulation rates and budgets of depositing particles of the East China Sea. *Deep Sea Research Part II: Topical Studies in Oceanography*, 50(2): 513-528.

- Qin, Y.S., Zhao, Y.Y., Chen, L.R. and Zhao, S.L., 1987. Geology of the East China Sea. China Science Press, Beijing, 290 pp (in Chinese).
- Stuiver, M. et al., 1998. INTCAL98 radiocarbon age calibration, 24,000-0 cal BP. *Radiocarbon*, 40(3): 1041-1083.
- Su, C.-C. and Huh, C.-A., 2002. ^{210}Pb , ^{137}Cs and $^{239,240}\text{Pu}$ in East China Sea sediments: sources, pathways and budgets of sediments and radionuclides. *Marine Geology*, 183(1-4): 163-178.
- Thompson, L.G. et al., 1989. Holocene-Late pleistocene climatic ice core records for Qinghai-Tibetan plateau. *Science*, 246: 474-477.
- Uehara, K. and Saito, Y., 2003. Late Quaternary evolution of the Yellow/East China Sea tidal regime and its impacts on sediments dispersal and seafloor morphology. *Sedimentary Geology*, 162(1-2): 25-38.
- Uehara, K., Saito, Y. and Hori, K., 2002. Paleotidal regime in the Changjiang (Yangtze) Estuary, the East China Sea, and the Yellow Sea at 6 ka and 10 ka estimated from a numerical model. *Marine Geology*, 183(1-4): 179-192.
- Wang, P. and Sun, X., 1994. Last glacial maximum in China: comparison between land and sea. *CATENA*, 23(3-4): 341-353.
- Wang, Z., Saito, Y., Hori, K., Kitamura, A. and Chen, Z., 2005. Yangtze offshore, China: highly laminated sediments from the transition zone between subaqueous delta and the continental shelf. *Estuarine, Coastal and Shelf Science*, 62(1-2): 161-168.
- Xia, X., Xie, Q., Li, Y., Li, B. and Feng, Y., 1999. ^{137}CS and ^{210}PB profiles of the seabed cores along the East China Sea coast and their implications to sedimentary

- environment. *Donghai Marine Science*, 17(1): 20-27 (in Chinese with English abstract).
- Xia, X., Yang, H., Li, Y., Li, B. and Pan, S., 2004. Modern Sedimentation Rates in the Contiguous Sea Area of Changjiang Estuary and Hangzhou Bay. *Acta Sedimentologica Sinica*, 22(1): 130-135 (in Chinese with English abstract).
- Xiao, S.B. et al., 2004a. Sedimentary record and climatic signal in the mud wedge of the inner shelf of East China Sea since 2 ka BP. *China Science Bulletin*, 49(21): 2233-2238 (in Chinese).
- Xiao, S.B. et al., 2004b. The history of the Yangtze River entering sea since last glacial maximum: a review and look forward. *Journal of Coastal Research*, 20(2): 599-604.
- Xiao, S.B. et al., 2005. Recent 8ka mud records of the east Asian winter monsoon from the inner shelf of the East China Sea. *Journal of China University of Geosciences (Earth Science)*, 30(5): 573-581 (in Chinese with English abstract).
- Xu, Z., 1996. Studies on late Quaternary sedimentary rate in western Taiwan Strait. *Journal of Oceanography in Taiwan Strait*, 15(3): 223-228 (in Chinese with English abstract).
- Ye, Y., Zhuang, Z., Liu, D., Feng, X. and Lin, L., 2002. Holocene Deposition Strength Zoning in the East China Sea. *Journal of Ocean University of Qingdao*, 32(6): 941-948 (in Chinese with English abstract).
- Yi, S., Saito, Y., Zhao, Q. and Wang, P., 2003. Vegetation and climate changes in the Changjiang (Yangtze River) Delta, China, during the past 13,000 years inferred from pollen records. *Quaternary Science Reviews*, 22(14): 1501-1519.

- You, Z. and Tang, J., 1992. Preliminary study on clay minerals of sediments in western Taiwan Strait. *Acta Sedimentologica Sinica*, 10(4): 129-136 (in Chinese with English abstract).
- Yu, P. and Li, N., 1992. The Crust Thermal Flux of the East China Sea. China Ocean Press, Beijing (in Chinese).
- Zhu, F., 1985. Clay minerals of the East China Sea shelf area in the recent epoch stratum. *Donghai Marine Science*, 3(4): 32-43 (in Chinese with English abstract).

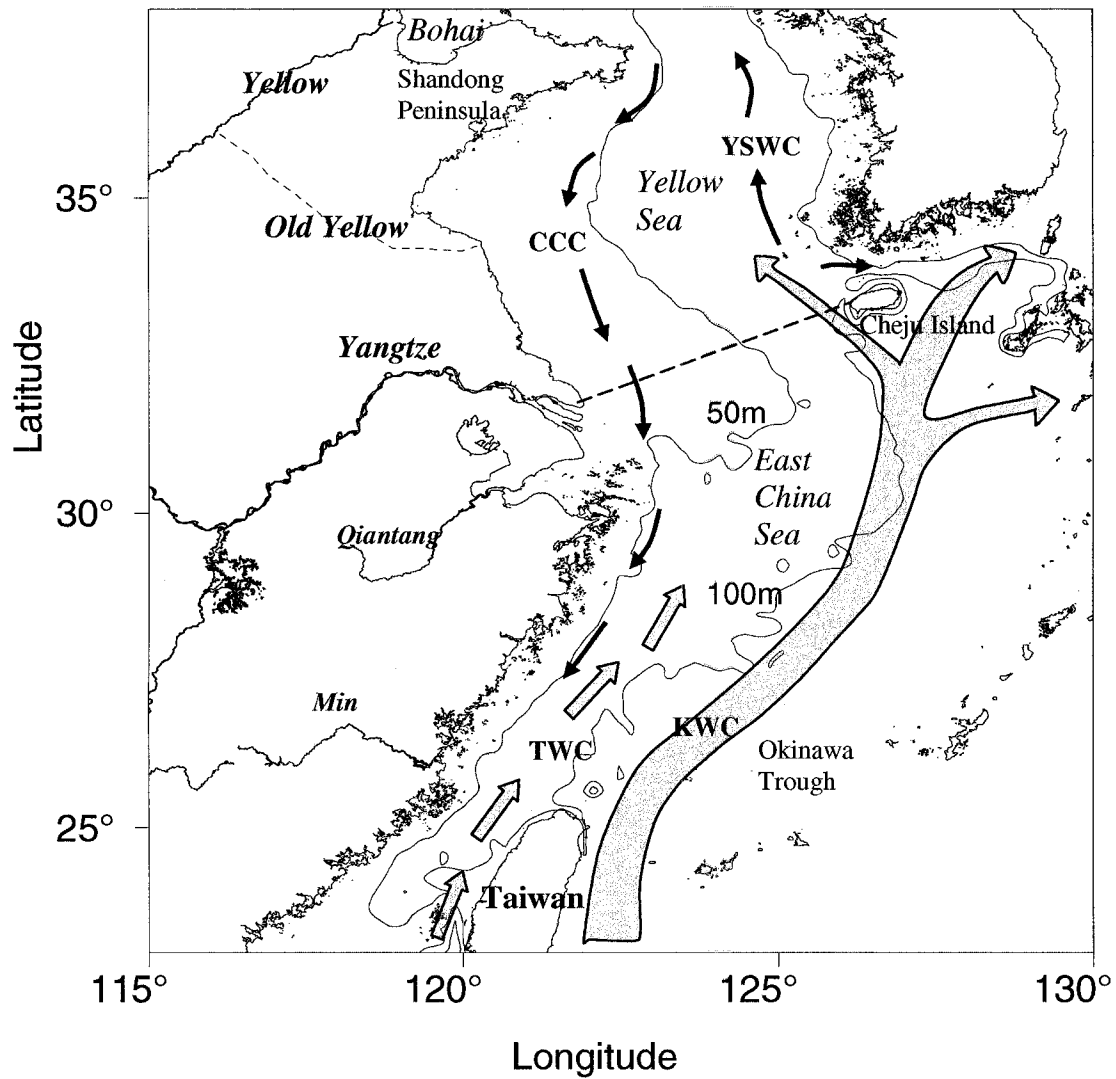


Fig. 1 Bathymetry and major currents in the East China Sea and Yellow Sea. KWC, Kuroshio Warm Current; TWC, Taiwan Warm Current; CCC, China Coastal Current; YSWC, Yellow Sea Warm Current. Dashed straight line from Yangtze mouth to Cheju Island is the dividing line between East China Sea and Yellow Sea. The old Yellow River entered the Yellow Sea from 1128 to 1855 AD (dashed course).

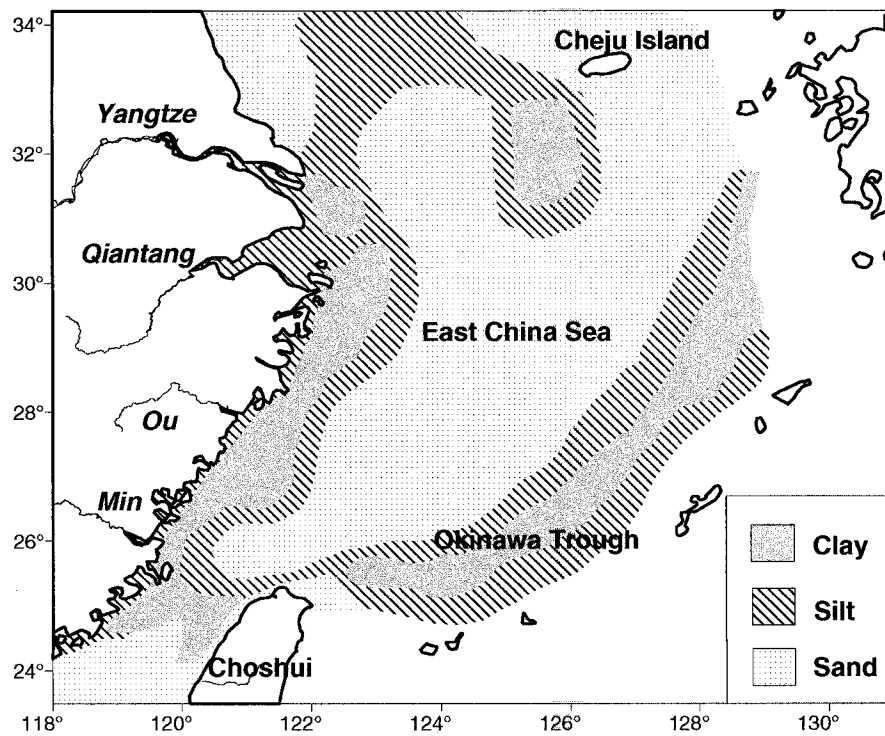


Fig. 2 Surficial sediment distribution in the East China Sea. Most surficial sediments are relict sands in the middle and outer shelf. There are three major mud deposits: inner shelf, southwest of Cheju Island and deeper Okinawa Trough.

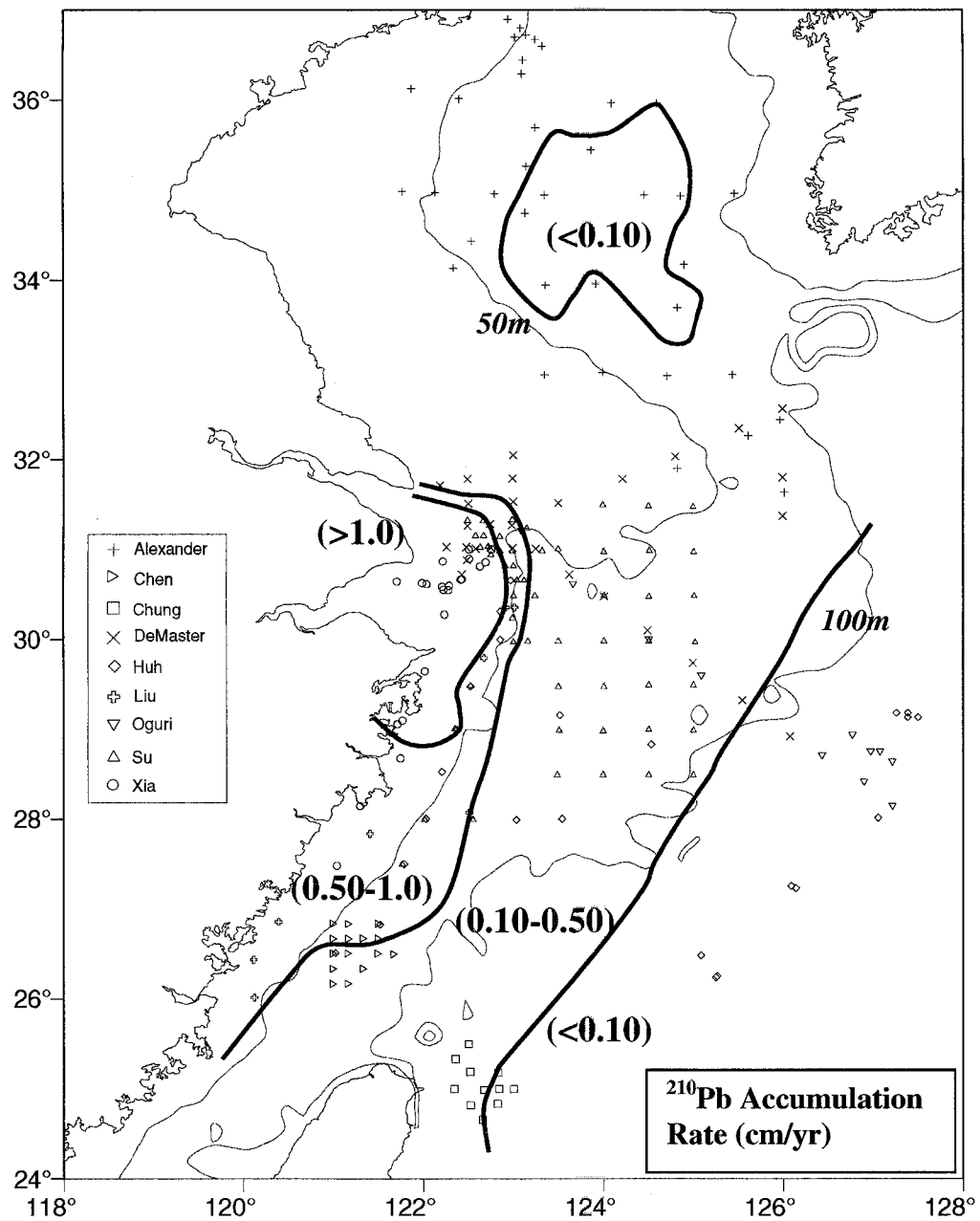


Fig. 3 Sediment accumulation rates based on ^{210}Pb analysis in the East China Sea. Isobaths are labeled as 50 and 100m. Data are from DeMaster et al., 1985; Alexander et al., 1991; Chen, 1995; Chung and Chang, 1995; Huh and Su, 1999; Xia et al., 1999 and 2004; Su and Huh, 2002; Oguri et al., 2003; Liu et al., 2006b.

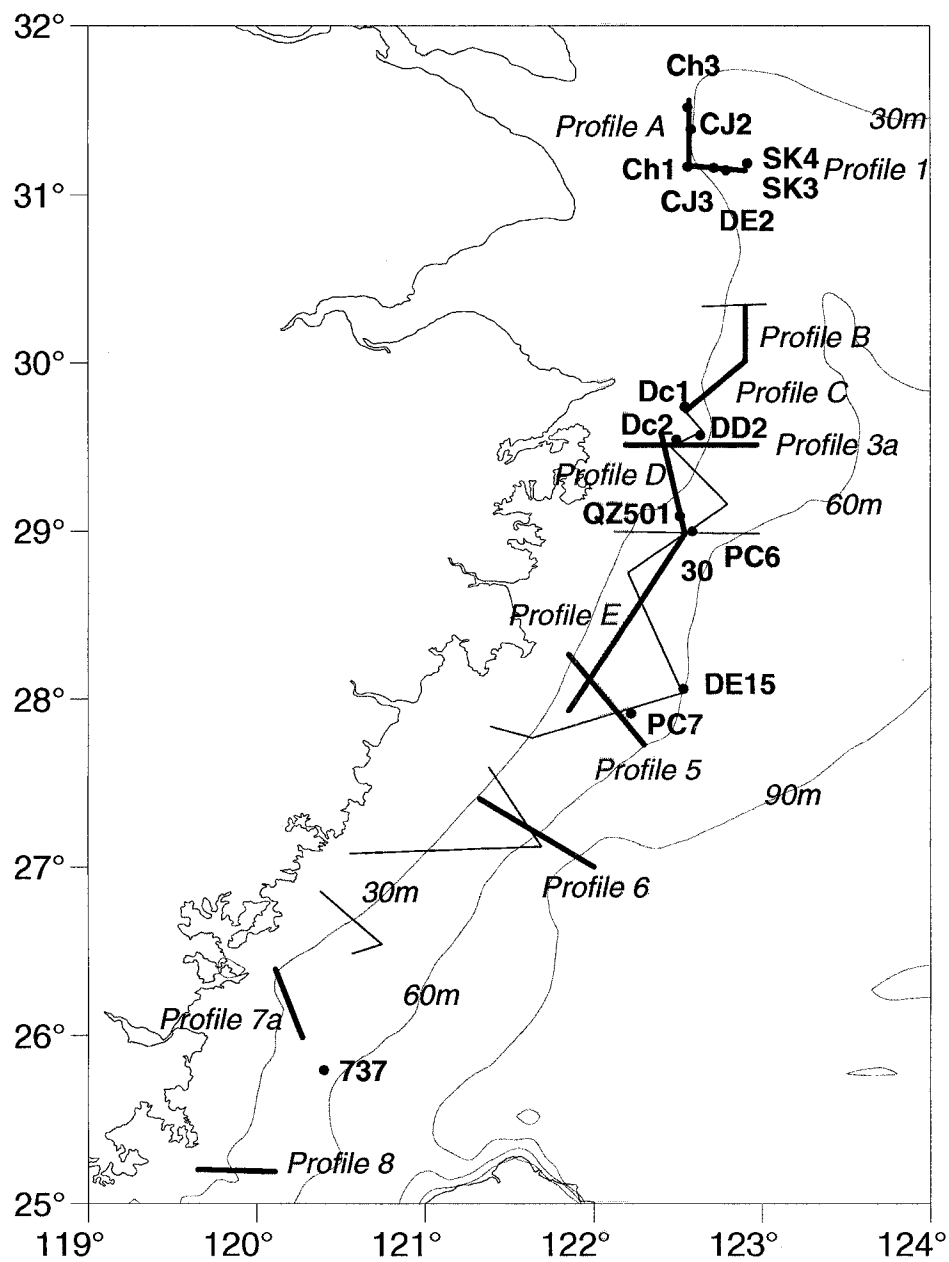
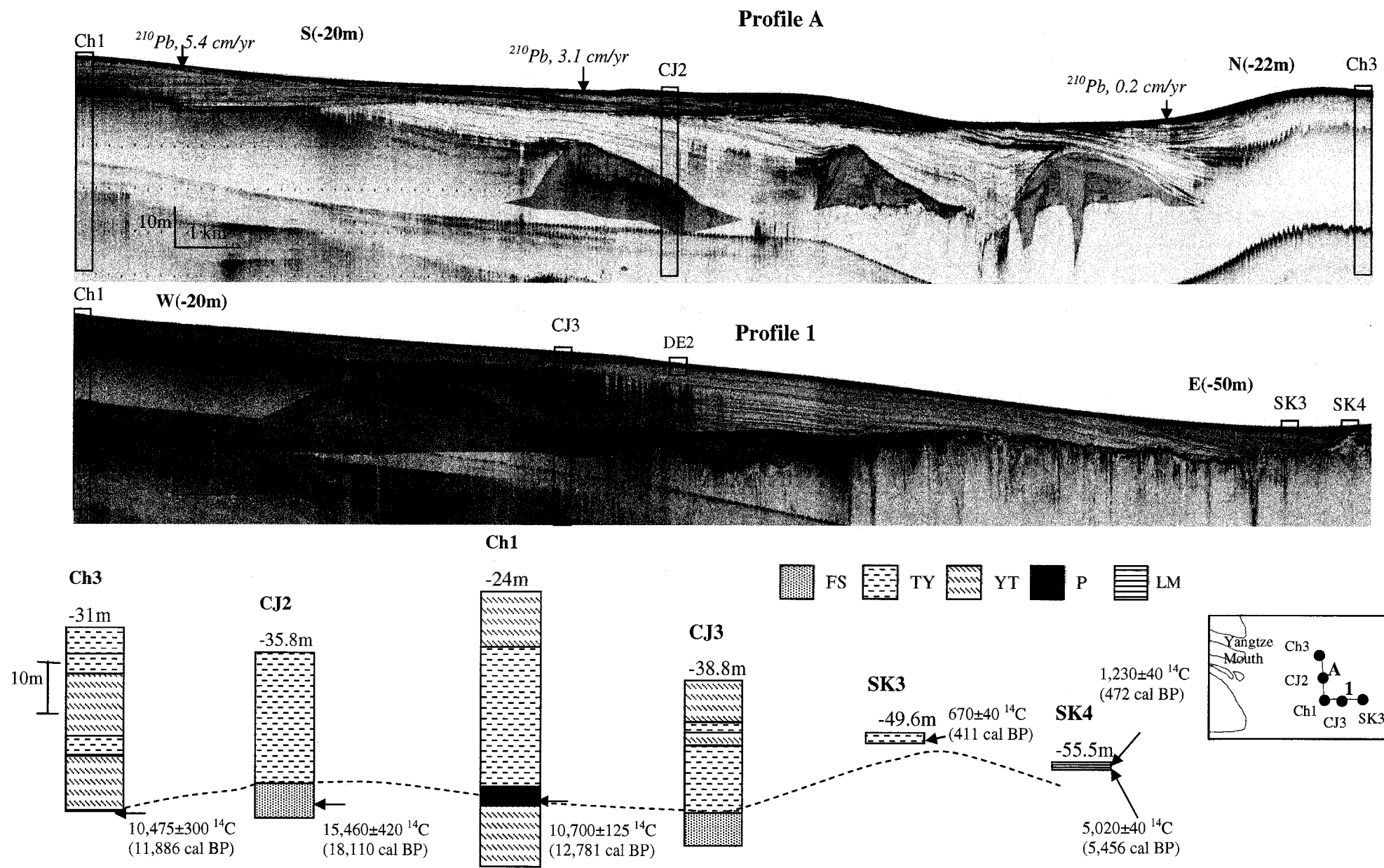
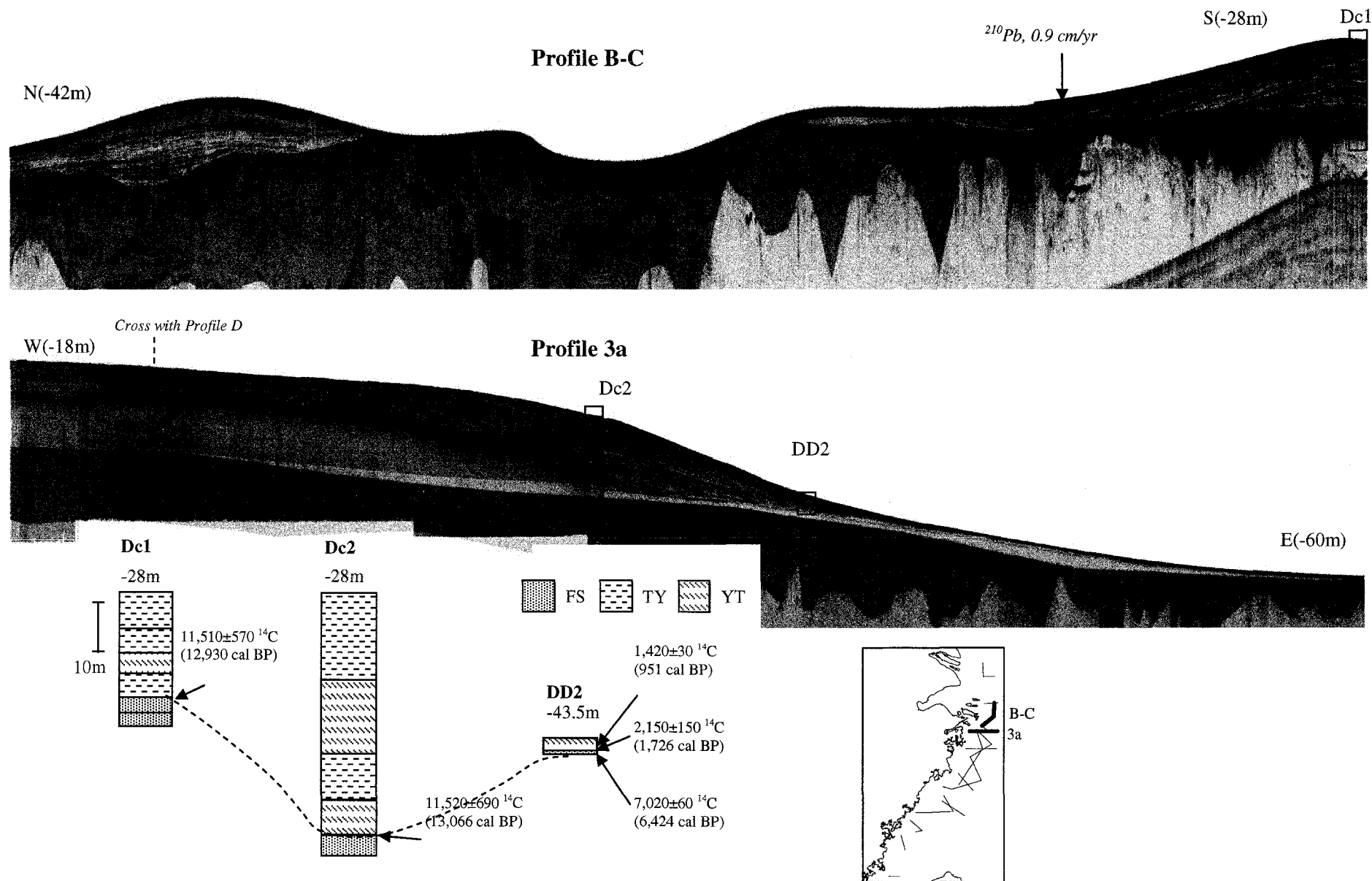


Fig. 4 Seismic profiles and cores in the East China Sea. Bold lines are shown in Fig. 5-10.

Figs. 5-9 Four facies (late-Pleistocene, Transgressive System Tract, early and late High-stand System Tracts, marked by blue, yellow, red and green, respectively) in the seismic profiles of inner East China Sea. Radiocarbon dates are reported in both ^{14}C and cal. BP. See Fig. 3 for the ^{210}Pb data sources. Sediment legends: FS, Fine Sand; TY, Silty Clay; YT, Clayey Silt; P, Peat; LM, laminated Mud.



(Fig. 5)



(Fig. 6)

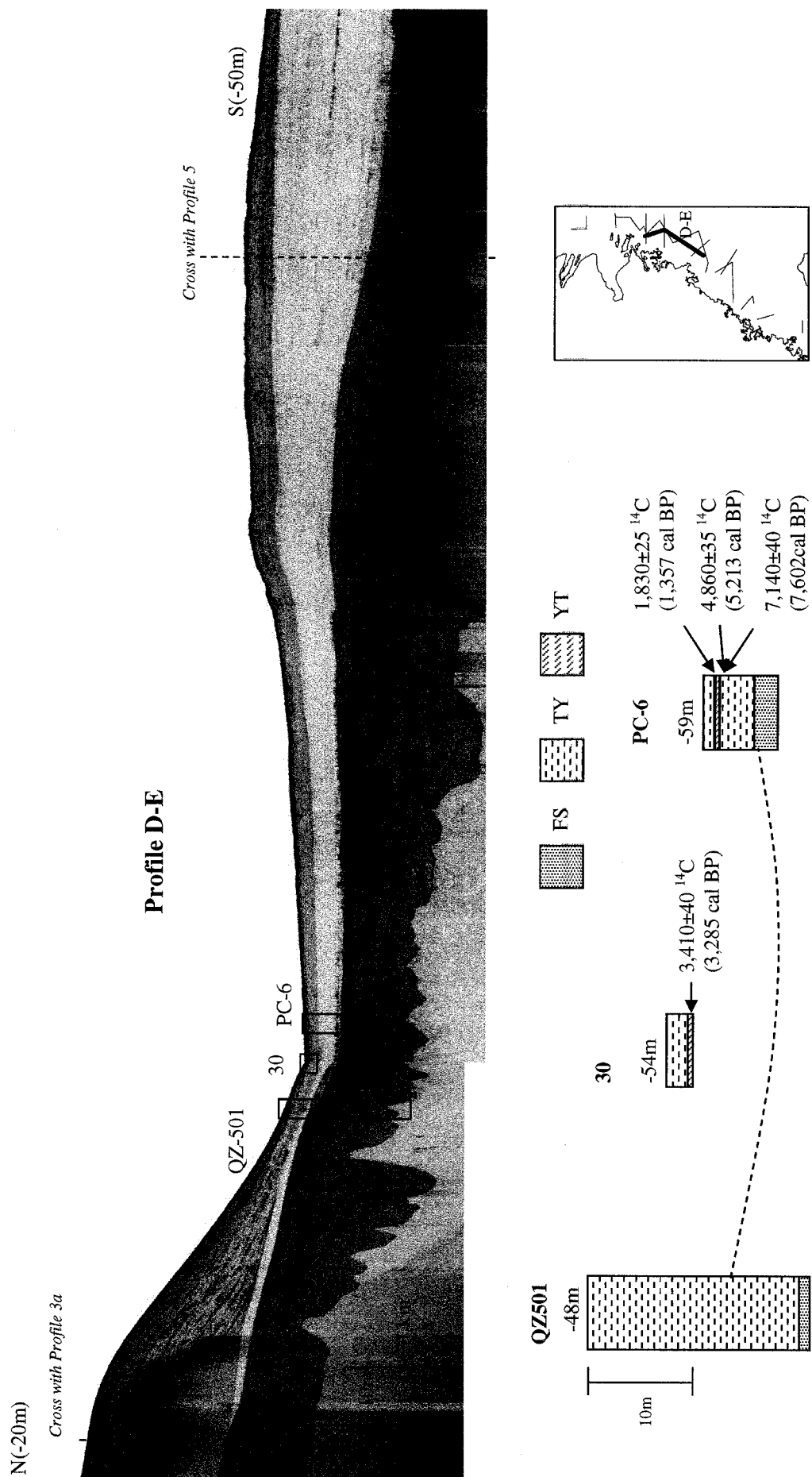


(Fig. 7)

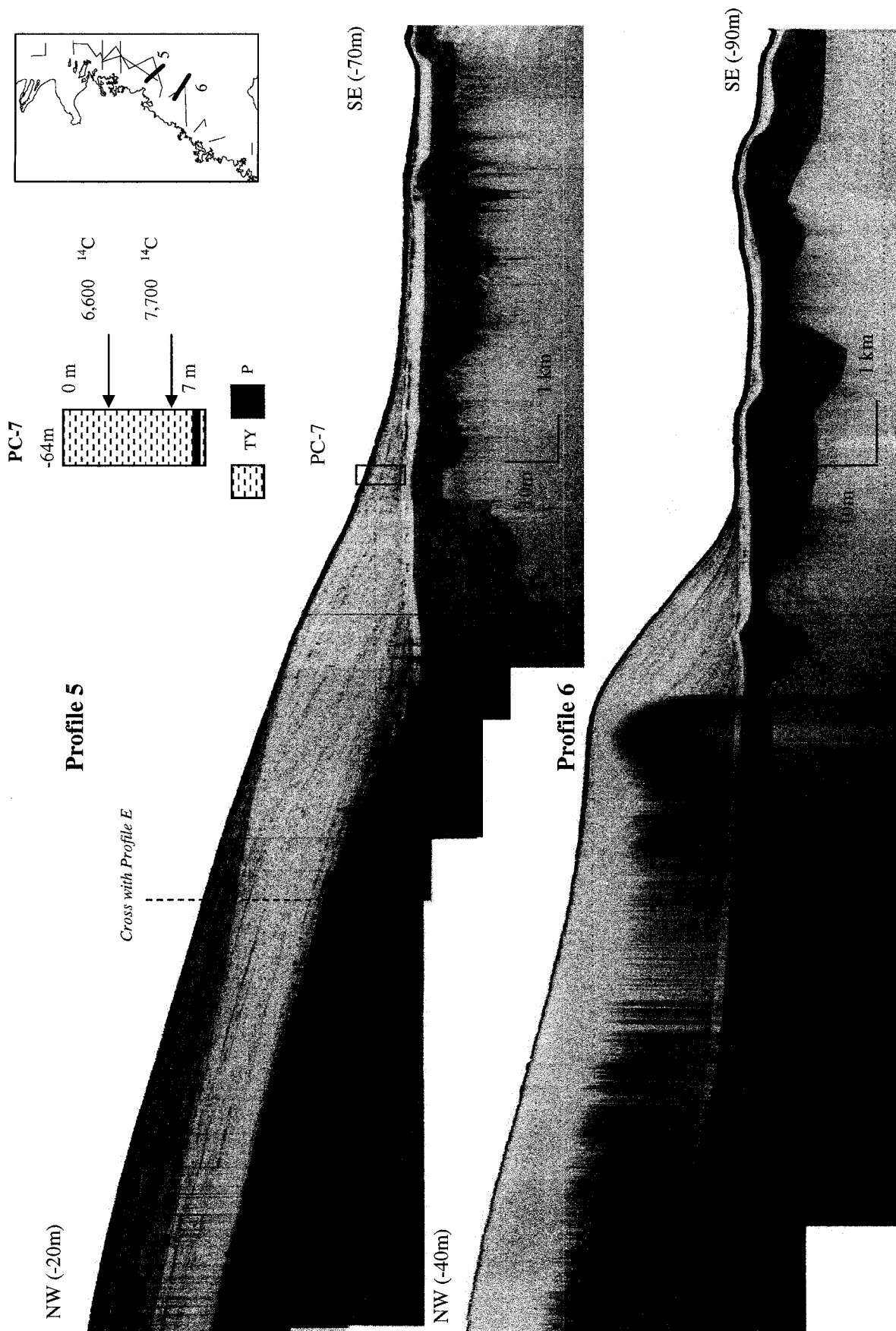


(Fig. 8)

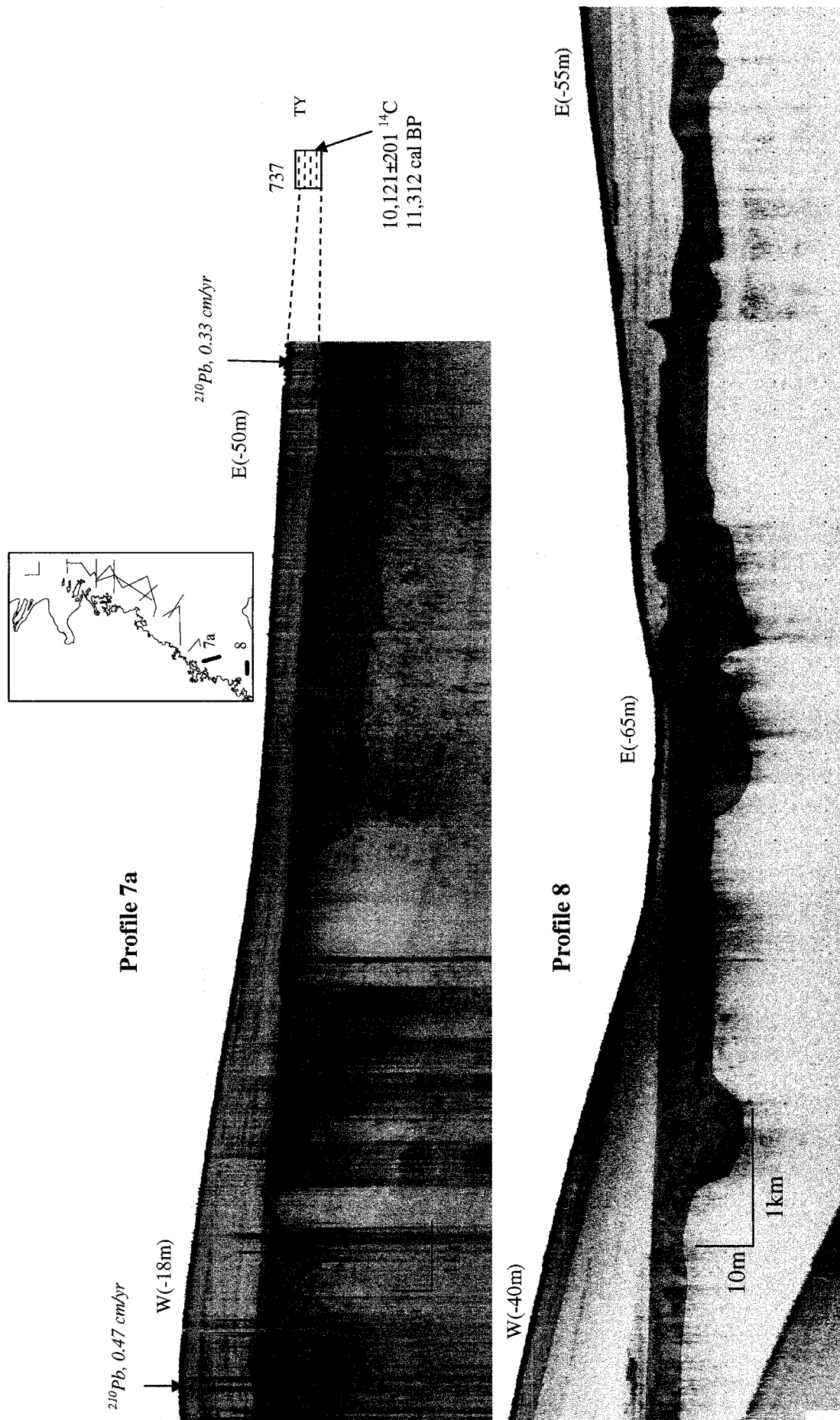


(Fig. 9)

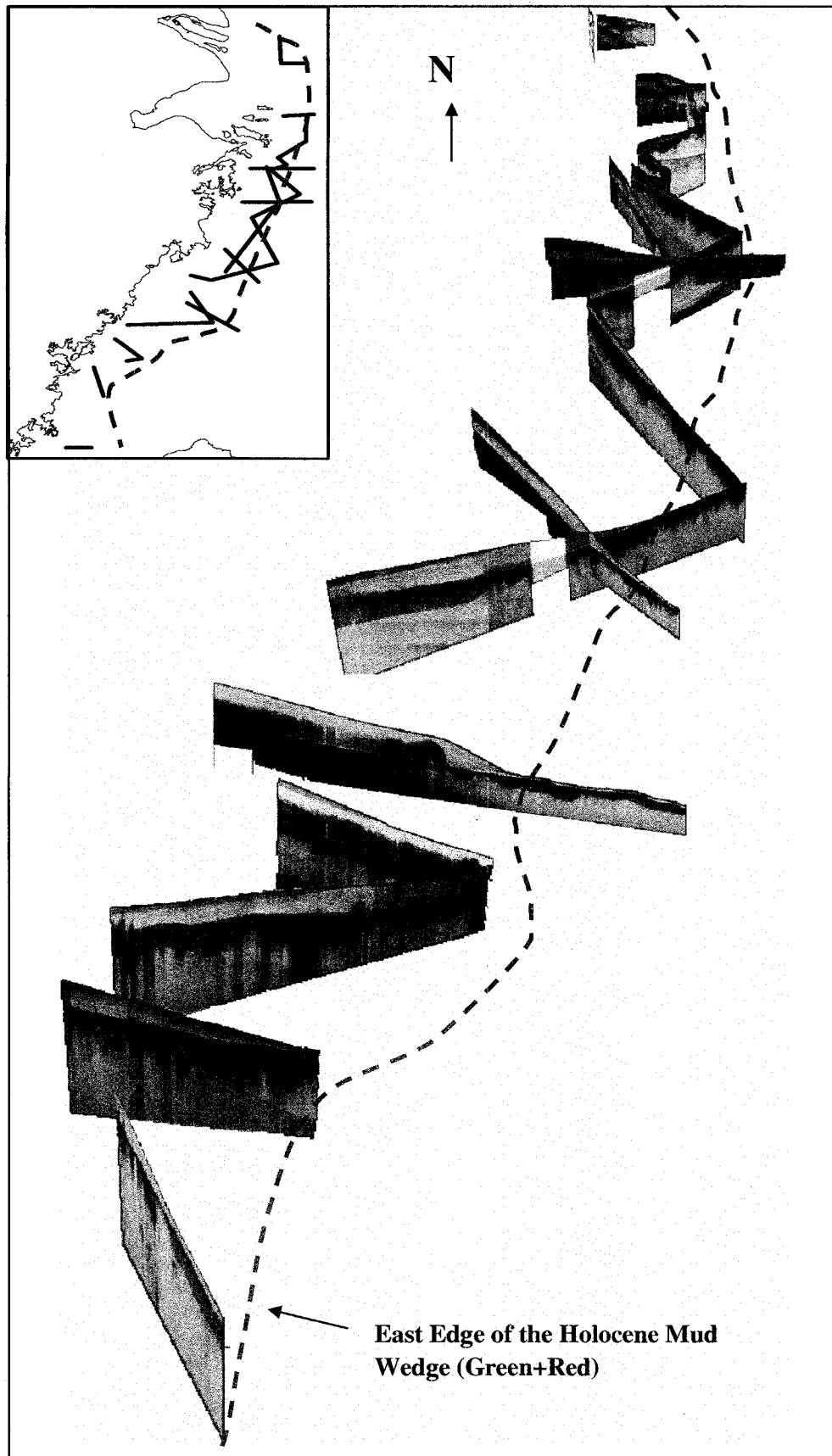


Fig. 10 Fence diagram of seismic profiles in the East China Sea. See color and strata descriptions in Fig. 5. Note that not all lines are shown here.

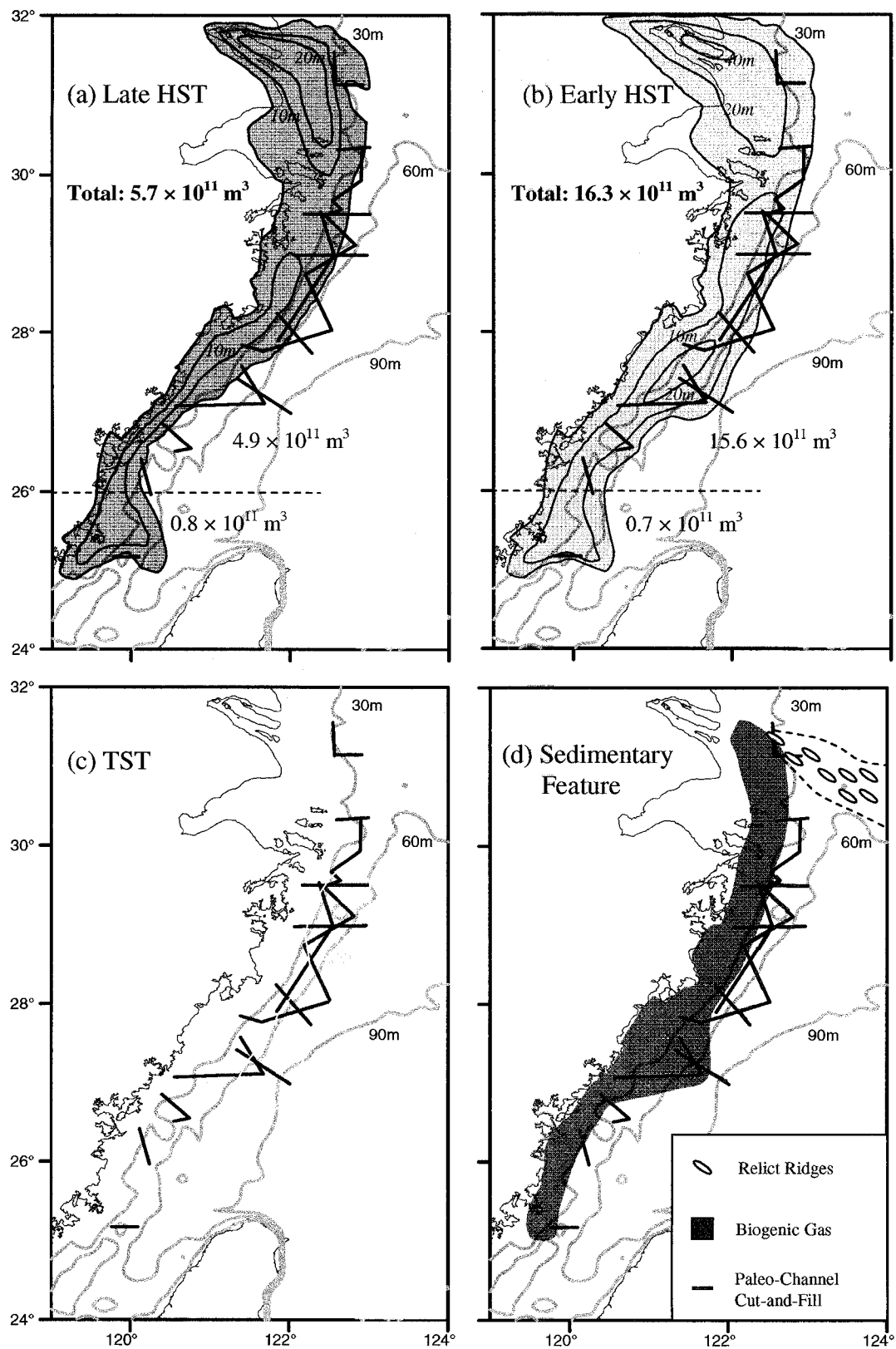


Fig. 11 (a) Late High-stand System Tract, (b) Early High-stand System Tract, (c) Transgressive System Tract and (d) Sedimentary feature. See explanation in Fig. 5.

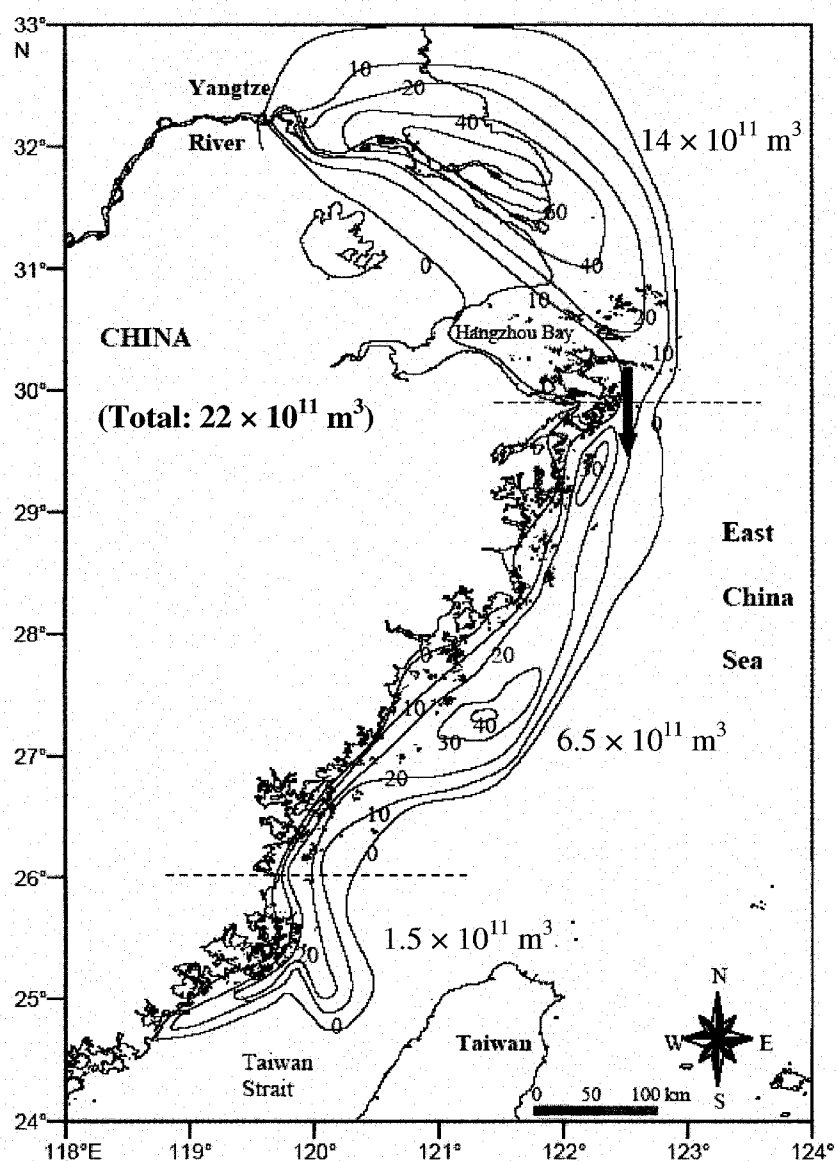


Fig. 12 Isopach of Holocene mud wedge in the inner shelf of East China Sea. The thickness is in meters. Total volume of this mud wedge is about $22 \times 10^{11} \text{ m}^3$, of which 14 , 6.5 and $1.5 \times 10^{11} \text{ m}^3$ are in >30 , $30-26$ and $<26^\circ\text{N}$ latitude ranges, respectively

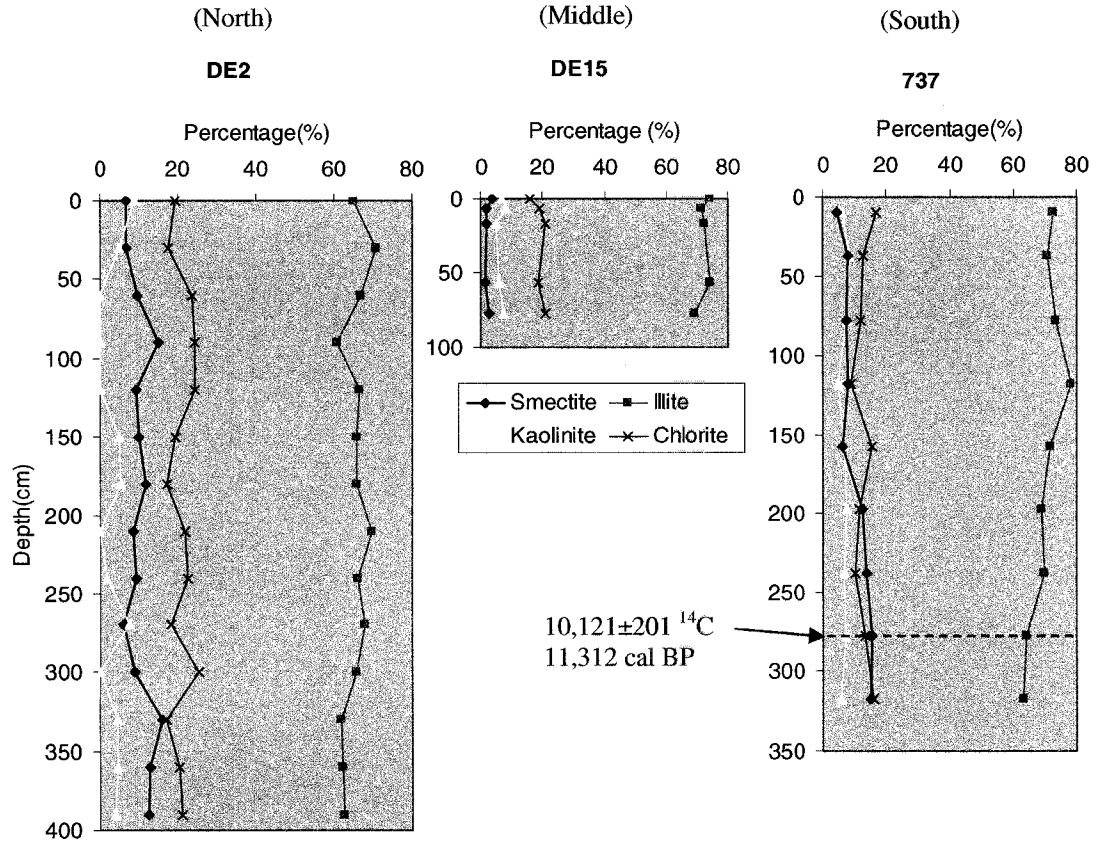


Fig. 13 Down-core clay mineral variations in the north (DE2), middle (DE15) and south (737) of the mud wedge. See Fig. 4 for the locations of cores.

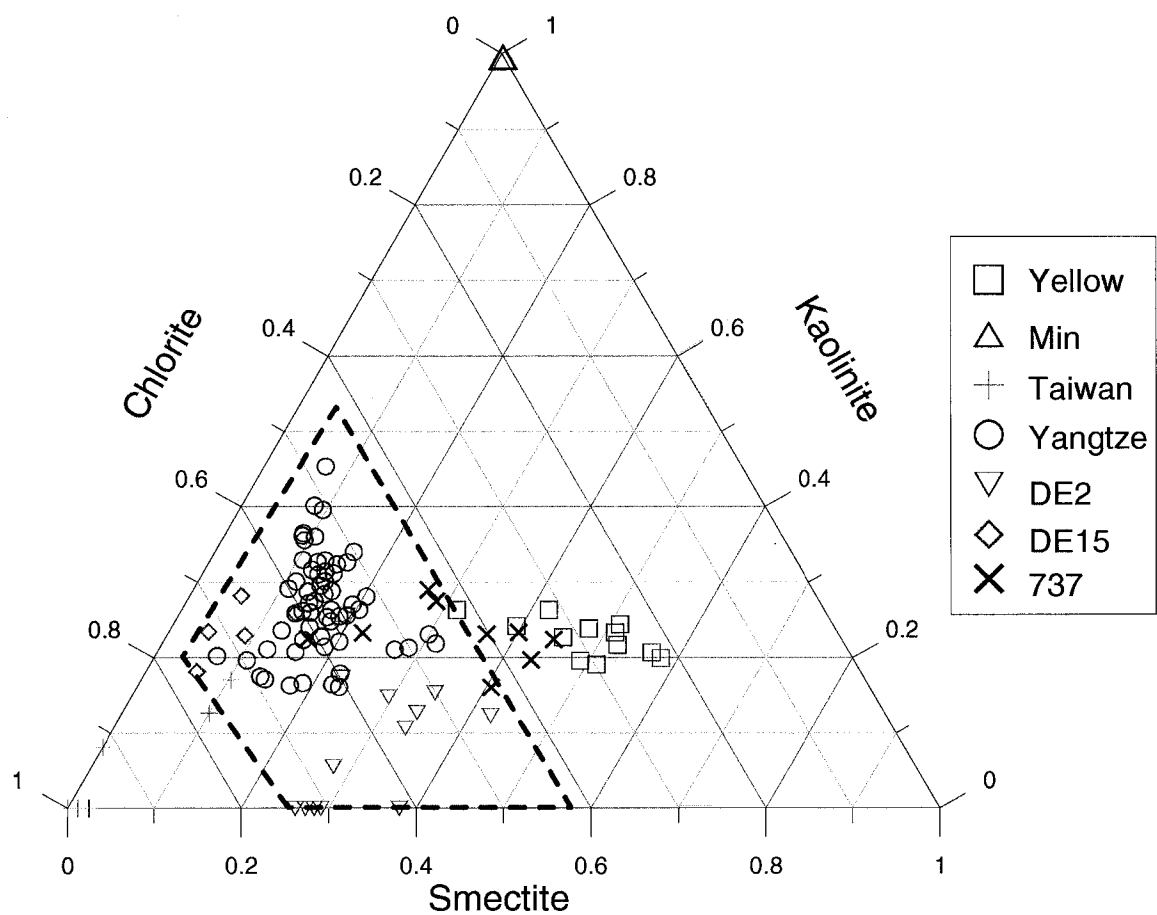


Fig. 14 Triangle plot of clay mineral assemblage from Yellow, Min, Taiwan, Yangtze and cores collected in ECS. See Fig. 4 for the locations of cores.

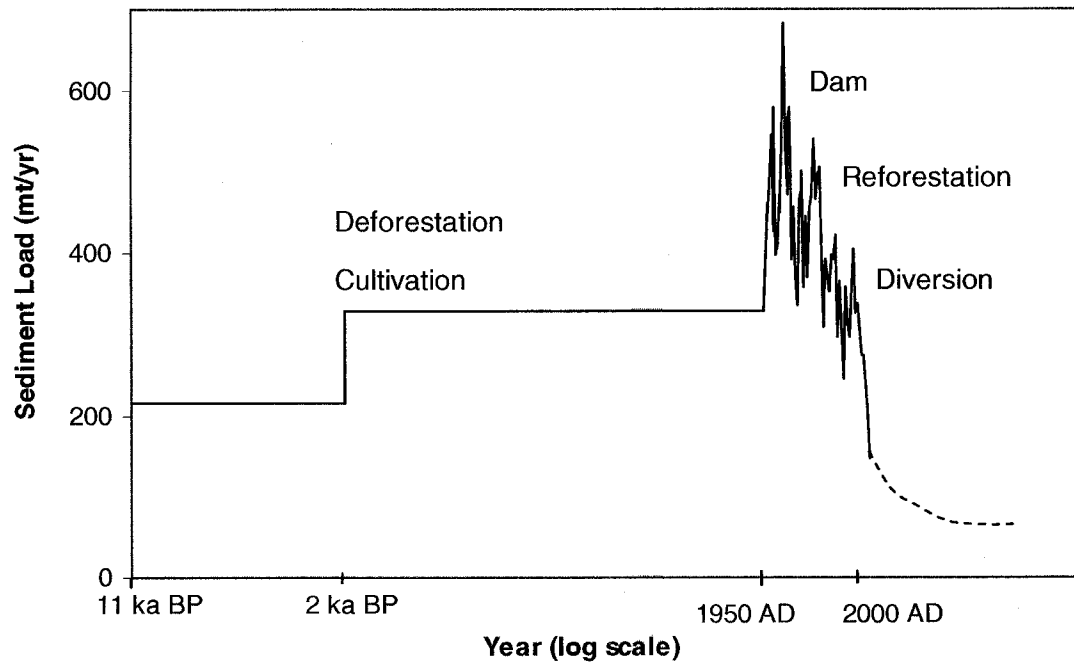


Fig. 15 Sediment load (mt/yr, million tons per year) from the Yangtze River to the East China Sea in the past 11,000 years and future decades.

VITA

Kehui Xu

Born in Weifang, Shandong Province in People's Republic of China on August 11th, 1977. Graduated from Weifang No. 1 High School in 1995. Earned B.S. in Geology & Computer Science from Ocean University of China in 1999. Received M.S. in Marine Geology from Ocean University of China in 2002. Entered doctoral program in the College of William and Mary, School of Marine Science in 2002.